

EFFECT OF ROAD BRIDGE ON WATER SURFACE PROFILE

A DISSERTATION

*Submitted in partial fulfillment of the requirements
for the award of the degree
of*

MASTER OF TECHNOLOGY

in

WATER RESOURCES DEVELOPMENT

By

**KHEM RAJ REGMI
(17548009)**



**DEPARTMENT OF WATER RESOURCES DEVELOPMENT AND MANAGEMENT
INDIAN INSTITUTE OF TECHNOLOGY ROORKEE
ROORKEE – 247 667 (INDIA)
MAY, 2019**



INDIAN INSTITUTE OF TECHNOLOGY ROORKEE

CANDIDATE'S DECLARATION

I hereby declare that the work presented in this Dissertation, entitled **EFFECT OF ROAD BRIDGE ON WATER SURFACE PROFILE**, in partial fulfilment of the requirement for the award of the degree of **Master of Technology in Water Resources Development** submitted to the **Department of Water Resources Development and Management, Indian Institute of Technology Roorkee** is an authentic and genuine record of my own work carried out during a period from July 2018 to May 2019 under the supervision and guidance of **Dr. S. K. Mishra**, Professor of WRD&M, IIT Roorkee and **Er. M. K. Jain**, DGM (Design), THDC India Ltd. Rishikesh, India.

I have not submitted the matter presented in this Dissertation Report for the award of any other Degree at any other Institute.

Date: 15th May, 2019

Place: IIT Roorkee

KHEM RAJ REGMI

Enrollment No. 17548009

CERTIFICATION

This is to certify that the above statement made by the candidate is correct to the best of my knowledge and belief.

.....

Er. Mayank Kumar Jain

DDG (Design)

THDC India Ltd. Rishikesh

.....

Dr. S.K. Mishra

Professor

DWRD&M, IIT Roorkee

ACKNOWLEDGEMENT

I would like to express my heartfelt gratitude and sincere thanks to my Supervisor **Dr. S. K. Mishra**, Professor, Department of Water Resources Development and Management, Indian Institute of Technology Roorkee for his valuable guidance, instructions, continuous feedback and co-operation for the completion of this Report. I am highly obliged to him for his keen interest, able guidance and encouragement throughout the writing. Working under his guidance is privilege and an excellent learning experience that I will flourish in my life time. I am extremely thankful to **Er. M. K. Jain**, DGM (Design), THDC India Ltd. Rishikesh, India for his kind guidance, continuous feedback and cooperation throughout the writing.

I am very much thankful to all authors, institutions and publishers whose books, papers have been used during this work.

Also, I would like to thank the entire team of the department including all the teaching and non-teaching staff members and my dear friends who have contributed directly or indirectly in successful completion of the work as well as report.

Finally, I must express my very profound gratitude to my parents, my wife (Sangita Subedi) and my baby (Tesla Regmi) for providing me with unfailing support and continuous encouragement throughout my years of study and in the process of research and writing this Dissertation Report. This accomplishment would not have been possible without them. Thank you.

Date: - 15th May, 2019

Place: IIT Roorkee

.....
KHEM RAJ REGMI

ABSTRACT

Bridges are constructed to ensure and facilitate the communication over the flow of waterways conveniently. However, these structures have detrimental effects on the hydrology and morphology of the adjacent area of the rivers/streams as the waterways get constricted. In this study, the effect of constriction of waterways due to bridge construction is reviewed through various literature available. A significant portion of waterways is occupied by bridge construction by bridge pier in case of small rivers compared to large rivers. The construction or renovation of bridges may require placement of bridge piers in the channel or floodplain of natural water ways. These piers will obstruct the flow i.e. the flow strikes piers and causes an increase in water levels upstream of the bridge for subcritical flows and hence considerable scours in bridge piers and its downstream side. The increase in water level is called as backwater or afflux. The extent of backwater caused by piers depends mainly on their geometric size, shape, their position in the stream or their spacing, the flow rate and the amount of channel blockage. Here the subject of study is to know how bridge influence channel flow and its effect in the water level variation at upstream and downstream of the bridge.

The effect of different parameters of Road Bridge on water surface profiles has been studied using popular HEC-RAS model. The variables under study are Manning's coefficient for different soils of the waterway, bridge pier shape and size, their spacing, contraction and expansion widths towards the flow direction. For this, the HEC-RAS model has been setup for water surface profiles for showing variation of afflux with variation of bridge parameters both upstream and downstream sides of the bridge under steady flow condition.

There has been found a significant change in water surface elevation with and without bridge condition in the river. The data of Alaknanda river reach starting from Devaprayag (a confluence of river Bhagirathi and Alaknanda) up to Lachmoli, which is about 10 km from Devaprayag are used in the study.

First the water surface elevation has been determined at the proposed bridge locations at various River Stations (RS) with HEC-RAS programming at various cross sections of river. Then the comparison has been made between the Water Surface Elevations for the same river

cross sections and at the same River Stations after placing the Bridge for the various values of steady flows (Discharge), Manning's coefficient n , Sizes of bridge piers, Spacing of piers, Piers geometry (shape), Contraction and expansion width of river etc. Then the corresponding water surface elevations are noted which are later used for plotting the water surface profiles. When there is no bridge at the proposed RS and for steady flow, for the constant discharge when Manning's coefficient n increases Water Surface Elevation increases, Velocity decreases, Flow area at Bridge site increases, and thus Froude no. (Fr) decreases. But after placing the bridge at the same location (RS), the bridge piers obstruct the flow at the upstream and downstream sides of the bridge and hence there is significant changes in water surface elevations at both sides of the bridge.

For the same Discharge, when Manning's coefficient n increases Water Surface Elevation increases, Velocity decreases, Flow area at Bridge site increases, and thus Froude no. (Fr) decreases. Also, providing the same Discharge, when bridge pier spacing increases, Water Surface Elevation decreases, Velocity increases, Flow area at Bridge site decreases, and thus Froude no. (Fr) increases. For different pier sizes i.e. 2.0, 2.5, 3.0 m piers @ 10 m spacing and for the same Q , when the bridge pier size increases, Water Surface Elevation increases, Velocity decreases, Flow area at Bridge site increases, and thus Froude no. (Fr) decreases.

Similarly, for same pier size (i.e. taking 2 m pier) at different spacing @ 10, 15, 20 m spacing and for the same steady flow Q , when the bridge pier spacing increases, Water Surface Elevation decreases, Velocity increases, Flow area at bridge site decreases, and thus Froude no. (Fr) increases.

Now, according to the Momentum method considering the shape of piers (or pier geometry), when the coefficient of discharge C_d ($C_d = 0.60$ for Elliptical piers with 2:1 length to width, 1.0 for Triangular nose with 30 degree angle, 1.2 for circular, 1.33 for Elongated with semicircular ends, 1.39 for Triangular nose with 60 degree angle and 2.0 for square nose) increases, Water Surface Elevation at u/s side of bridge increases whereas it is constant at d/s side, Velocity at u/s side decreases and there is no change at d/s side, similarly flow area at u/s bridge location increases but no change at d/s side, and thus Froude no. (Fr) at u/s side decreases and is constant at d/s side.

To determine the effect of Yarnell coefficient k ($k = 0.90$ for semi-circular nose and tail, 0.90 for 90 degree nose and tail and 1.25 for square nose and tail), for the same steady flow Q , it has no effect on any of the above parameters. Providing the constant k i.e. for a particular pier when the flow Q increases, there is no change in Water Surface Elevation, Velocity, Flow area and Froude no. (Fr). Also for the same coefficient of discharge C_d and n at the same time, when the Discharge Q increases, Water Surface Elevation increases, Velocity also increases, Flow area at Bridge site increases but the Froude no. (Fr) at u/s side increases while it is decreased at d/s side. And for the constant n , when flow Q increases, Water Surface Elevation increases, Velocity also increases, Flow area at Bridge site increases but the Froude no. (Fr) at u/s side increases while it decreased at d/s side of the bridge.

Also for the particular soil having constant n and same pier size, if Spacing of piers increases, Water Surface Elevation decreases, u/s velocity increases but d/s velocity decreases, Flow area at u/s decreases and increases at d/s side, thus Froude no. (Fr) at u/s side increases while it decreased at d/s side of bridge.

But for the multiple bridges, the effect of backwater is of local nature and does not extend largely towards the u/s and d/s sides of bridge (here the spacing between the each successive bridges is 1500 m) but it should be considered for the flood, river training and other hydraulic effects of the river as well as bridge.

CONTENTS

CANDIDATE’S DECLARATION	i
ACKNOWLEDGEMENT.....	ii
ABSTRACT	iii
CONTENTS	vi
LIST OF FIGURES.....	viii
LIST OF TABLES.....	xi
LIST OF ABBREVIATIONS	xiii
CHAPTER – 1 INTRODUCTION.....	1
1.1 GENERAL BACKGROUND OF THE STUDY.....	1
1.2 OBJECTIVES OF THE STUDY.....	3
1.3 RESEARCH GAP/RATIONALE.....	4
1.4 STUDY AREA	4
1.5 ORGANIZATION OF THESIS.....	7
CHAPTER – 2 SELECTION OF MATHEMATICAL MODEL	8
2.1 INTRODUCTION	8
2.2 HYDRAULIC CAPABILITY OF HEC – RAS	9
2.3 HEC – RAS IN BRIDGE MODELLING.....	10
2.4 LITERATURE REVIEW	11
CHAPTER – 3 HYDRAULIC SIMULATION OF FLOW THROUGH HEC-RAS	21
3.1 INTRODUCTION	21
3.2 METHODOLOGY/FLOW – CHART.....	24
3.3 PREPARATION AND RUN HEC-RAS MODEL.....	26
3.3.1 Geometric Data.....	26
3.3.2 Flow Data	26

3.4 CALCULATION AND RESULT EXTRACTION.....	30
3.4.1 WITH NO BRIDGE CONDITION.....	30
3.4.1.1 Variation of Water Surface Profiles with Manning’s coefficient n.....	30
3.4.2 WITH BRIDGE AND COMPARISON WITH NO BRIDGE CONDITION	45
3.4.2.1 Variation of Water Surface Profiles with Manning’s coefficient n.....	45
3.4.2.2 Variation of Water Surface Profiles with Contraction and Expansion Reach Length.....	54
3.4.2.3 Variation of Water Surface Profiles with Pier Size (2.0, 2.5, 3.0 m)	65
3.4.2.4 Variation of Water Surface Profiles with Pier Spacing (10.0, 15.0 and 20.0 m)	74
3.4.2.5 Variation of Water Surface Profiles with Pier Shape (Drag Coefficient C_d) (Momentum Method).....	85
3.4.2.6 Variation of Water Surface Profiles with Pier Shape (Yarnell Coefficient k)... ..	90
3.4.3 VARIATION OF WATER SURFACE PROFILES WITH AND WITHOUT BRIDGES IN SERIES (5 nos.)	92
3.4.3.1 Data extraction for No Bridge Condition	92
3.4.3.2 Data extraction for Five Bridges in Series.....	94
3.4.3.2 Comparison of Water Surface Elevations with and without Bridges	96
CHAPTER – 4 SUMMARY AND DISCUSSION OF RESULTS.....	100
4.1 SUMMARY AND CONCLUSION.....	100
4.2 FUTURE SCOPE OF WORKS	103
REFERENCES:.....	104

LIST OF FIGURES

Figure 1.1: DEM of Study Area extracted from HEC-RAS	4
Figure 1.2: Schematic of Alaknanda River Reach (at 500 m interval) after Georeferencing .	5
Figure 1.3: Schematic of Whole River showing all the Cross Sections in HEC - RAS	5
Figure 1.4: Schematic of Bridge Location at River Station 928 m	5
Figure 1.5: Cross Sections at Bridge Locations (River Stations 928, 2428, 3928, 5428 and 6928 m).....	6
Figure 2.1: Definition sketch of flow through a bridge constriction.	12
Figure 2.2: Measurement of the backwater of the bridges: (a) plane view; (b) side view	14
Figure 2.3: Bridge Reach (HEC, 1997)	18
Figure 3.1: Representation of Terms in the Energy Equation	21
Figure 3.2: Methodology through HEC – RAS	24
Figure 3.3: Water Surface Elevation vs Manning's no. n	31
Figure 3.4: Water Surface Elevation vs Velocity	31
Figure 3.5: Water Surface Elevation vs Flow area	32
Figure 3.6: Water Surface Elevation vs Fr	32
Figure 3.7: Velocity vs Fr.....	33
Figure 3.8: Velocity vs Flow area at Q = 200 cumecs.....	33
Figure 3.9: Fr vs Manning's no. n.....	34
Figure 3.10: Velocity vs Manning's no. n at Q = 200 cumecs.....	34
Figure 3.11: Water Surface Elevation vs Manning's no. n at Q = 400 cumecs	35
Figure 3.12: Water Surface Elevation vs Velocity	36
Figure 3.13: Water Surface Elevation vs Flow area	36
Figure 3.14: Water Surface Elevation vs Fr	37
Figure 3.15: Velocity vs Fr.....	37
Figure 3.16: Velocity vs Flow area.....	38
Figure 3.17: Fr vs Manning's no. n.....	38
Figure 3.18: Velocity vs Manning's no. n.....	39
Figure 3.19: Water Surface Elevation vs Manning's coefficient n at various Q.....	41
Figure 3.20: Water Surface Elevation vs Flow Area at various Q	41

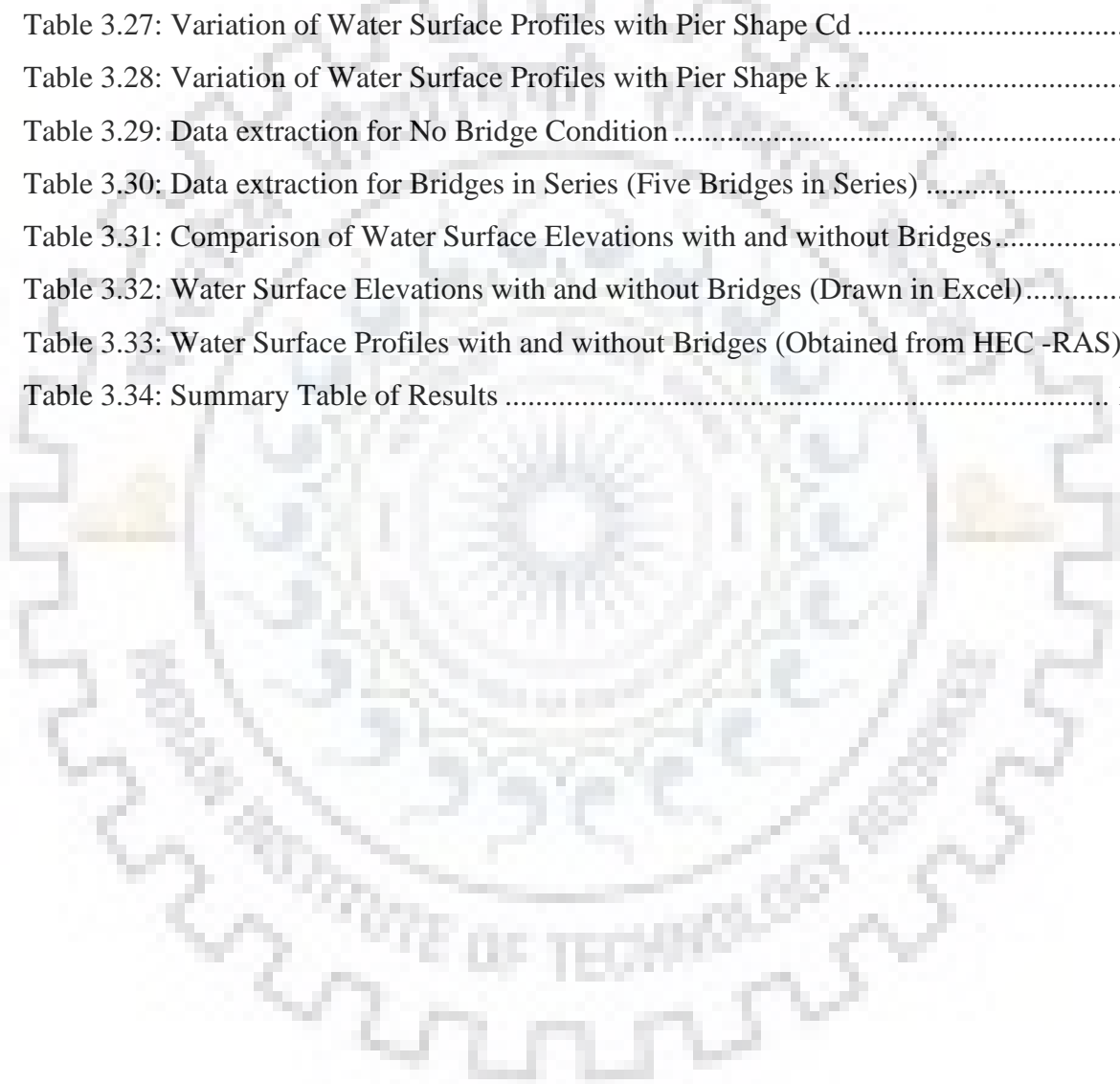
Figure 3.21: Velocity vs Froude no. (Fr) at various Q	42
Figure 3.22: Velocity vs Fr at Q = 200 cumecs with various n (No Bridge).....	47
Figure 3.23: Velocity vs Fr at Q = 200 cumecs (With Bridge)	47
Figure 3.24: Water Surface Elevation vs Contraction Length at Q = 200 cumecs.....	56
Figure 3.25: Velocity vs Fr	57
Figure 3.26: Water Surface Elevation vs Fr	57
Figure 3.27: Water Surface Elevation vs Contraction Length at Q = 400 cumecs.....	58
Figure 3.28: Velocity vs Fr	59
Figure 3.29: Water Surface Elevation vs Fr	59
Figure 3.30: Water Surface Elevation vs Contraction Length at Q = 600 cumecs.....	60
Figure 3.31: Velocity vs Fr	61
Figure 3.32: Water Surface Elevation vs Fr	61
Figure 3.33: Water Surface Elevation vs pier spacing at Q = 200 cumecs	65
Figure 3.34: Water Surface Elevation vs Velocity	66
Figure 3.35: Water Surface Elevation vs flow area	66
Figure 3.36: Water Surface Elevation vs Fr	67
Figure 3.37: Velocity vs Fr.....	67
Figure 3.38: Water Surface Elevation vs Pier spacing for same pier size 2.5 m at Q = 200 cumecs	68
Figure 3.39: Water Surface Elevation vs Velocity	68
Figure 3.40: Water Surface Elevation vs Flow area.....	69
Figure 3.41: Velocity vs Fr.....	69
Figure 3.42: Water Surface Elevation vs Pier spacing for same pier size 3.0 m at Q = 200 cumecs	70
Figure 3.43: Water Surface Elevation vs Velocity	70
Figure 3.44: Water Surface Elevation vs Flow area at Q = 200 cumecs.....	71
Figure 3.45: Velocity vs Fr.....	71
Figure 3.46: Water Surface Elevation vs Pier size at Q = 200 cumecs and 10 m pier spacing	74
Figure 3.47: Water Surface Elevation vs Velocity	74
Figure 3.48: Water Surface Elevation vs Flow area.....	75

Figure 3.49: Velocity vs Pier size.....	75
Figure 3.50: Velocity vs Fr.....	76
Figure 3.51: Fr vs Pier size.....	76
Figure 3. 52: Water Surface Elevation vs Pier size at Q = 200 cumecs and 15 m pier spacing	77
Figure 3.53: Water Surface Elevation vs Velocity.....	77
Figure 3.54: Water Surface Elevation vs Flow area.....	78
Figure 3.55: Velocity vs Pier size.....	78
Figure 3.56: Velocity vs Fr.....	79
Figure 3.57: Fr vs Pier size.....	79
Figure 3.58: Water Surface Elevation vs pier size at Q = 200 cumecs and 20 m pier spacing	80
Figure 3.59: Water Surface Elevation vs Velocity.....	80
Figure 3.60: Water Surface Elevation vs Flow area.....	81
Figure 3.61: Velocity vs Pier size.....	81
Figure 3.62: Velocity vs Fr.....	82
Figure 3.63: Fr vs Pier size.....	82
Figure 3.64: Water Surface Elevation vs Cd at Q = 200 cumecs and 10 m pier spacing, 2 m pier size.....	86
Figure 3.65: Water Surface Elevation vs Velocity.....	86
Figure 3.66: Velocity vs Cd.....	87
Figure 3.67: Fr vs Cd.....	87
Figure 3.68: (a) Water Surface Elevation vs k at Q = 200 cumecs and 10 m pier spacing, 2 m pier size (b) Velocity vs k.....	90

LIST OF TABLES

Table 3.1: Manning’s coefficient n for various types of soils and waterways	29
Table 3.2: For No Bridge Condition and $Q = 200 \text{ m}^3/\text{sec}$	30
Table 3.3: For No Bridge Condition and $Q = 400 \text{ m}^3/\text{sec}$	35
Table 3.4: For No Bridge Condition and $Q = 600 \text{ m}^3/\text{sec}$	39
Table 3.5: For No Bridge Condition and $Q = 800 \text{ m}^3/\text{sec}$	40
Table 3.6: For No Bridge Condition and $Q = 1000 \text{ m}^3/\text{sec}$	40
Table 3.7: Variation of Water Surface Profiles with Manning’s coefficient n ($Q = 200 \text{ m}^3/\text{s}$)	45
Table 3.8: Variation of Water Surface Profiles with Manning’s coefficient n ($Q = 400 \text{ m}^3/\text{s}$)	48
Table 3.9: Variation of Water Surface Profiles with Manning’s coefficient n ($Q = 600 \text{ m}^3/\text{s}$)	50
Table 3.10: Variation of Water Surface Profiles with Manning’s coefficient n ($Q = 800 \text{ m}^3/\text{s}$)	50
Table 3.11: Variation of Water Surface Profiles with Manning’s coefficient n ($Q = 1000 \text{ m}^3/\text{s}$)	51
Table 3.12: Variation of Water Surface Profiles with Contraction and Expansion Reach Length (for contraction length 20 m).....	54
Table 3.13: Variation of Water Surface Profiles with Contraction and Expansion Reach Length (for contraction length 25 m).....	54
Table 3.14: Variation of Water Surface Profiles with Contraction and Expansion Reach Length (for contraction length 30 m).....	55
Table 3.15: Variation of Water Surface Profiles with Contraction and Expansion Reach Length (for contraction length 35 m).....	55
Table 3.16: Rearranging data for various Contraction Lengths ($Q = 200 \text{ cumecs}$).....	56
Table 3. 17: Rearranging data for various Contraction Lengths ($Q = 200 \text{ cumecs}$).....	58
Table 3.18: Rearranging data for various Contraction Lengths ($Q = 600 \text{ cumecs}$).....	60
Table 3.19: Rearranging data for various Contraction Lengths ($Q = 800 \text{ cumecs}$).....	62
Table 3.20: Rearranging data for various Contraction Lengths ($Q = 1000 \text{ cumecs}$).....	62

Table 3.21: Variation of Water Surface Profiles with Pier Size (2 m pier size).....	65
Table 3.22: Variation of Water Surface Profiles with Pier Size (2.5 m pier size).....	68
Table 3.23: Variation of Water Surface Profiles with Pier Size (3 m pier size).....	70
Table 3.24: Variation of Water Surface Profiles with Pier Spacing (10 m pier spacing).....	74
Table 3.25: Variation of Water Surface Profiles with Pier Spacing (15 m pier spacing).....	77
Table 3.26: Variation of Water Surface Profiles with Pier Spacing (20 m pier spacing).....	80
Table 3.27: Variation of Water Surface Profiles with Pier Shape Cd	85
Table 3.28: Variation of Water Surface Profiles with Pier Shape k	90
Table 3.29: Data extraction for No Bridge Condition	92
Table 3.30: Data extraction for Bridges in Series (Five Bridges in Series)	94
Table 3.31: Comparison of Water Surface Elevations with and without Bridges.....	96
Table 3.32: Water Surface Elevations with and without Bridges (Drawn in Excel).....	98
Table 3.33: Water Surface Profiles with and without Bridges (Obtained from HEC -RAS)	99
Table 3.34: Summary Table of Results	100



LIST OF ABBREVIATIONS

C: Expansion or Contraction loss coefficient	k: Yarnell's pier shape coefficient
Cd: Coefficient of discharge (pier shape coefficient)	km: kilometer
ch.: chainage	Lat.: Latitude
cumecs: cubic meter per second	Lon.: Longitude
CWSE: Critical Water Surface Elevation	m: meter
d/s: downstream	n: Manning's coefficient (roughness coefficient)
DEM: Digital Elevation Model	N: North
E: East	Q: Steady flow (Discharge)
GIS: Geographical Information System	RS: River Station
GUIC: Graphical User Interface	u/s: upstream
h_e : head loss	WSE: Water Surface Elevation
HEC-RAS: Hydraulic Engineering Center River Analysis System	

INTRODUCTION

1.1 GENERAL BACKGROUND OF THE STUDY

When the bridge is constructed across the river, there is a significant increase in water level at the upstream which creates an obstruction in the flow and local loss of stream energy. This is due to the fluid friction in contact with the structure, and the stagnation zones that border the contracting and expanding flow reaches. To maintain a steady flow, this local loss of energy is compensated by an increase in potential energy immediately upstream of the structure. A backwater is thus created which begins at the afflux location.

Information about the flow regime of any open channels (River) under different discharge conditions is essential for the water resources engineers, planners and managers. In order to know the depth of flow at different downstream reaches, water surface profiles are computed using the information on channel geometry and roughness coefficient of the river reach.

River training works modify the existing flow conditions. For example, construction of levees for the protection of a village or town increases the depth of flood flow. The human activities and encroachment in the flood plain affects the river environment. Construction of embankments along the river reaches drastically changes the river regime which has to attain a new equilibrium state under changed condition. For releasing water from a reservoir, knowledge of depth of flow at different downstream stations are required, to avoid damage to lives and properties.

As mentioned above, in many engineering applications, it is necessary to compute the flow conditions in channels having gradually varied flow. These computations, generally referred to as water surface profile calculations, determine the water surface elevations along the channel for a specified discharge. The water surface elevations are required for the planning, design and operation of open channels so that the effects of engineering works and channel modifications on water levels may be assessed.

The continuity, momentum, and energy equations describe the relationships among various flow variables, such as the flow depth, discharge and flow velocity. By solving these equations, it is possible to determine the flow conditions throughout a specified channel length. These analyses yield the change in flow depth in a given distance or compute the distance in which a specified change in flow depth will occur. The channel cross-section, Manning's n, bottom slope and the rate of discharge are usually known for these steady state flow computations.

By differentiating the energy equation for a channel section between two river sections, the governing equation for gradually varied flow can be expressed as;

$$dx/dy = (S_0 - S_f) / [1 - (\alpha B Q^2 / g A^3)] \dots \dots \dots (i)$$

where, S_f is the slope of the energy grade line, S_0 is the slope of the channel bottom, α is the velocity head coefficient, B is the bottom width of the channel, Q is the discharge and A is the cross sectional area of the channel.

For the derivation of this governing equation, some assumptions are made. They are;

- ✓ The slope of the channel bottom is small.
- ✓ Channel is prismatic and there is no lateral inflow or outflow from the channel.
- ✓ Pressure distribution at a channel section is hydrostatic.

Several procedures to compute the water surface profiles have been developed. Some of the earlier procedures used varied flow functions developed by integrating the differential equation describing the gradually varied flow. Several graphical and mathematical methods were developed for the integration of this equation or for solving the energy equation between two sections. Some of these methods have been used in the various general purpose computer programs for computing water surface profiles (Soil Conservation Service, 1976; US Geological Survey, 1976; US Army Corps of Engineers, 1982). Some of the generally used methods are listed below:

The most common and simple method is to calculate the profile reach by reach;

- Direct Step Method
- Standard Step Method

Methods in which numerical integration of differential equation for gradually varied flow is used;

- ✓ Single Step Method: Euler Method, Modified Euler Method, Improved Euler Method, Fourth-Order Runge-Kutta method etc.
- ✓ Predictor-Corrector methods.

HEC-2 or HEC-RAS, developed by Hydrologic Engineering Centre, US Army Corps of Engineers (1982), is based on Standard Step Method. It is being widely used in many countries for Water Surface Profile computations and proved to be very useful. This method uses river cross section data to define channel geometry; Manning's roughness coefficient to define flow characteristic along the main channel as well as for flood plain; and initial and boundary conditions to arrive at the profile characteristics for different reaches.

Other than the water surface Profile calculations, HEC-RAS is used for many other applications such as planning of various river training works, river and flood plain encroachment studies, flood plain zoning, etc. It can also be used to prepare rating curves for different reaches of a river network, which can be useful during floods, for the planning and design of flood protection works along various reaches of the stream network.

1.2 OBJECTIVES OF THE STUDY

The Main objectives of the study are:

- i.** To determine the nature of change of water surface profile along the length of open channel at the steady flow condition using HEC-RAS.
- ii.** To determine the backwater (afflux) at upstream due to bridge effect (its piers, nos., shape, spacing, contraction and expansion widths etc.) on water surface profiles.
- iii.** To create a comprehensive and solid idea that how the single and multiple bridges (bridges in series) effects the backwater.
- iv.** To compare the model for Water Surface Profile providing steady flow with and without bridge conditions.

1.3 RESEARCH GAP/RATIONALE

Found lack of comprehensive and cumulative study of road bridge effects on water surface profile at various cross section of natural channel considering the shape, size, nos., spacing of piers. Also there is no such a literature available which can explain the effect of multiple bridges (bridges in series) along the channel and effect of expansion and contractions portions of river reach due to bridge at steady flow condition using HEC-RAS.

1.4 STUDY AREA

- ✓ Alaknanda River reach (A major tributary of River Ganga) Starts from Devaprayag (a confluence of River Bhagirathi and Alaknanda) and ends at near Lachmoli, 10 km upstream From Devaprayag (near Srinagar), Uttarakhand State of India.
- ✓ Lat. $30^{\circ} 08' 43''$ N to $30^{\circ} 14' 20''$ N and Lon. $78^{\circ} 36' 02''$ E to $78^{\circ} 41' 17''$ E.
- ✓ River Cross – Section taken at 500 m interval are georeferenced with ArcGIS and then interpolated at 50 m intervals in HEC - RAS.
- ✓ Bridges are assumed to be located/placed at River Stations 928 m , 2428 m, 3928 m, 5428 m and 6928 m of river reach (from d/s to u/s side)
- ✓ Simulation performed for 200, 400, 600, 800 and 1000 cumecs steady flow.

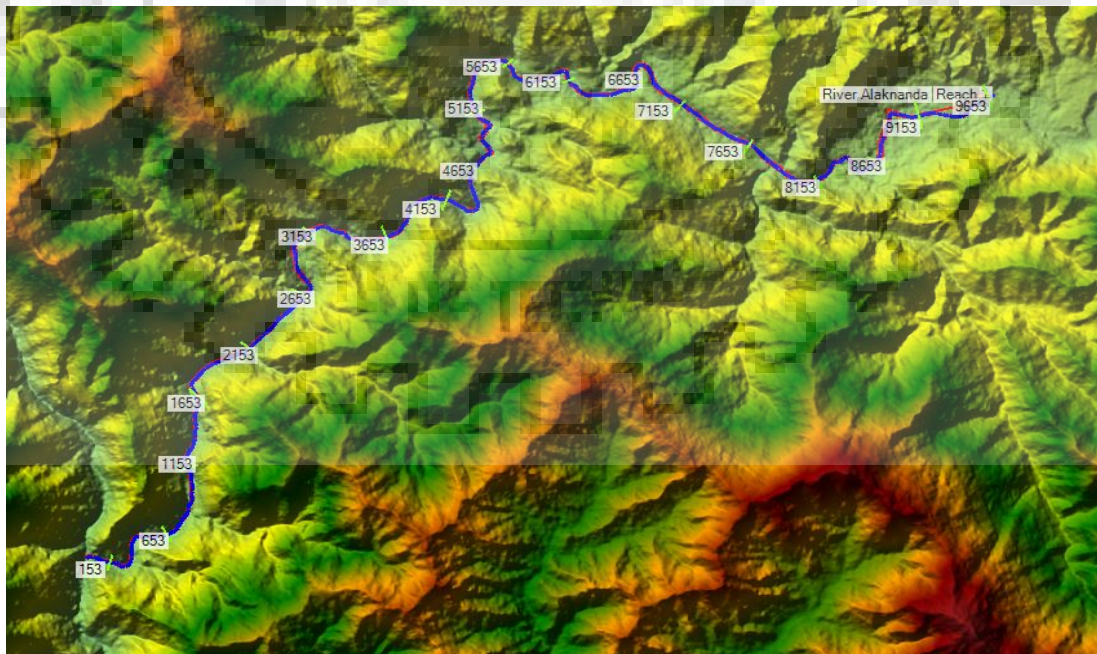
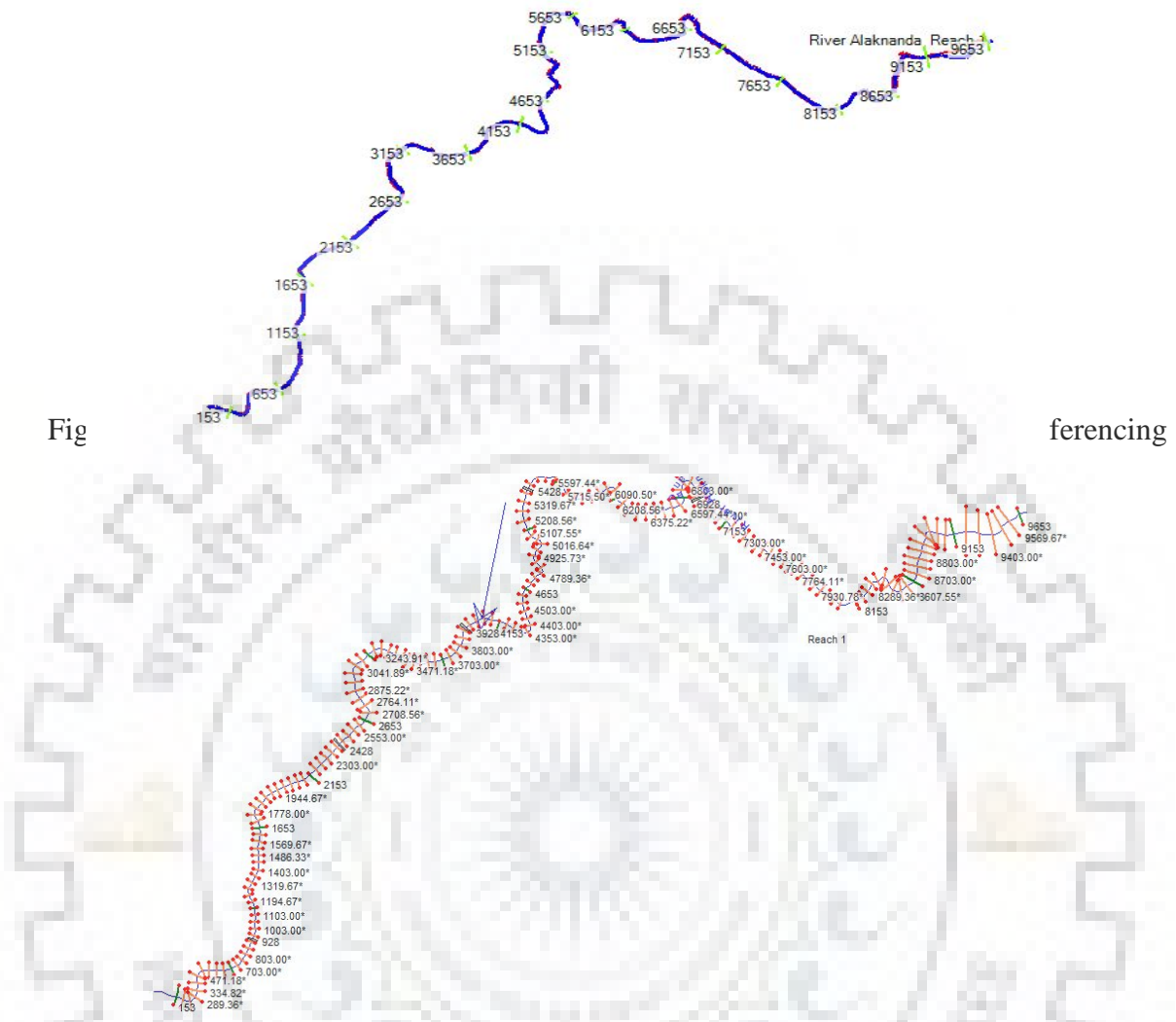


Figure 1.1: DEM of Study Area extracted from HEC-RAS



Fig

ferencing

Figure 1.3: Schematic of Whole River showing all the Cross Sections in HEC - RAS

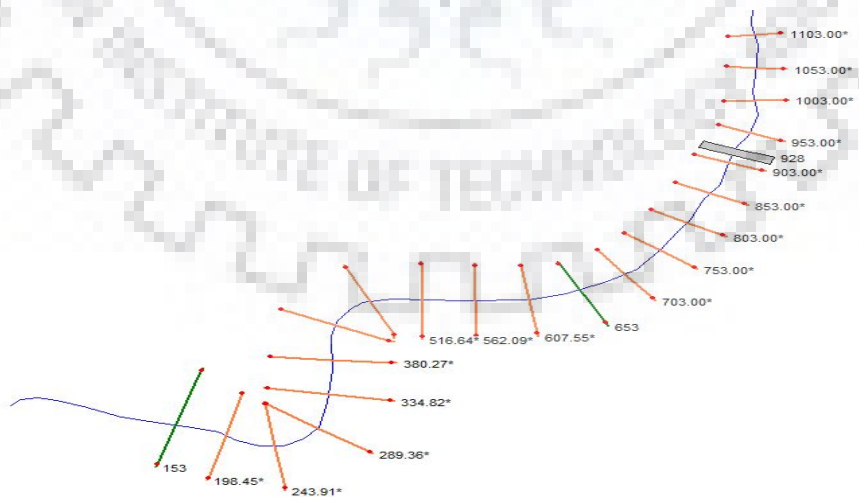


Figure 1.4: Schematic of Bridge Location at River Station 928 m

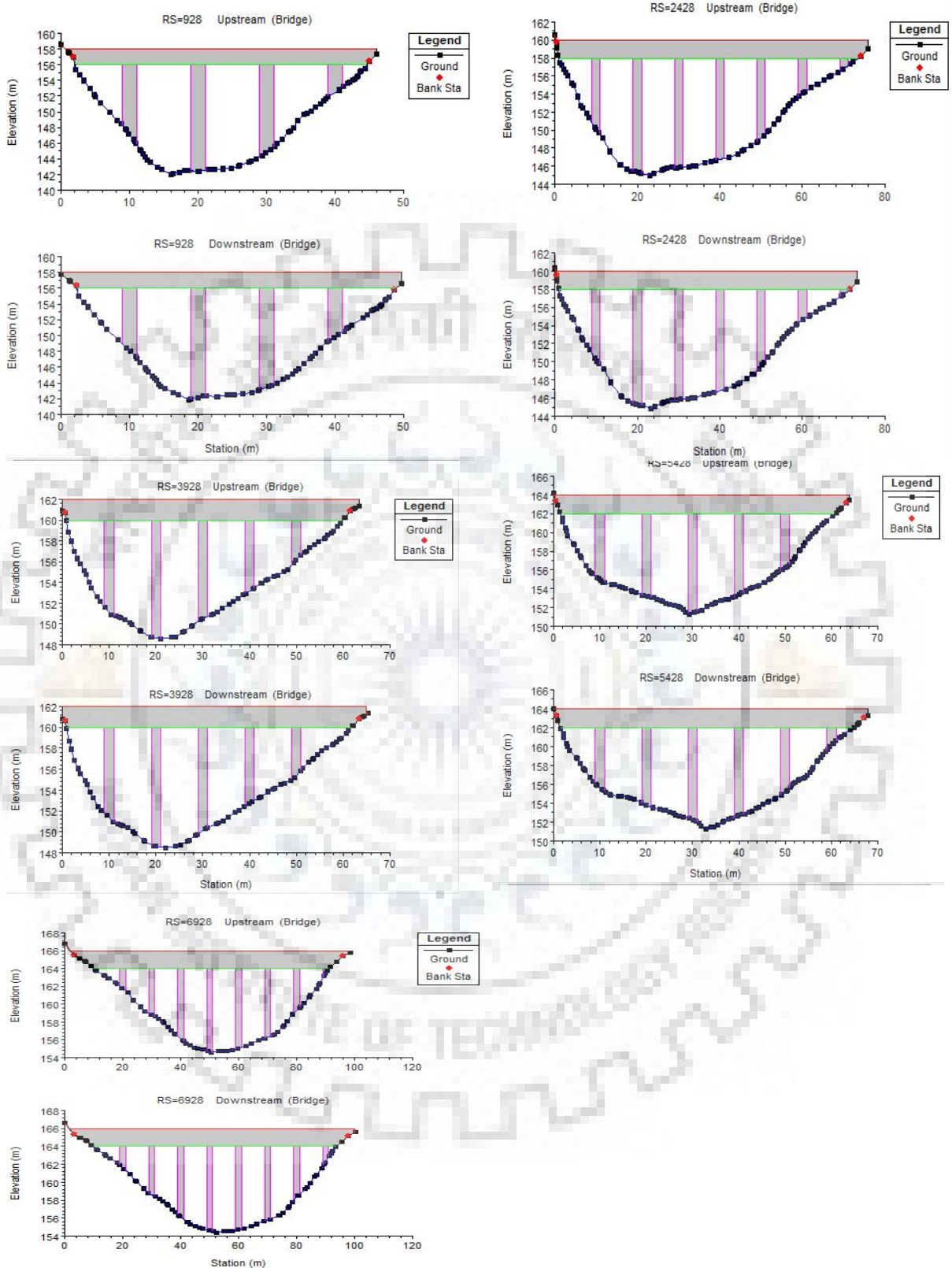


Figure 1.5: Cross Sections at Bridge Locations (River Stations 928, 2428, 3928, 5428 and 6928 m)

1.5 ORGANIZATION OF THESIS

Chapter 1: Describes the General Background of the Study and the importance of the topic. The chapter also includes the Objectives of the study, Research gaps/rationale and the description of the Study area.

Chapter 2: Discusses about HEC –RAS and its hydraulic capability in Bridge Modelling. This chapter also includes Literatures Review by different authors based on the water surface profiles in the natural channels.

Chapter 3: Discusses the materials and method adopted for the hydraulic simulation of flow at bridge locations. This chapter also includes methodology adopted for HEC-RAS model setup, Calculation and Results extraction for no bridge condition and its comparison with the bridge provided condition. It also covers the variation of Water Surface Profiles with and without bridge condition (five bridges in series) including graphs and tables and finally the results are analyzed for the various bridges in the river Alaknanda.

Chapter 4: The overall summary and conclusions are derived from the analysis, and future scope of work presented in this chapter.

SELECTION OF MATHEMATICAL MODEL

2.1 INTRODUCTION

In this study, a popular and well known model namely, Hydrologic Engineering Center’s River Analysis System (HEC-RAS) is used for Hydraulic simulation of flow around the bridge in the rivers. This model is developed by the U.S. Army Corps of Engineers and it allows performing one-dimensional steady, unsteady flow hydraulics, sediment transport/mobile bed computations for quantifying the effects of new structures and their operation in the river. HEC-RAS is an integrated system of software, designed for interactive use in a multi-tasking, multi-user network environment. The system is comprised of a graphical user interface (GUIC), separate hydraulic analysis components, data storage and management capabilities, graphics and reporting facilities. The HEC-RAS system contains many one-dimensional river analyses including the components for:

- (1) Steady flow water surface profile computations;
- (2) Unsteady flow simulation and
- (3) Movable boundary sediment and transport computations.

A key element is that all the components use common geometric data representation and common geometric and hydraulic computation routines. In addition to the three river analysis components, the system contains several hydraulic design features that can be used in the water surface profiles computation.

2.2 HYDRAULIC CAPABILITY OF HEC – RAS

General Capability of the HEC-RAS is to calculate the water surface profiles for steady and gradually varied flow. The system can handle a single river reach or a full network of channels. The steady flow component is capable of modeling subcritical, supercritical and mixed flow regime water surface profiles. The computational procedure is based on the solution of the one-dimensional energy equation. Energy losses are evaluated by friction (Manning's equation) and contraction/expansion (coefficient multiplied by the change in velocity head). The momentum equation is utilized in situations where the water surface profile is rapidly varied. These situations include hydraulics of bridges and evaluating profiles at river confluences (stream junctions). The effects of various obstructions such as bridges and other structures on the flood plain are considered in the computations. The steady flow system is designed for application in floodway encroachments. Also, capabilities are available for assessing the change in water surface profiles due to channel improvements, and levees. Unsteady Flow Simulation component of the HEC-RAS modeling system is capable of simulating one dimensional unsteady flow through a full network of open channels. The hydraulic calculations for cross-sections, bridges, and other hydraulic structures that had been developed for the steady flow component are incorporated into the unsteady flow module. Additionally, the unsteady flow component has the ability to model storage areas and hydraulic connections between storage areas as well as between stream reaches. Sediment Transport/Movable Boundary Computations component of the modeling system is intended for the simulation of one dimensional sediment transport/movable boundary calculations resulting from scour and deposition over moderate time periods; typically days, months or years. Applications to single flood events are also possible. The sediment transport potential is computed by grain size fraction, thereby allowing the simulation of hydraulic sorting and armoring, if the case be. The model is designed to simulate long-term trends of scour and deposition in a stream channel that might result from modifying the frequency and duration of the water discharge and stage or modifying the channel geometry.

Here, the water surface profile determination and plotting is done with HEC-RAS for steady flow and mixed regime condition for without and with bridge condition with contraction and expansion coefficients of 0.1 and 0.3 respectively. Also for the bridges in

series, the water surface elevations are determined with energy and momentum method taking the shape, size, nos. of piers and lengths of contraction and expansion reach just upstream and downstream sides of bridge (s).

2.3 HEC – RAS IN BRIDGE MODELLING

HEC-RAS, is one of the mostly widely used computer program for bridge modelling and is one dimensional hydraulic analyses program with water surface elevation computation. The basic computational procedure in HEC-RAS is based on solving the one dimensional energy equation. Energy losses are accounted for by friction (Manning's equation) and contraction/expansion (coefficient multiplied by the change in velocity head). The momentum equation is utilized in situations where the water surface profile is rapidly varied. These situations include mixed flow regime calculations (i.e., hydraulic jumps), hydraulics of bridges, and evaluating profiles at river confluences (stream junctions). Scour occurring at bridge crossing generally include three components: 1) Long-term aggradation and degradation of the river bed, 2) general scour at bridge (including contraction scour and other general scour), and 3) local scour at the piers or abutments. Local scour in bridge piers (Kothyari 2007, Mazumder 2008) occur due to obstruction by pier and pier foundation and the consequent changes in the flow field around the piers. Because of variation in velocity from top to bottom of a pier, the stagnation pressure head is the highest at top and lowest at the bottom of pier, thereby inducing a pressure gradient, since the potential head is highest at the top and lowest at the bottom of the pier. This causes a downward vertical flow impinging the bed. At the pier base, two horse-shoe vortices develop due to flow separation. It is primarily due to the vortex formation and the downward flow impinging on the bed that causes scour at the base of the pier. Here only the effect of pier shape, size, spacing, contraction and expansion widths on water surface profile has been considered rather than the scour.

2.4 LITERATURE REVIEW

Various literatures available in the different sources can be reviewed thoroughly as below:

Kocaman Selahattin et al., (2014)

Accurate estimation of flow characteristics at and around bridge locations is main concern for the bridge engineers both in terms of stability of bridge itself and the problems caused by insufficient hydraulic design of it such as flooding due to the sudden increase in water level upstream.

Depending on the flow situation, estimation of these characteristics can be difficult. Flow in a compound channel is an example of such flow situation as there is a strong transfer of longitudinal momentum from the fast moving flow in the main channel to the slow-moving flow in the floodplain. This transfer is more pronounced at the interface between the floodplain and the main channel.

The complexity of flow can increase by placing hydraulic structures such as abutments and piers, which block the part of flow area. In such conditions, rapidly varied flow develops near the structures due to the presence of the obstruction. Consequently, the flow is separated downstream of the structure and a reverse flow and an adverse pressure gradient occur. The water surface upstream of the structure increases and forms a backwater profile. A jet is generally established in the bridge opening and continues into the region of expansion immediately downstream of the bridge, where there is a strong turbulent diffusion and mixing as well as a large amount of energy losses.

In the case of a bridge pier, occurrences of a horseshoe vortex in front of the pier and lee-wake vortices behind it increase the complexity and are very important for the scour and scour protection studies. Similar flow pattern can be observed for the bridge abutments. Development of scour has to be well understood by bridge engineers as most of the bridge failures occur due to the local scour, which is highly correlated with the flow processes, around bridge piers and abutments. Moreover, a significant amount of problems caused by bridge constructions is corresponding to the backwater. It is essential to estimate the increase in the water surface level due to bridge constrictions especially in flood conditions. Maximum backwater height called afflux is also one of the key parameters in bridge design.

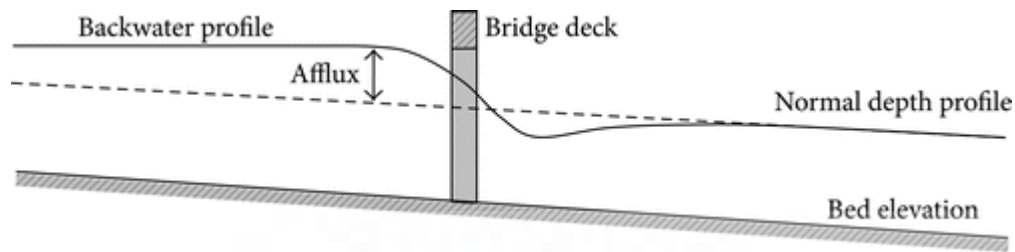


Figure 2.1: Definition sketch of flow through a bridge constriction.

The water surface profiles obtained from different flow conditions show similar trends; they rise upstream, forming backwater profiles and show a sudden drop through the bridge contraction. Later, they are fluctuated further downstream and reach normal depth downstream of the channel. As can be seen, reasonable agreement between the measured and computed water surface profiles was captured in the upstream directions of the bridges.

The maximum increase in water level above the normal unobstructed level due to the constriction is known as afflux (maximum backwater). It occurs along the upstream region of the bridge constriction at a distance which is approximately equal to bridge opening. Accurate estimation of the afflux is the main objective in the design of a bridge construction and studies regarding backwater calculation.

Bridges act as an obstruction against river flow, resulting in alteration of the flow characteristics and a change in the original geometry of the nearby river bed. In subcritical flow, one typical kind of flow alteration caused by bridges is the back-water phenomenon, which results in an increase in the water surface level upstream and a reduction downstream of the bridge; a wide longitudinal extent of the river reach is also affected. The interaction between bridge obstruction and river flow increases flooding risks and thus the probability of bridge damage, traffic disruption, loss of human life and economic losses. Researching the influence of bridges on flood control is therefore of critical importance.

The variation in the water surface level and the extent of the backwater-affected river reach are highly dependent on the river section, bridge geometry and characteristics of the flow and the floodplain (Luigia and Kebede, 2013). Many methods for investigating the backwater at bridge crossing sections have been developed. Yarnell (1934) developed the most widely used empirical equation for calculating the increase in water level caused by bridge piers. In that study, 2600 experiments were carried out considering the influence of several parameters on the afflux, including the shape of the piers, the width, the length, the angle and the flow rate. However, Yarnell (1934) did not compare the equation developed with the large amount of data collected through the experiments. Moreover, Yarnell's experiments involved a relatively small percentage of circular columns, which are now a commonly used pier shape. Through experimental studies using a large physical model, Charbeneau and Holley (2001) developed a new equation including a further two parameters as a modification of the equation proposed by Yarnell (1934). Suribabu et al. (2011) also suggested a modified equation, including one more parameter. Regrettably, neither of these two modifications gave a clear physical explanation of the newly added parameters in the equations. Charbeneau and Holley (2001) also reported that the length of the two-dimensional mound of water immediately upstream of a bridge pier is no greater than the channel width.

Salah El-Alfy Kassem et al., 2009: The flow constriction due to piers of Road bridges results in producing backwater rise upstream such bridges, especially at floodplain periods. This backwater rise depends mainly on both flow properties and geometrical characteristics of piers. In the research, the backwater rise due to bridge piers was experimentally investigated for extreme ratios of piers thickness to channel width (t_{ps}/B) under a wide range of both subcritical and supercritical flow conditions between bridge piers. The backwater rise upstream bridge piers depends mainly on both flow type between piers and constriction ratio, while it is secondary depends on geometrical shape of pier end noses. Also, the experimental results illustrates that the backwater rise at supercritical flow conditions between piers agreed satisfactory with the corresponding computed values from the most widely relationships published by Yarnell than that for subcritical flow conditions between piers. The results of the backwater rise due to constriction of flow by bridge piers presented in his research paper are employed in development of two formulas, which could be used in computing backwater rise at both subcritical and supercritical flows between bridge piers.

Seckin et al. (2009a, 2009b) applied artificial neural network techniques to derive a regression-based formula for estimating bridge backwater based on laboratory and field data.

In many countries, rapid economic development has led to a sharp increase in traffic volume, thus requiring the construction of additional bridges across rivers and canals. Such construction could cause interactions with existing bridges and affect the characteristics of river flow and sediment motion (Wang et al., 2016a, 2016b). Most of the studies considered single bridges or piers, and little research considering the backwater of a group of bridges has been reported.

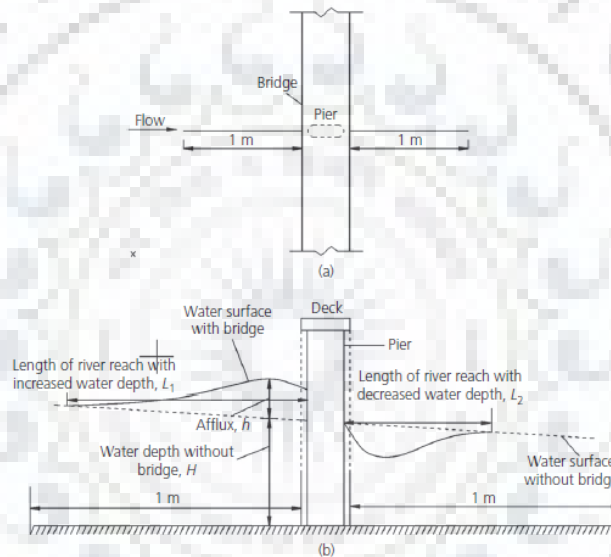


Figure 2.2: Measurement of the backwater of the bridges: (a) plane view; (b) side view

Peck W. W. et al., (2001).

It was found that transition reach lengths recommended by HEC-RAS documentation were the most accurate, and recommendations made as part of the HEC-2 program result in over calculation of water surface elevations. It was also found that use of the energy method for bridge calculations during high flow events which experience only pressure flow results in calculated water surface elevations that are much higher than observed data indicates.

In 1976 the Corps Hydraulic Engineering Center (HEC) introduced HEC-2 'Water Surface Profiles' (HEC, 1982). This computer program was designed to compute water surface

elevations along a stream or river reach. It was designed to accommodate bridges, culverts, dams, and weirs, as well as unconfined reaches.

HEC-2 provided two methods for computing flow profiles through bridges: the normal bridge and special bridge methods.

The normal bridge method computes a water surface profile through bridges by use of the energy equations and the standard step method. This method assumes energy losses are caused by flow contraction and expansion upstream and downstream of the bridge, and by friction. Water surfaces are computed by use of the standard step method while energy losses are added at the required places. Empirical methods are used to compute losses due to contraction and expansion of flow and friction losses are computed using Manning's n factor. The normal bridge method requires six river cross-sections to compute a water surface profile through the bridge.

The special bridge method uses a method developed by Yarnell for factoring in the hydraulic effects of bridge piers. This empirical method was developed based upon over 2,100 flume experiments utilizing various shapes and sizes of bridge piers. Based upon these experiments, pier coefficients were developed to account for the most common shapes of bridge piers. This method requires only four cross-sections for computations. The bridge opening is approximated by a trapezoid.

The Corps was quick to take advantage of this technological improvement. In 1995 HEC introduced the River Analysis System (RAS) (HEC, 1995). HEC's stated intention is for RAS to replace HEC-2. RAS provides capabilities similar to HEC-2. The major improvement however, is the addition of a graphical user interface. While requirements for data input by the user are similar between HEC-2 and RAS, the graphical capabilities of RAS provide great assistance in detecting bugs and errors in data input. Graphic capabilities for output data are much improved as well. Users can plot cross-sections and bridges and overlay water surface elevations as needed. This provides extensive help in visualizing situations and comparing alternatives. RAS also provides improved computation methods based upon new advances in hydraulic engineering theory since the introduction of HEC-2.

Due to its increased flexibility and user-friendly graphics, RAS is becoming the method of choice for hydraulic bridge design. Based upon an informal survey conducted by the author of state Departments of Transportation in the southeast United States, WSPRO was the software of choice for the 1980's and early 1990's. The majority of state DOTs contacted are now using or considering the use of RAS for bridge designs.

Extensive documentation concerning RAS is available from HEC. An experienced RAS user will find the Hydraulic Reference Manual (HEC, 1997) the most useful of these. HEC provides a detailed discussion of the theory of RAS in this manual. It also contains recommendations for dealing with various modeling situations the user may encounter. Further details and discussion can be found within the course notes provided as part of RAS training classes offered by HEC and the National Highways Institute.

While HEC (1997) provides an overview of RAS's application of the WSPRO method, Sherman et.al. (1986) discuss the WSPRO methodology in detail as it was originally implemented. Shearman provides theoretical background and data requirements for using this method for bridge analysis.

Shearman also provides charts and tables for assistance in determining the discharge coefficient (K') which is required for the WSPRO analysis method. The concept of the discharge coefficient was first presented by Kindsvater, Carter, and Tracy (1953) for use in indirect measurement of flow through bridges. The authors present four categories of bridge constriction based upon the type of bridge abutment and roadway embankment. The base coefficient is determined based upon the type of bridge opening and the degree of floodplain constriction caused by the bridge. The base coefficient is then modified for several factors based upon charts developed empirically from laboratory data. These charts were later modified by Matthai (1967) to reflect additional data.

Brunner and Hunt (1995) performed a comparison of RAS, WSPRO, and HEC-2. Their study contains a discussion of the similarities and differences of the fundamental computational methods of each. Using a sample consisting of thirteen bridge sites located in Louisiana, Alabama, and Mississippi with seventeen flood flows they determined the mean average absolute error for each computation method by comparing calculated water surface elevations

to observed field data. Based on these results they concluded that all three programs computed water surface elevations "within the tolerances of observed data".

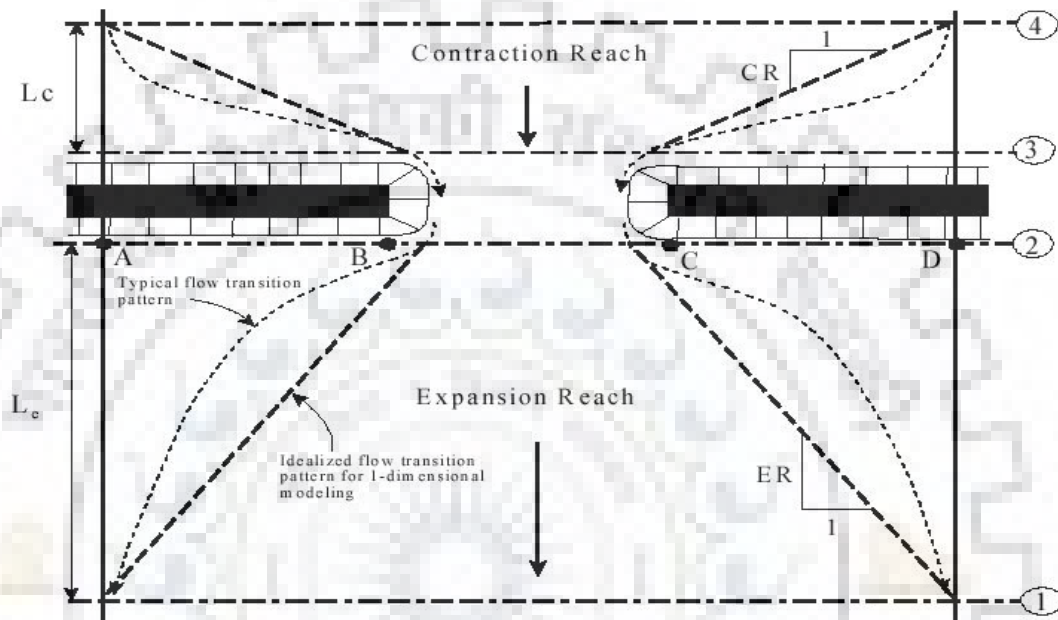
Biery and Delleur et al., (1962) developed a method for the prediction of the afflux at bridges based on laboratory studies using rectangular channels. However, it was found this method could lead to errors when applied to compound channels (Atabay et. al., 2008a, 2008b). Many other laboratory and field studies (Kaatz and James, 1997; Seckin, 2004; Seckin et. al., 1998) have shown that the energy equation used by the bridge sub-routine in HEC-RAS (Hydrologic Engineering Center River Analysis System) (HEC, 2002) is capable of producing accurate estimates of water surface levels in river reaches constricted by bridges. However, considerable inaccuracies may arise in its application depending on the parameters chosen by the user (Seckin et. al., 2007). Raju et al. (1983) used experiments to investigate the effect of blockages on the drag coefficient of circular cylinders and obtained a relationship between the energy loss, afflux and drag force.

The Bridge Reach

One element common to nearly all literature concerning bridge hydraulics is the concept of the bridge reach. The bridge reach is the portion of the river that contains the bridge. It is normally defined by a four to six cross-sections. Energy losses within the bridge reach are greater and much harder to predict than in an unstricted river reach. As a consequence, water surface elevations may vary greatly within the bridge reach.

The Corps (1959) divides the bridge reach into three sections based upon the primary method of energy loss. These are the transition length downstream of the bridge crossing, the transition length upstream of the bridge crossing, and the width of the bridge. The Corps concluded that energy losses in the downstream reach are primarily due to expansion as the active flow area expands from the constricted bridge area to the larger unstricted floodplain flow area. This downstream transition is referred to as the expansion reach. Losses in transition area upstream of the bridge are caused by contraction of the active flow area from the large floodplain into the smaller bridge area. This upstream bridge reach is called the

contraction reach. Losses within the bridge area itself are due primarily to friction, impact, and eddies caused by the bridge piers and abutments. Exact computation of losses in the bridge length depends upon the method used. Figure below illustrates the sections of the bridge reach **Figure 2.3** below.



As previously mentioned, a bridge reach is defined by a minimum of four cross-sections. The most downstream cross-section is located at the point where the active flow area has expanded to the full, unconfined floodplain width. This is called the exit section (1).

The most upstream section is located at the point where flow is just about to begin to contract from the full floodplain width to the width of the constricted bridge opening. This is referred to as the approach section (4).

When modeling a bridge, it is generally advisable to include cross-sections some distance upstream and downstream of the bridge reach. This ensures that all other influences on the local water surface elevations are included.

Cross-section Spacing

Spacing of cross-sections within a hydraulic model is an issue of some importance. HEC and FHWA recommend that cross-sections be placed where the channel experiences some significant change (i.e. sudden channel widening or constriction). RAS has built-in provisions for monitoring this and a successful RAS run can often have numerous warnings concerning cross-section spacing. A large change in depth, conveyance, or velocity head triggers a warning to the user that cross-section spacing may be too great.

There is some discussion as to how often cross-sections should be placed. In the comparison of modeling software types Brunner and Hunt (1995) find location of cross-sections to be more important than the type of model used, however, they do not provide guidance concerning this. Gates et al. (1998) performed a study of this issue. Numerous cross-sections on a river reach were surveyed. They then did a statistical analysis of how the various cross-section properties varied with different sampling resolutions. Average slope, cross-section area, and other hydraulic parameters were determined using cross-sections at various spacing resolutions. Average slope was shown to vary significantly when using small spacing increments, but this stabilized quickly at larger increments. They also found that differences in elevations over long distance appear to be influenced by large-scale trends, but differences over small distances appear to be nearly random.

Selection of Bridge Modeling Method

RAS provides four different methods for modeling bridges in low-flow situations, and two for bridges in high-flow situations.

RAS documentation (HEC, 1997) provides the following guidelines for selection of a low flow modeling method:

- ✓ Where losses are predominately friction and piers are a small obstruction, the energy, momentum and WSPRO methods may all be used accurately.
- ✓ Where pier losses are experienced in addition to friction, the momentum method is recommended.
- ✓ The Yarnell and WSPRO method are capable of modeling only subcritical flow. The energy or momentum methods must be used if flow passes through critical depth within the bridge reach.

- ✓ For supercritical flow, the momentum method is recommended where pier impact and drag losses are large.
- ✓ At bridges where piers are the major cause of energy loss the Yarnell and momentum methods are best.
- ✓ During high flows, when flow through the bridge is not pressurized the energy method is recommended.
- ✓ When the bridge deck and roadway embankments are a large obstruction the pressure and weir method should be used.
- ✓ When flow over the bridge and embankment is large, the energy method is best.

Various methods concerning the selection of bridge modeling methods are available in the literatures. The most valid method for each bridge site will be determined by comparing results of all methods to observed data. These results should provide some recommendations for selection of low and high flow methods.

Johnson et al. pointed out that bridge piers, bridge abutments, and roadway embankments all create local obstructions that cause the flow to become highly three-dimensional. In fact, it is believed that any vertical obstruction in a channel makes formerly unidirectional flow become highly three-dimensional. Biglari and Sturm have also recommended using 3D model in order to capture the local flow characteristics causing local scour around bridge abutments.

One-dimensional numerical models have been widely used for prediction of water surface profile around bridges such as HEC2, HECRAS, ISIS, and MIKE11. Alternatively, Mantz and Be on developed two one-dimensional analytical models, namely, Afflux Estimator (AE) for more detailed analysis of the water surface profiles and Afflux Advisor (AA) for the rapid estimate of the afflux rating. They verified their models with the experimental data used in their study and a large-scale field data.

HYDRAULIC SIMULATION OF FLOW THROUGH HEC-RAS

3.1 INTRODUCTION

Though there are various methods like Standard Step Backwater Method, Afflux Estimator Models with consideration of expansion and contraction losses etc. available, Water Surface Profile in this case is calculated using the HEC-RAS programs for effective and better results.

Water Surface Profiles are computed from one cross section to the next by solving an energy equation with an iterative procedure called Standard Step Method. The Energy Equation can be written as follows.

$$Z_2 + Y_2 + (\alpha_2 V_2^2 / 2g) = Z_1 + Y_1 + (\alpha_1 V_1^2 / 2g) + h_e \dots\dots\dots (1)$$

Or, $WS_2 + (\alpha_2 V_2^2 / 2g) = WS_1 + (\alpha_1 V_1^2 / 2g)$

Where, WS_1 and WS_2 = Water Surface Elevations at sections 1 and 2 resp.

V_1 and V_2 = Average velocities

α_1 and α_2 = Velocity weighting coefficients

g = Acceleration due to gravity

h_e = Energy head loss

A diagram showing the terms of the energy equation is shown below:

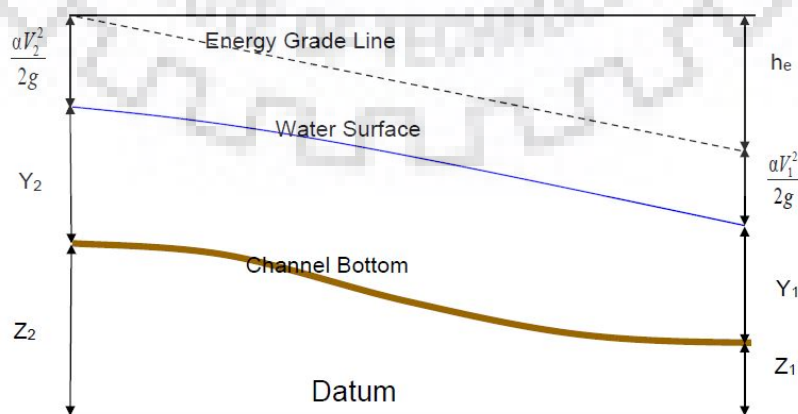


Figure 3.1: Representation of Terms in the Energy Equation

The energy head loss (h_e) between two cross section is comprised of friction losses and contraction or expansion losses. The equation for the energy head loss is as follows:

$$h_e = LS_f + C \left| \alpha_2 V_2^2 / 2g - \alpha_1 V_1^2 / 2g \right| \dots\dots\dots(2)$$

Where, L = Discharge weighted reach length

S_f = Representative friction slope between two sections

C = expansion or contraction loss coefficient

The unknown water surface elevation at a cross section is determined by an iterative solution of equations 1 and 2. The computational procedure is as follows:

1. Assume a water surface elevation at the upstream cross section (or downstream cross section if a super critical profile is being calculated).
2. Based on the assumed water surface elevation, determine the corresponding total conveyance and velocity head.
3. With values from step 2, compute S_f and solve equation 2 for h_e .
4. With values from step 2 and 3, solve equation 1 for WS_2 .

Compare the computed value of WS_2 with the value assumed in step 1; repeat steps 1 through 4 until the values agree to within 0.01 feet (0.003 m), or the user defined tolerance.

The criterion used to assume water surface elevations in the iterative procedure varies from trial to error. The first trial water surface is based on projecting the previous cross section's water depth on to the current cross section. The second trial water surface elevation is set to the assumed water surface elevations plus 70% error from the first trial (computed water surface – assumed water surface). The third and subsequent trials are generally based on a 'Secant' method of projecting the rate of change of the difference between computed and assumed elevations for the previous two trials.

For a sub-critical profile, a preliminary check for proper flow regime involves checking the Froude number. The program calculates the Froude number of the balanced water surface for both the main channel and the entire cross section. If either of these two Froude numbers are greater than 0.94, then the program will check the flow regime by calculating a more accurate estimate of critical depth using the minimum specific energy method. A

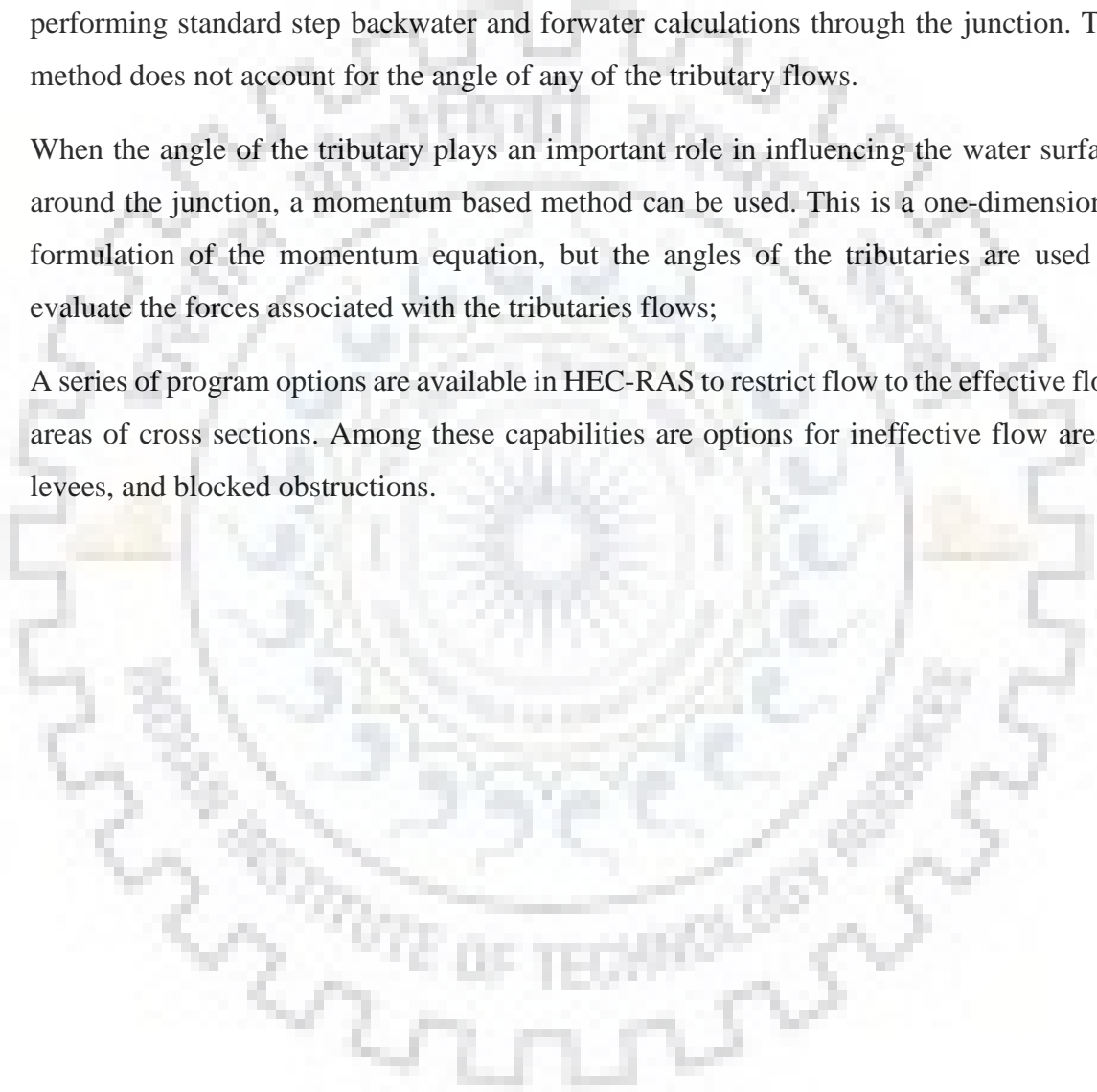
Froude number of 0.94 is used instead of 1, because the calculation of Froude number in irregular channels is not accurate.

For a super critical profile, critical depth is automatically calculated for every cross section, which enables a direct comparison between balanced and critical elevations.

Stream junctions can be modelled in two different ways in HEC-RAS. The default method is an energy based solution. This method solves for water surfaces across the junction by performing standard step backwater and forwater calculations through the junction. The method does not account for the angle of any of the tributary flows.

When the angle of the tributary plays an important role in influencing the water surface around the junction, a momentum based method can be used. This is a one-dimensional formulation of the momentum equation, but the angles of the tributaries are used to evaluate the forces associated with the tributaries flows;

A series of program options are available in HEC-RAS to restrict flow to the effective flow areas of cross sections. Among these capabilities are options for ineffective flow areas, levees, and blocked obstructions.



3.2 METHODOLOGY/FLOW – CHART

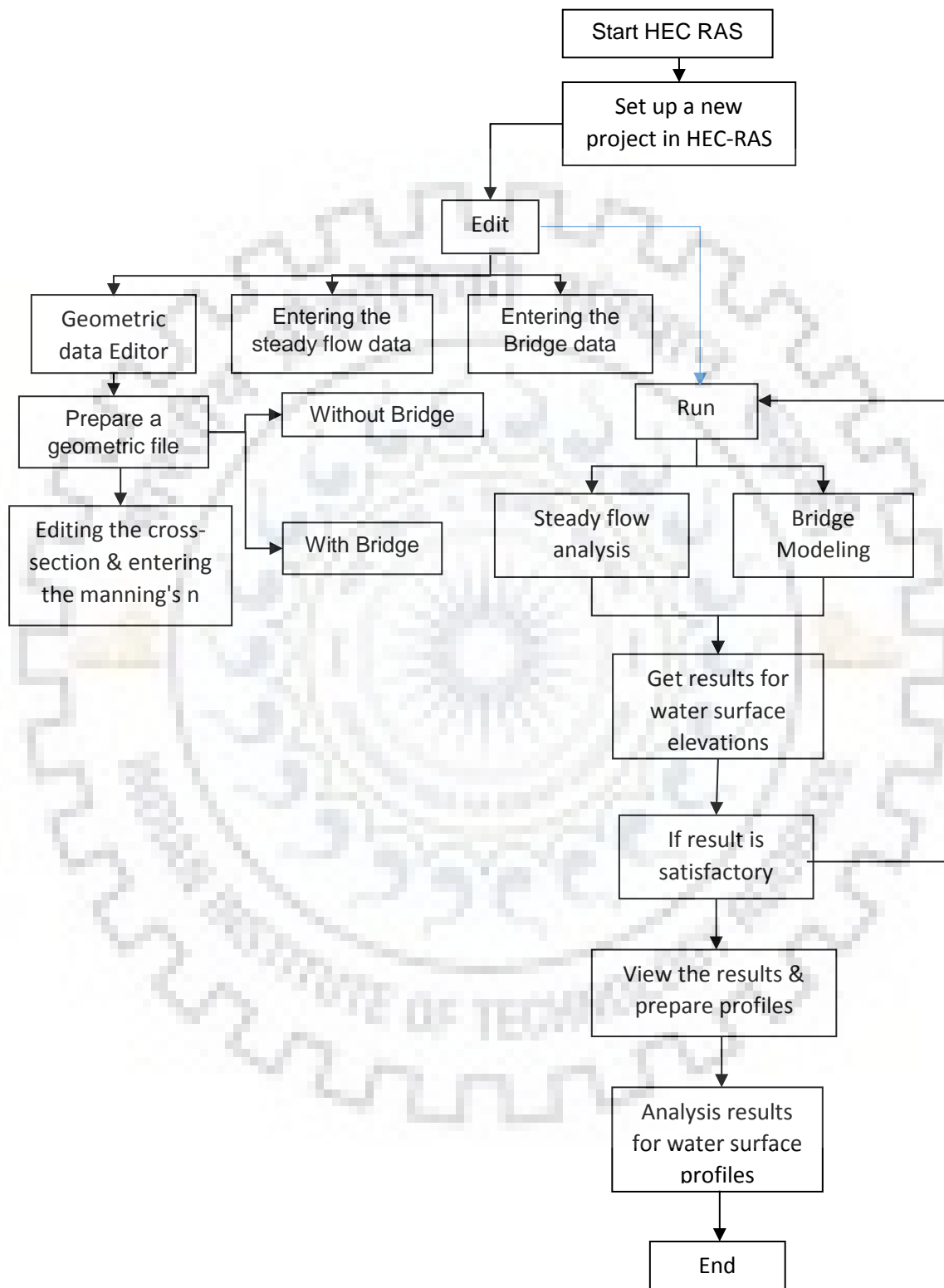


Figure 3.2: Methodology through HEC – RAS

Here, HEC-RAS is adopted for determining water surface elevation and then water surface profiles are plotted either using the same or through Microsoft Excel spreadsheet. The programming uses two types of data namely, River data and Bridge data. The river data includes river cross section, geometry of section, flow data like discharge, boundary condition etc. whereas the bridge data includes the deck size, shape and sizes of piers, nos., spacing, expansion and contraction reach lengths etc. The Bridge data are used for bridge modelling which are necessary for the water surface elevation. After getting the water surface elevation one can easily determine or plot the water surface profiles which are closely interrelated with the flow area, velocity at the section of measurement, Froude no. etc.

After getting the River data and Bridge data, they are entered in to the HEC-RAS programming and data analysis is done. The analysis is done for Steady flow along with Bridge modelling condition. For steady flow we use 200, 400, 600, 800 and 1000 cumecs adopting mixed regime flow with 0.012 as boundary condition. For bridge modelling, deck width 10.0 m in the direction of flow is taken. Also we use the pier size of 2.0, 2.5 and 3.0 m for the simulation. Similarly pier spacing of 10.0, 15.0 and 20.0 m is used in the analysis. For the analysis of results for pier shape we use different pier coefficients (coefficients of discharges C_d) from 0.60 to 2.00 for various pier shapes. Also to find out the effects of contraction and expansion widths due to bridge we use the equal contraction and expansion width 20.0, 25.0, 30.0 and 35.0 m at the upstream and downstream of the bridge section and the water surface elevations are noted for the section at 50.0 m upstream and downstream of the bridge axis. For various cases we vary Manning's coefficient from 0.025 to 0.045 for different types of soils as waterway of river may contain different types of soils having different n .

3.3 PREPARATION AND RUN HEC-RAS MODEL

For the preparation of one dimensional HEC-RAS model for steady flow analysis, following two types of data are entered as described below and the model run accordingly.

3.3.1 Geometric Data

- ✓ River Cross - Section data obtained from DEM image using ArcGIS for 10 km river reach at 500 m interval has been entered.
- ✓ The river cross sections is then interpolated at every 50 m intervals.
- ✓ Bridge data at different locations are not available, so bridges are assumed to be located at different locations for bridge modelling (i.e. bridges are located at 928 m, 2428 m, 3928 m, 5428 m and 6928 m chainage of river reach length).

3.3.2 Flow Data

- ✓ Flow regime is considered as a Mixed Regime (supercritical, subcritical and mixed).
- ✓ Steady flow 200, 400, 600, 800 and 1000 m³/sec has been used for steady flow analysis.
- ✓ Water Surface Elevations for different cases of steady flow (discharges) with variation of different parameters (i.e. water surface elevation vs Manning's coefficient n, water surface elevation vs velocity, water surface elevation vs flow area, velocity vs flow area, velocity vs Froude no. (Fr), Fr vs n, velocity vs n) at the upstream and downstream side of the **proposed bridge location (with no bridge condition)** obtained from HEC-RAS are then plotted in graphs to find the water surface profiles.
- ✓ Similarly, Water Surface Elevations for different cases of steady flow (discharges) with variation of different parameters (i.e. water surface elevation vs Manning's coefficient n, water surface elevation vs velocity, water surface elevation vs flow area, velocity vs flow area, velocity vs Froude no. (Fr), Fr vs n, velocity vs n) at the upstream and downstream side of the **bridge location (with bridge condition) for single and multiple bridges** as obtained from HEC-RAS are then plotted in graphs.
- ✓ Since there is no observed afflux due to bridge piers is available, afflux obtained from HEC-RAS is to be used for Water Surface Profile determination for single and multiple bridges.
- ✓ Afflux obtained after placing the bridges are then compared with no bridge conditions.

- ✓ Steady flow for Single and Multiple bridges and their backwater effect has been analyzed.

Suggested values for the Manning roughness coefficient for designing soil and water conservation earthworks, such as grassed waterways, grade banks and shallow relief drains for various waterways are given below.

Typical values for Manning's coefficient n for different types of waterways are:

Waterway type - bare soil	Minimum	Design Value	Maximum
Fine sand colloidal	-	0.020	-
Sandy loam non colloidal	-	0.020	-
Loam	-	0.020	-
Fine gravel > 2 mm	-	0.020	-
Coarse gravel < 60 mm	-	0.025	-
Low Plasticity (stiff) clay	-	0.025	-
Soils with stony surface - rounded	-	0.035	-
Soils with stony surface - angular	-	0.040	-

Waterway type - grassed, constructed waterway, in sand to fine gravel soils	Minimum	Design Value	Maximum
Average depth of flow is 2 or more times grass height	0.025	-	0.030
Average depth of flow is 1 to 2 times grass height	0.030	-	0.040
Average depth of flow is similar to grass height	0.045	-	0.070
Average depth of flow is less than one half grass height	0.070	-	0.120

Waterway type - grassed, constructed waterway, with pasture species	Minimum	Design Value	Maximum
Average depth of flow greater than height of grass	-	-	-
Low grass (<250mm)	0.025	0.030	0.035
Tall grass (250–500mm)	0.030	0.035	0.050

Waterway type - grassed, constructed waterway, in stiff (low plasticity) clay and coarse gravel soils	Minimum	Design Value	Maximum
Average depth of flow is 2 or more times grass height	0.030	-	0.035
Average depth of flow is 1 to 2 times grass height	0.035	-	0.045
Average depth of flow is similar to grass height	0.050	-	0.075
Average depth of flow is less than one half grass height	0.075	-	0.125

Waterway type - minor natural streams <30m wide	Minimum	Design Value	Maximum
Straight bank, full stage, no rifts (shallow stony sections) or deep pools	0.025	0.030	0.033
Straight bank, full stage, no deep pools, some weeds and stones	0.030	0.035	0.040
Winding bank, some pools and shoals	0.033	0.040	0.045
Winding bank, some pools, shoals, weeds and stones	0.035	0.045	0.050
Light shrubs and trees – natural vegetation	0.040	0.060	0.080
Medium to dense shrubs and trees – natural vegetation	0.070	0.100	0.160
Scattered shrubs, grasses and weeds – degraded natural vegetation	0.035	0.050	0.070

Waterway type - major natural streams >30m wide	Minimum	Design Value	Maximum
Regular cross-section with no boulders or shrubs	0.025	-	0.060
Irregular and rough cross-section	0.035	-	0.100

Table 3.1: Manning's coefficient n for various types of soils and waterways

After analyzing the above values of Manning's coefficient n we take the value for River waterway type (**major natural streams >30m wide**) as varying from 0.025 to 0.045 for water surface elevation determination in HEC-RAS programming.



3.4 CALCULATION AND RESULT EXTRACTION

3.4.1 WITH NO BRIDGE CONDITION

3.4.1.1 Variation of Water Surface Profiles with Manning's coefficient n

u/s RS 953					d/s RS 903				
WSE (m)	Velocity (m/s)	Flow area m^2	Fr	n	WSE (m)	Velocity (m/s)	Flow area m^2	Fr	n
145.43	4.41	45.31	0.93	0.025	145.27	4.26	46.94	0.91	0.025
145.76	3.85	51.95	0.77	0.03	145.61	3.7	54.09	0.75	0.03
146.05	3.45	57.91	0.66	0.035	145.89	3.31	60.37	0.65	0.035
146.3	3.16	63.31	0.59	0.04	146.14	3.03	66.02	0.57	0.04
146.54	2.93	68.33	0.53	0.045	146.36	2.81	71.28	0.52	0.045

Table 3.2: For No Bridge Condition and $Q = 200 \text{ m}^3/\text{sec}$

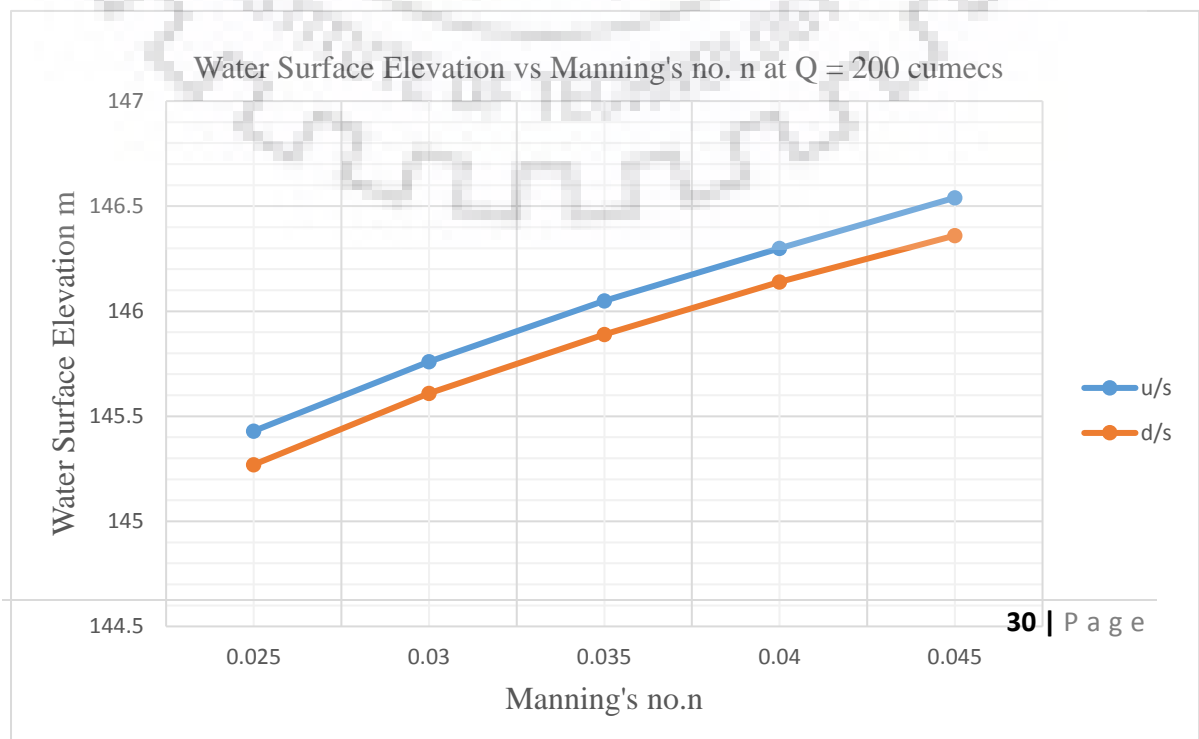


Figure 3.3: Water Surface Elevation vs Manning's no. n

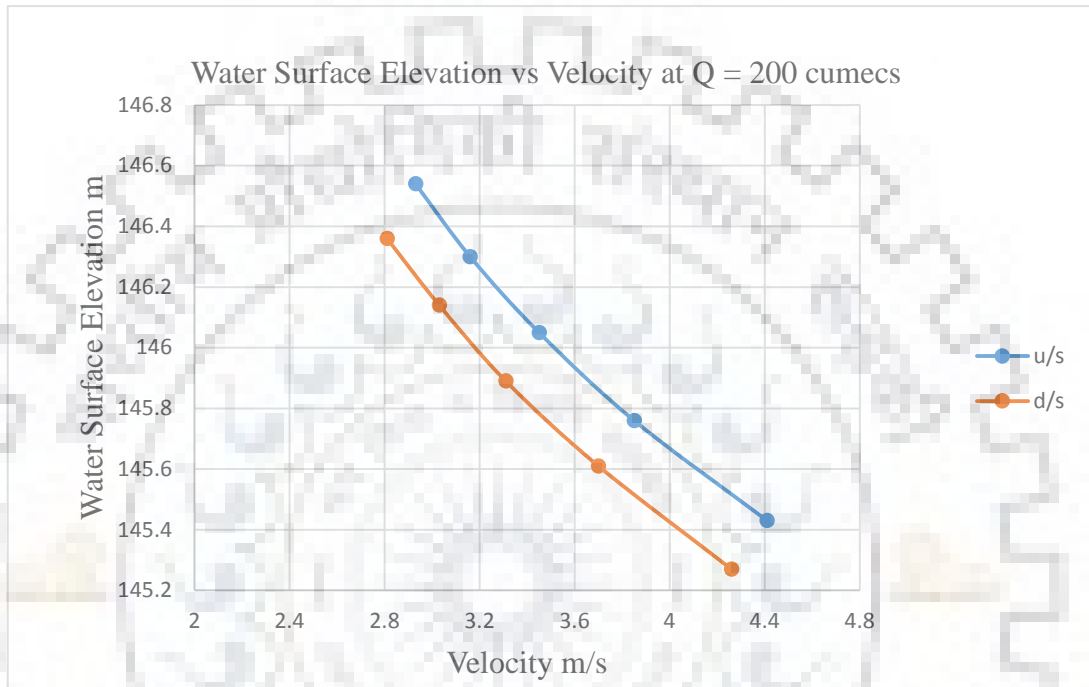


Figure 3.4: Water Surface Elevation vs Velocity

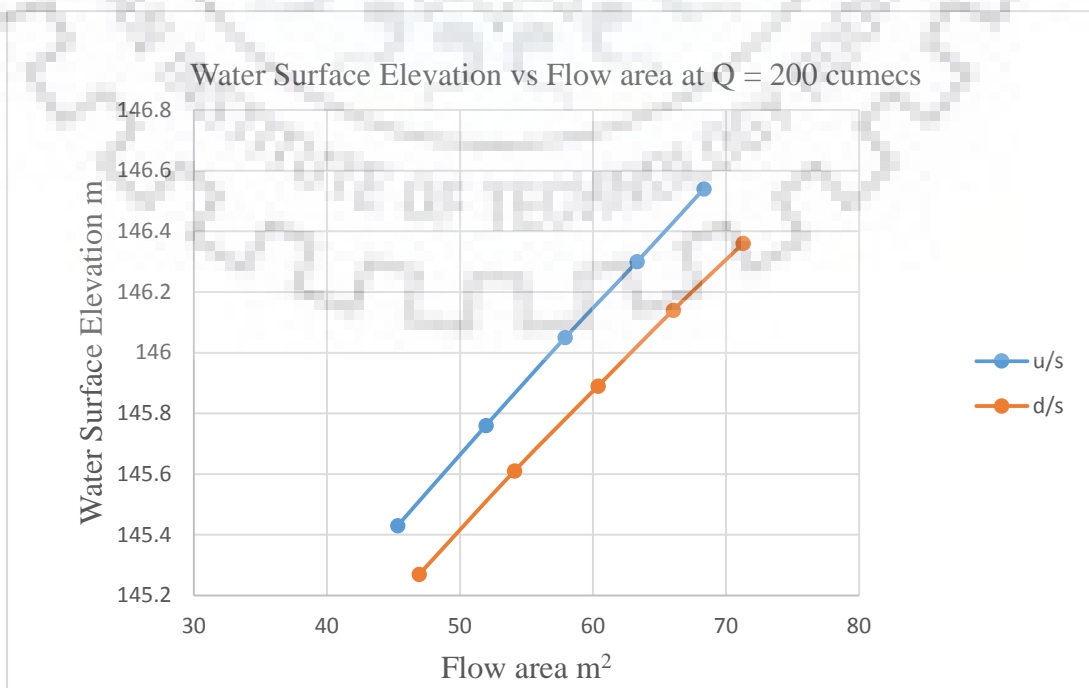


Figure 3.5: Water Surface Elevation vs Flow area

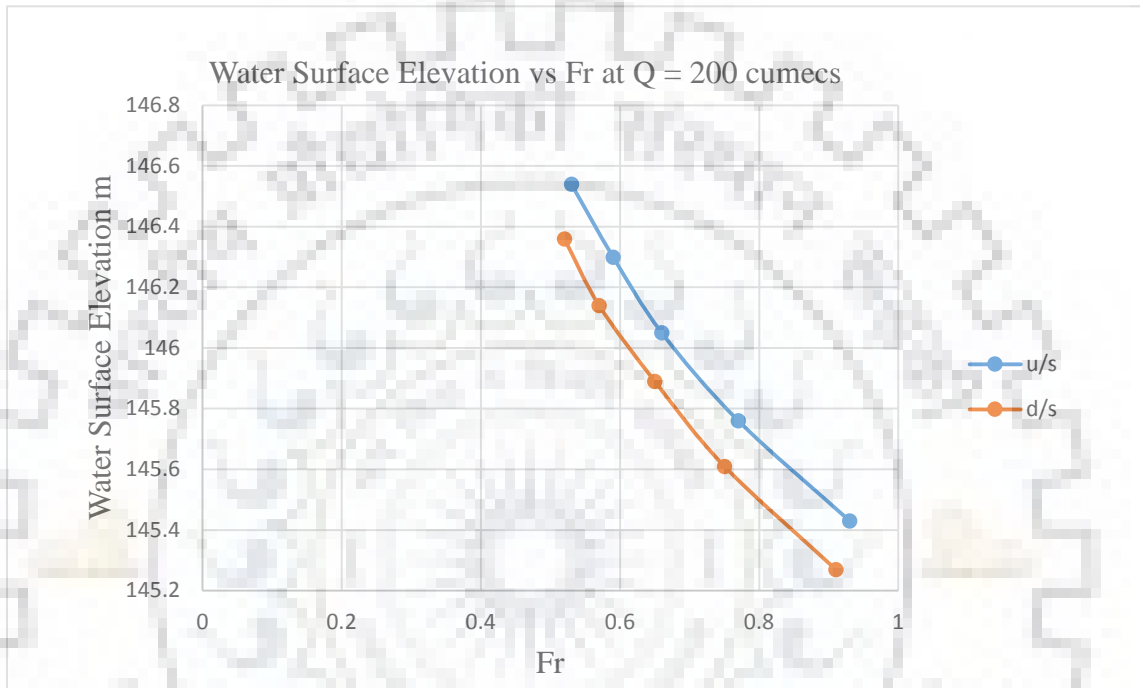


Figure 3.6: Water Surface Elevation vs Fr

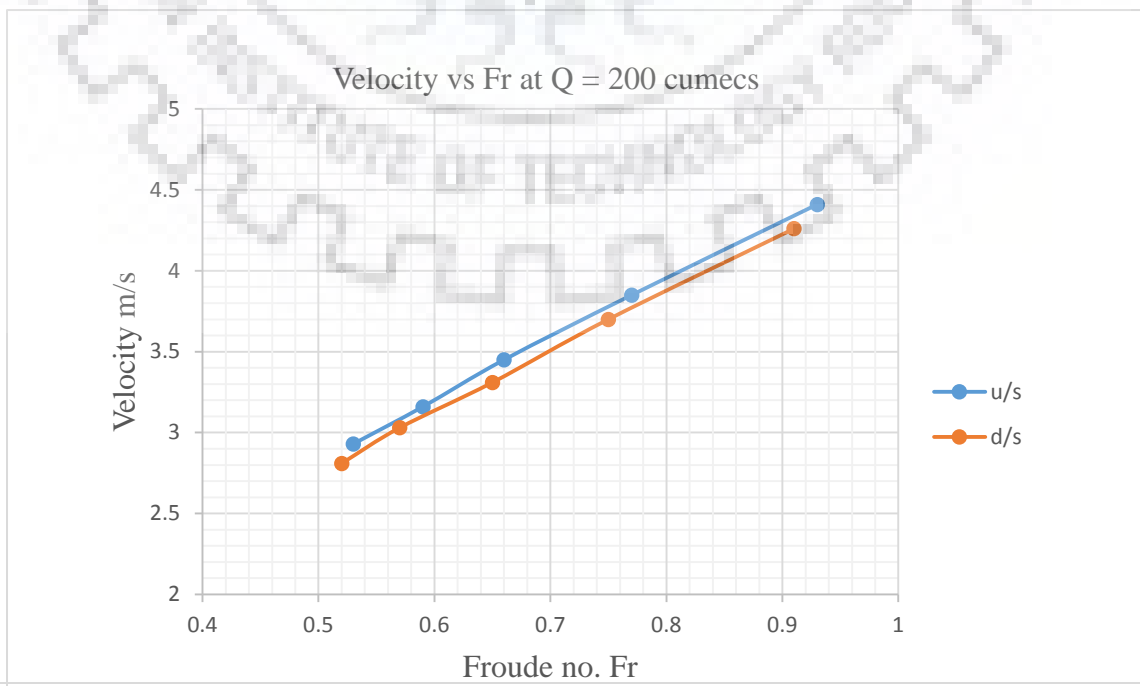


Figure 3.7: Velocity vs Fr

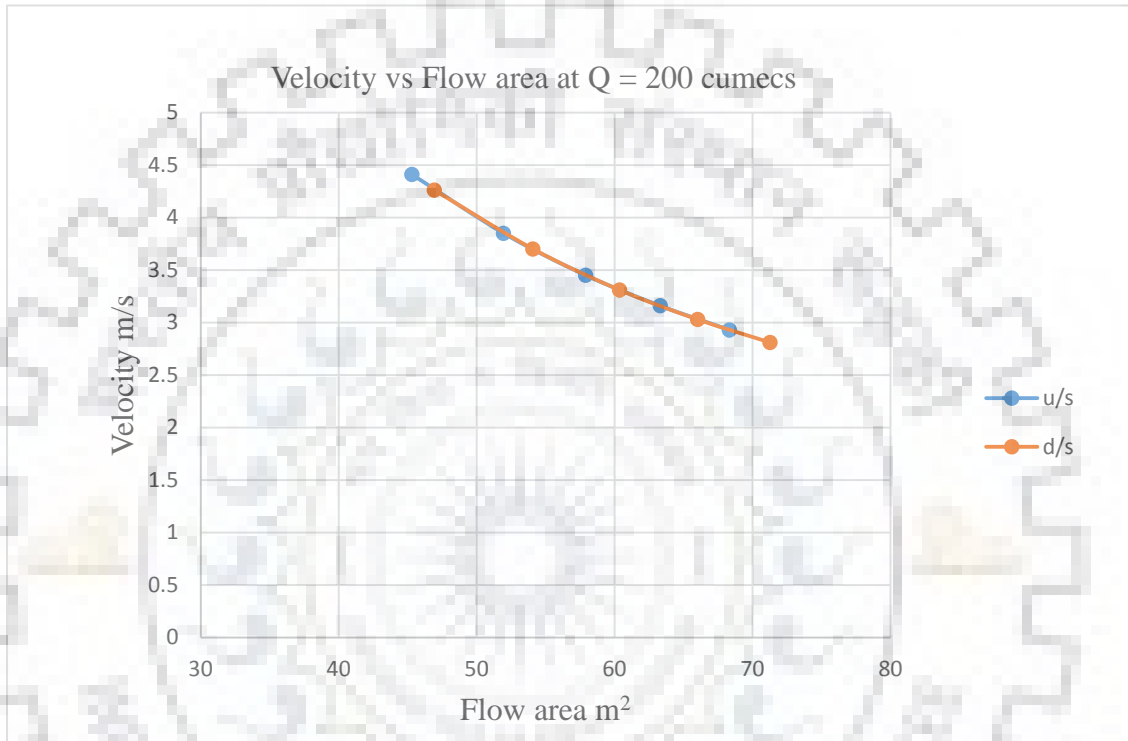


Figure 3.8: Velocity vs Flow area

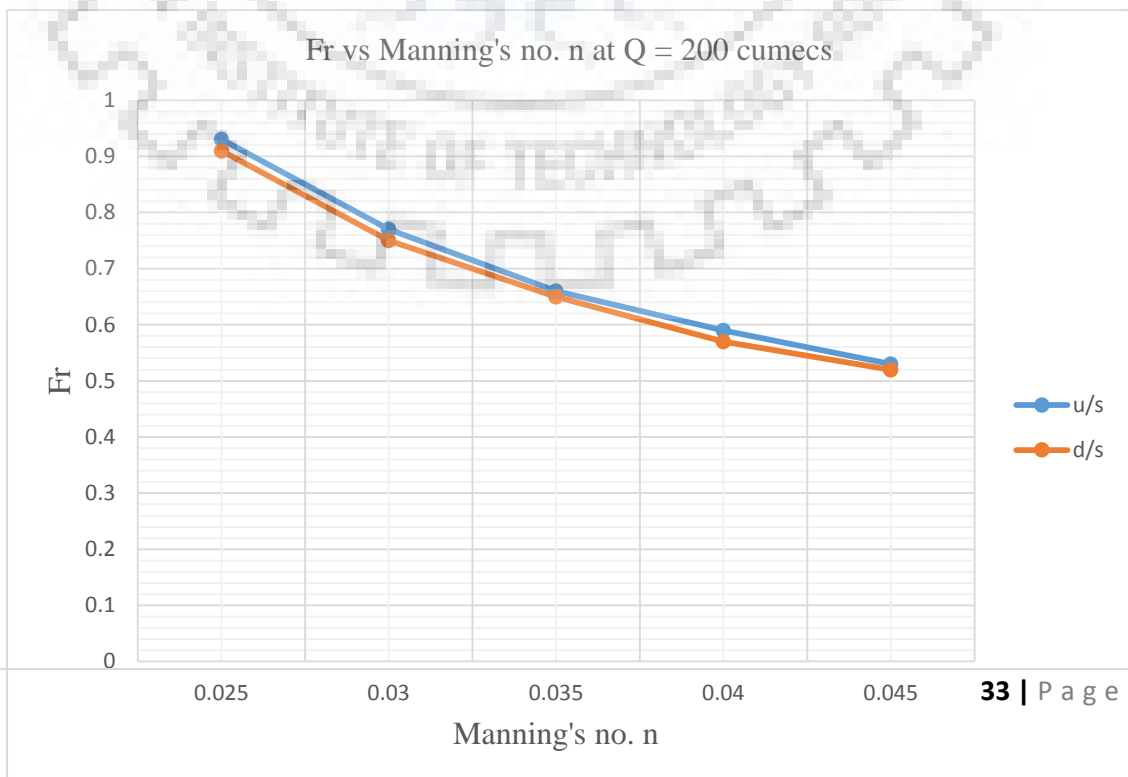


Figure 3.9: Fr vs Manning's no. n

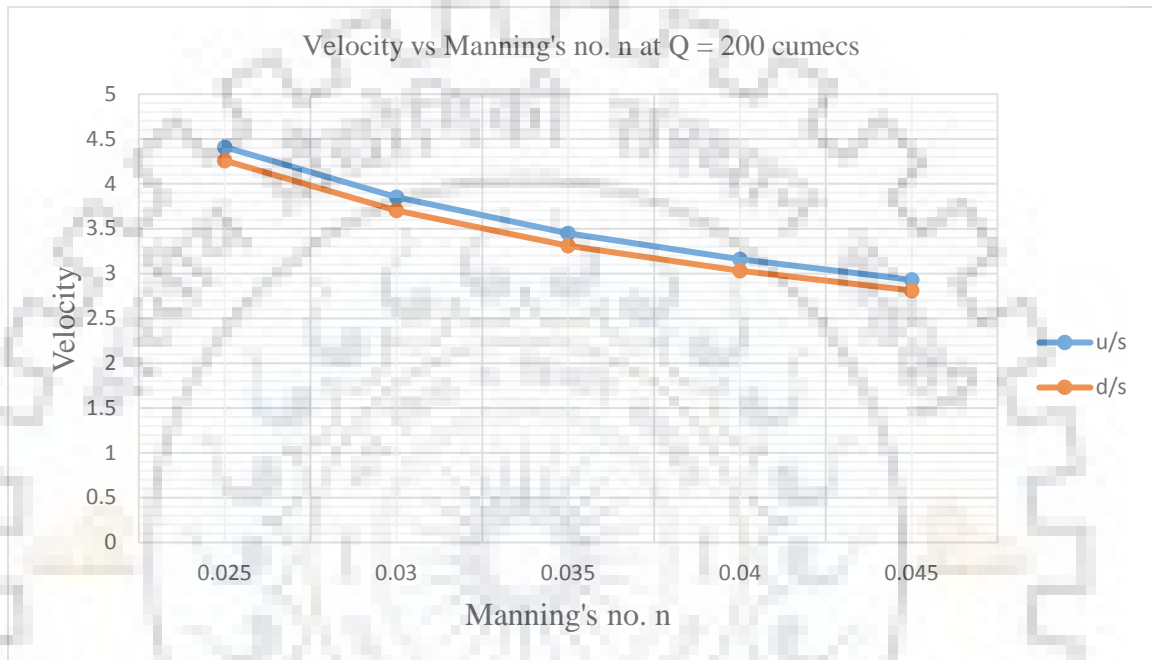


Figure 3. 10: Velocity vs Manning's no. n

(For No Bridge Condition and $Q = 400 \text{ m}^3/\text{sec}$)

u/s RS 953					d/s RS 903				
WSE (m)	Velocity (m/s)	Flow area m^2	Fr	n	WSE (m)	Velocity (m/s)	Flow area m^2	Fr	n
146.45	6.02	66.48	1.1	0.025	146.38	5.57	71.79	1.02	0.025
146.89	5.26	76.09	0.91	0.03	146.72	5.01	79.81	0.89	0.03
147.31	4.66	85.74	0.78	0.035	147.13	4.44	90.02	0.75	0.035
147.67	4.24	94.29	0.68	0.04	147.48	4.04	98.94	0.66	0.04

147.99	3.92	102.07	0.61	0.045	147.78	3.74	107.0	4	0.6	0.045
--------	------	--------	------	-------	--------	------	-------	---	-----	-------

Table 3.3: For No Bridge Condition and $Q = 400 \text{ m}^3/\text{sec}$

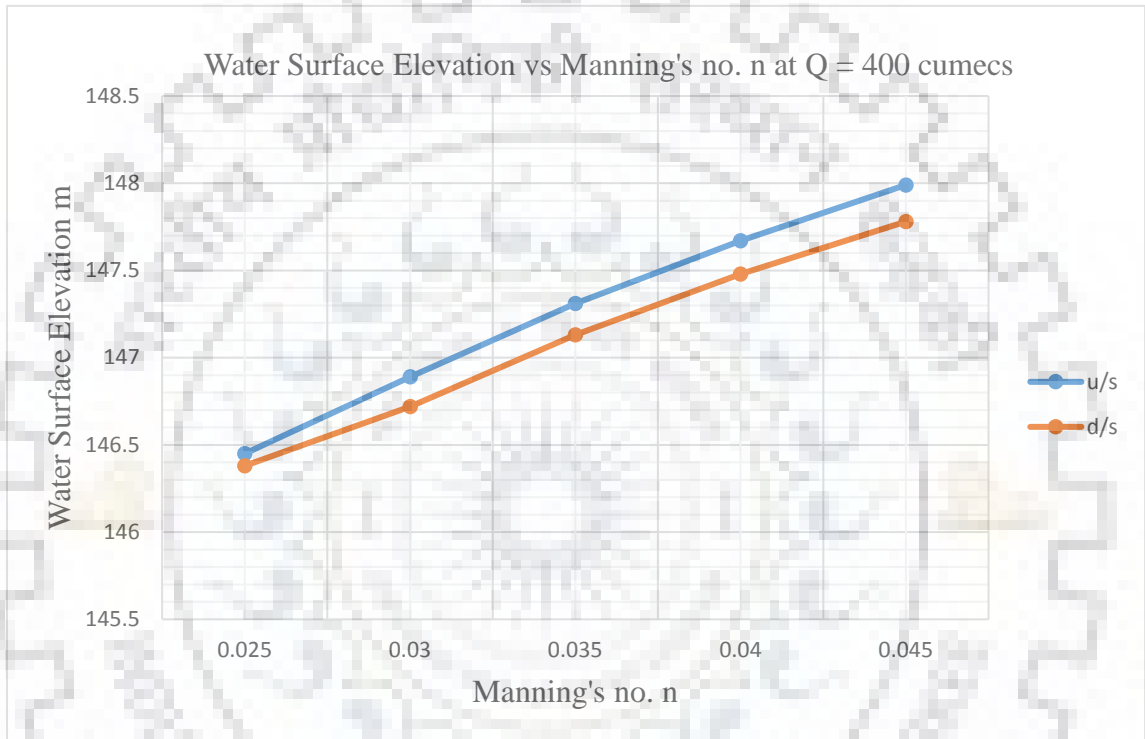


Figure 3.11: Water Surface Elevation vs Manning's no. n at $Q = 400$ cumecs

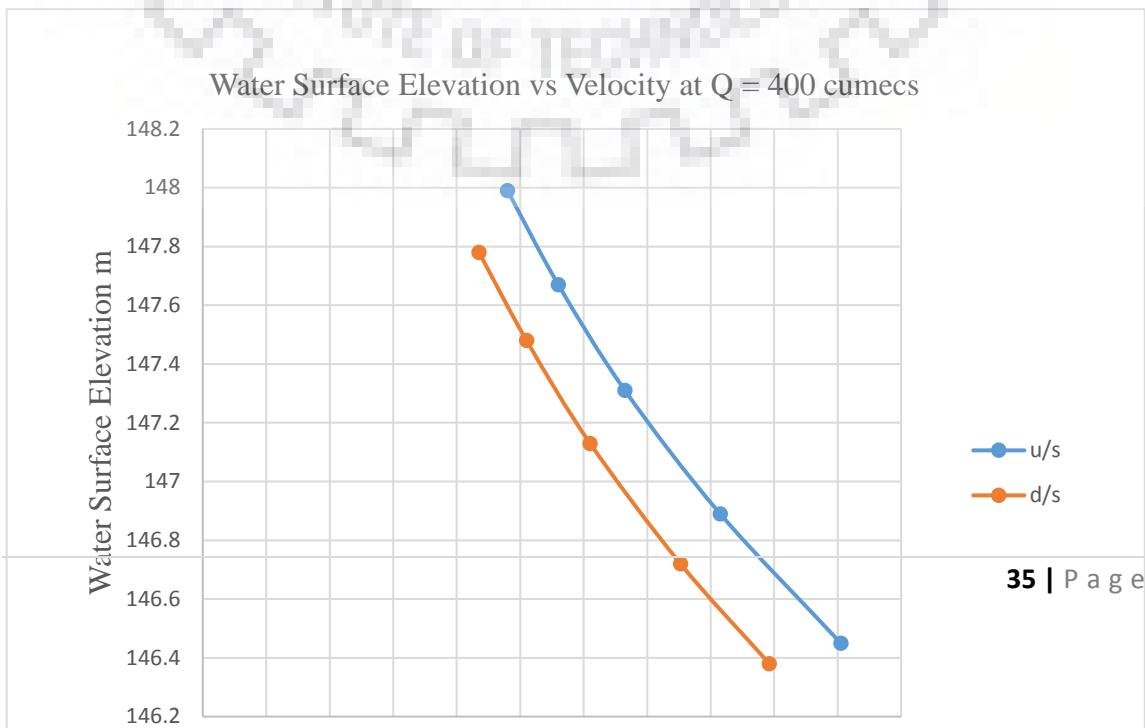


Figure 3.12: Water Surface Elevation vs Velocity

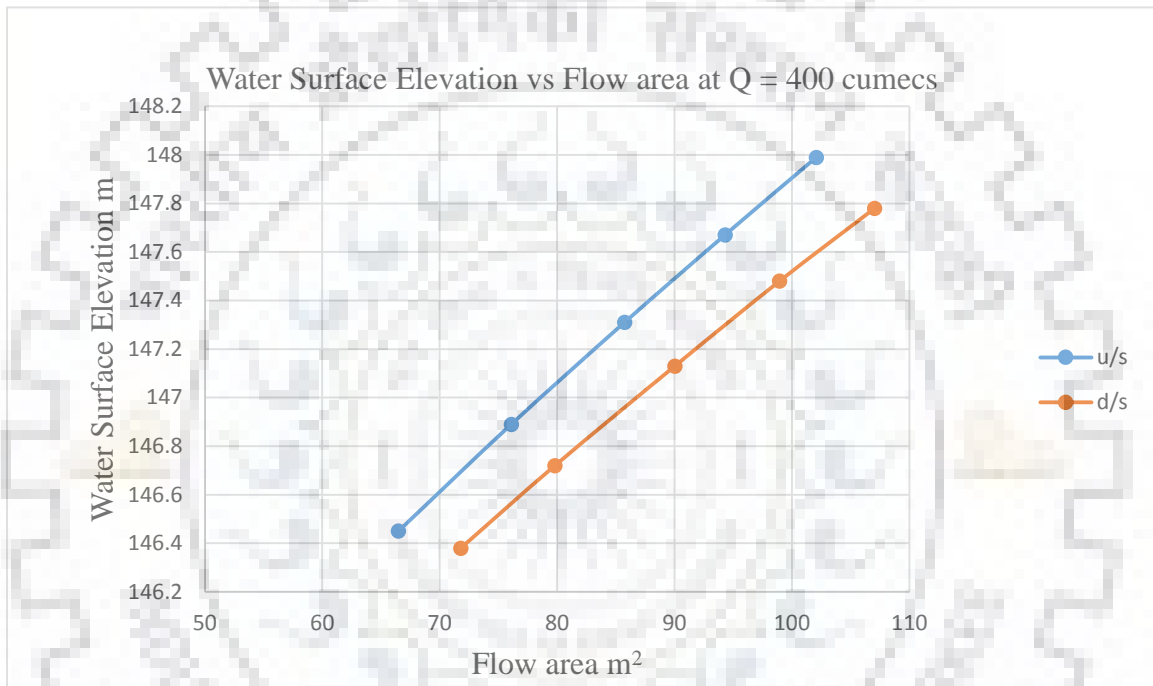


Figure 3.13: Water Surface Elevation vs Flow area

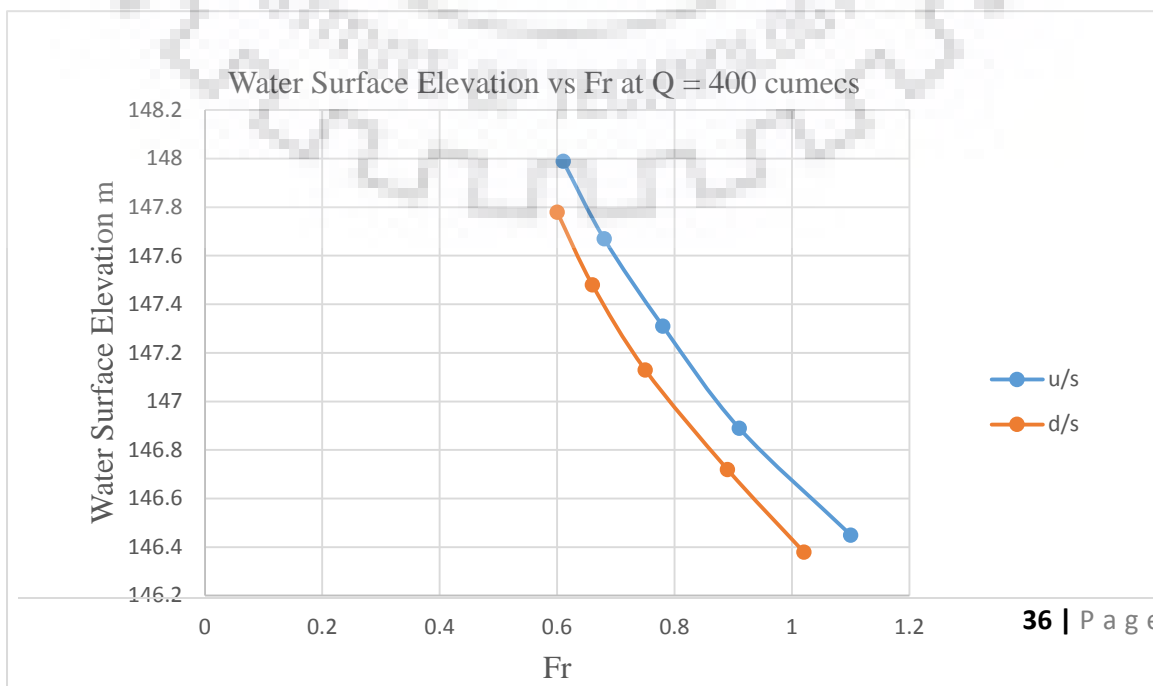


Figure 3.14: Water Surface Elevation vs Fr

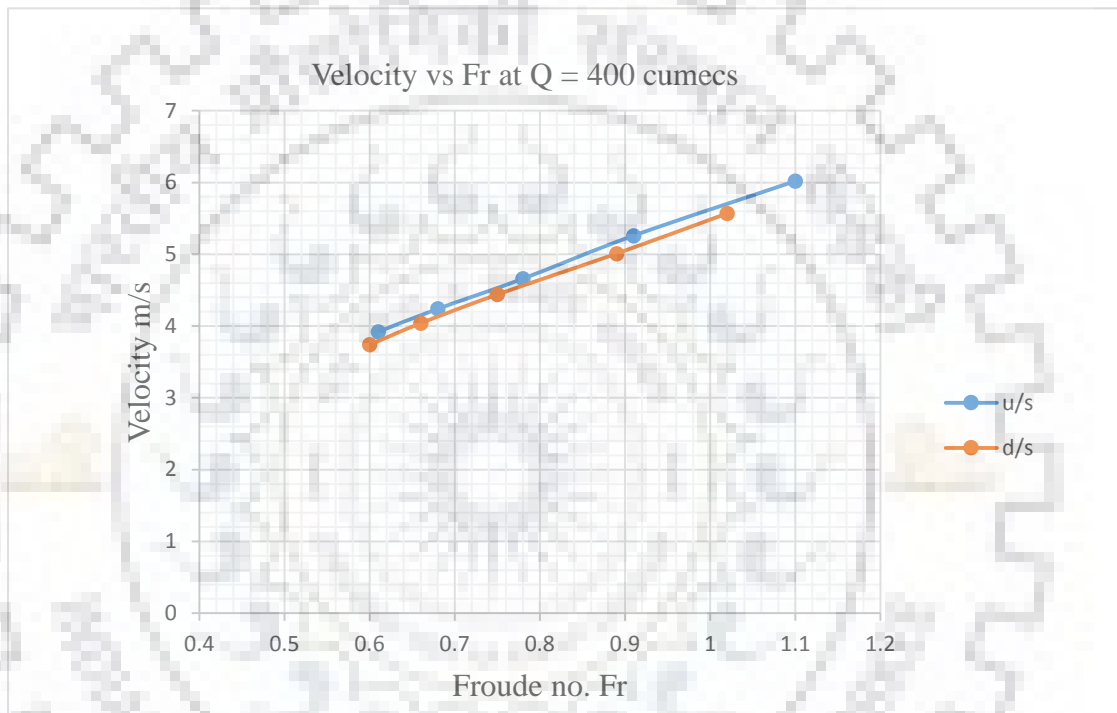


Figure 3.15: Velocity vs Fr

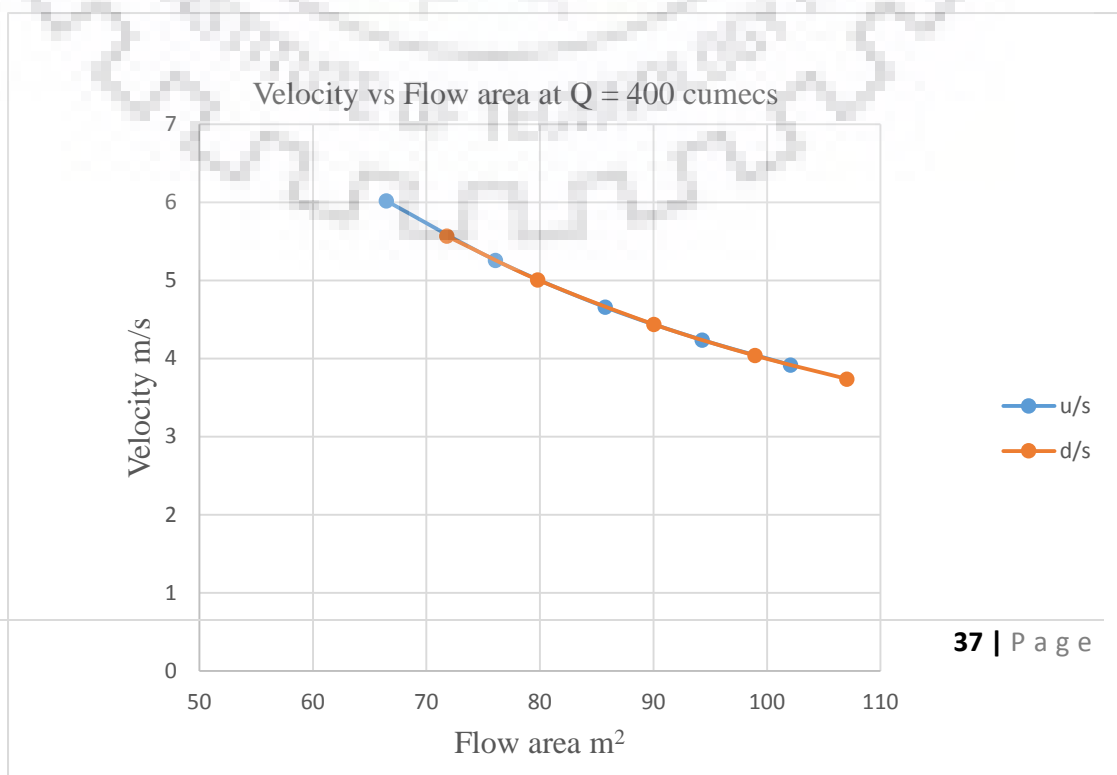


Figure 3.16: Velocity vs Flow area

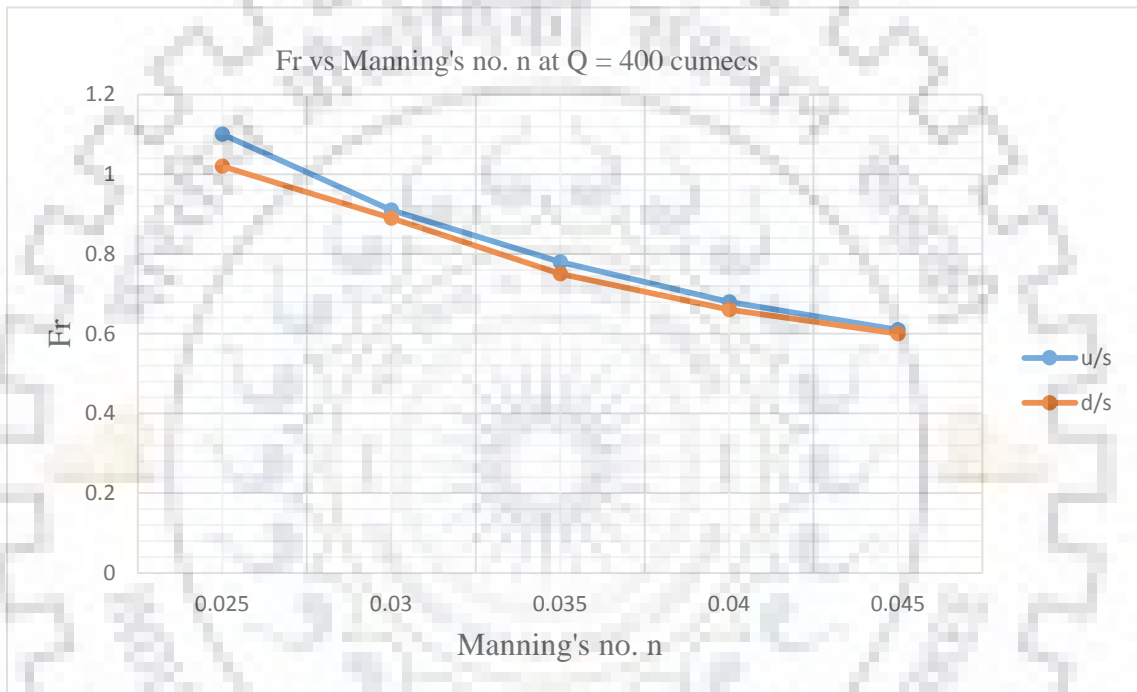


Figure 3.17: Fr vs Manning's no. n

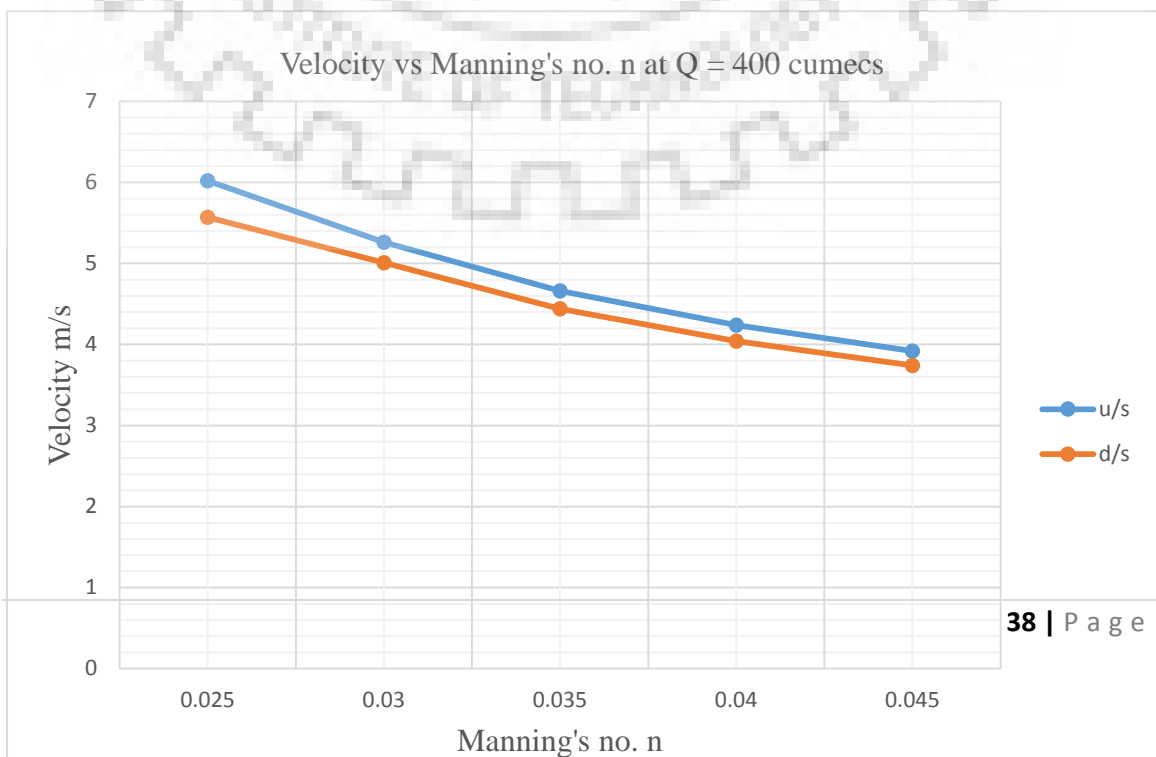


Figure 3.18: Velocity vs Manning's no. n

(For No Bridge Condition and $Q = 600 \text{ m}^3/\text{sec}$)

u/s RS 953					d/s RS 903				
WSE (m)	Velocity (m/s)	Flow area m^2	Fr	n	WSE (m)	Velocity (m/s)	Flow area m^2	Fr	n
147.1	7.41	80.98	1.26	0.025	146.86	7.19	83.41	1.25	0.025
147.47	6.69	89.67	1.1	0.03	147.15	6.63	90.5	1.12	0.03
148.18	5.62	106.8	0.87	0.035	147.99	5.33	112.54	0.84	0.035
148.63	5.08	118.18	0.76	0.04	148.42	4.82	124.48	0.73	0.04
149.02	4.67	128.46	0.68	0.045	148.79	4.44	135.19	0.66	0.045

Table 3.4: For No Bridge Condition and $Q = 600 \text{ m}^3/\text{sec}$

(For No Bridge Condition and $Q = 800 \text{ m}^3/\text{sec}$)

u/s RS 953					d/s RS 903				
WSE (m)	Velocity (m/s)	Flow area m^2	Fr	n	WSE (m)	Velocity (m/s)	Flow area m^2	Fr	n
147.66	8.5	94.16	1.37	0.025	147.39	8.27	96.74	1.36	0.025
148.15	7.54	106.04	1.17	0.03	148	7.09	112.81	1.11	0.03
148.85	6.45	124.06	0.95	0.035	148.65	6.1	131.22	0.91	0.035
149.39	5.77	138.56	0.82	0.04	149.17	5.46	146.48	0.79	0.04

149.85	5.28	151.57	0.73	0.045	149.61	5	160	0.71	0.045
--------	------	--------	------	-------	--------	---	-----	------	-------

Table 3.5: For No Bridge Condition and $Q = 800 \text{ m}^3/\text{sec}$

(For No Bridge Condition and $Q = 1000 \text{ m}^3/\text{sec}$)

u/s RS 953					d/s RS 903				
WSE (m)	Velocity (m/s)	Flow area m^2	Fr	n	WSE (m)	Velocity (m/s)	Flow area m^2	Fr	n
148.19	9.33	107.2	1.44	0.025	147.87	9.15	109.26	1.45	0.025
148.73	8.27	120.91	1.23	0.03	148.44	7.99	125.1	1.21	0.03
149.49	7.08	141.23	1	0.035	148.8	7.38	135.43	1.09	0.035
150.04	6.37	156.92	0.88	0.04	149.82	6.01	166.41	0.84	0.04
150.56	5.8	172.56	0.78	0.045	150.31	5.48	182.62	0.75	0.045

Table 3.6: For No Bridge Condition and $Q = 1000 \text{ m}^3/\text{sec}$

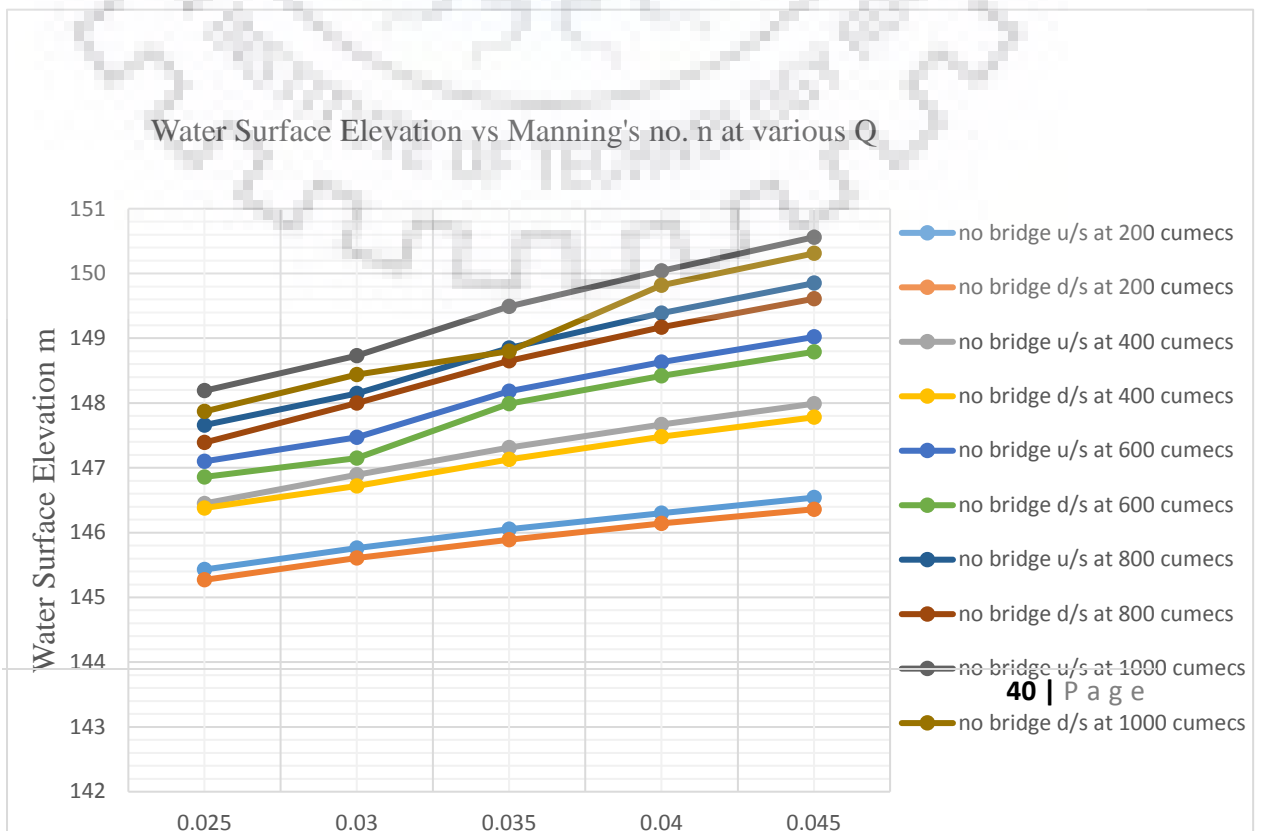


Figure 3.19: Water Surface Elevation vs Manning's coefficient n at various Q

(Water Surface Elevation vs Flow Area at various Q)

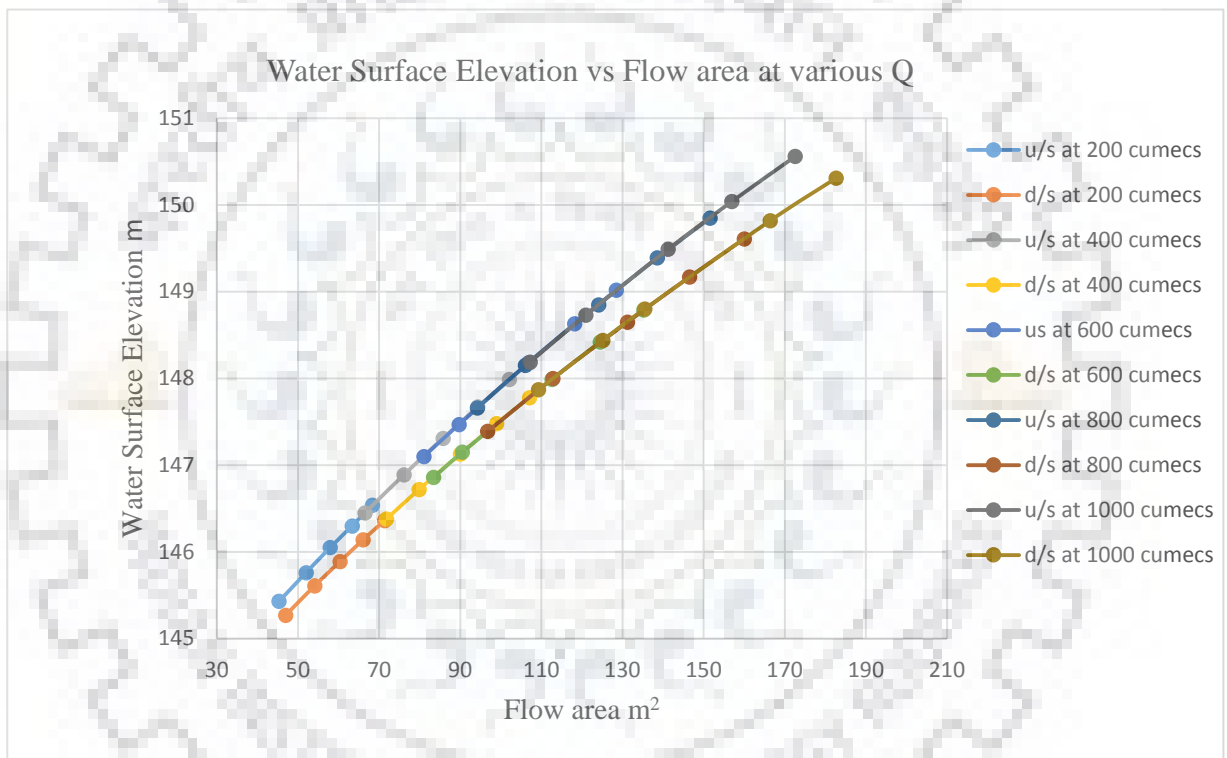
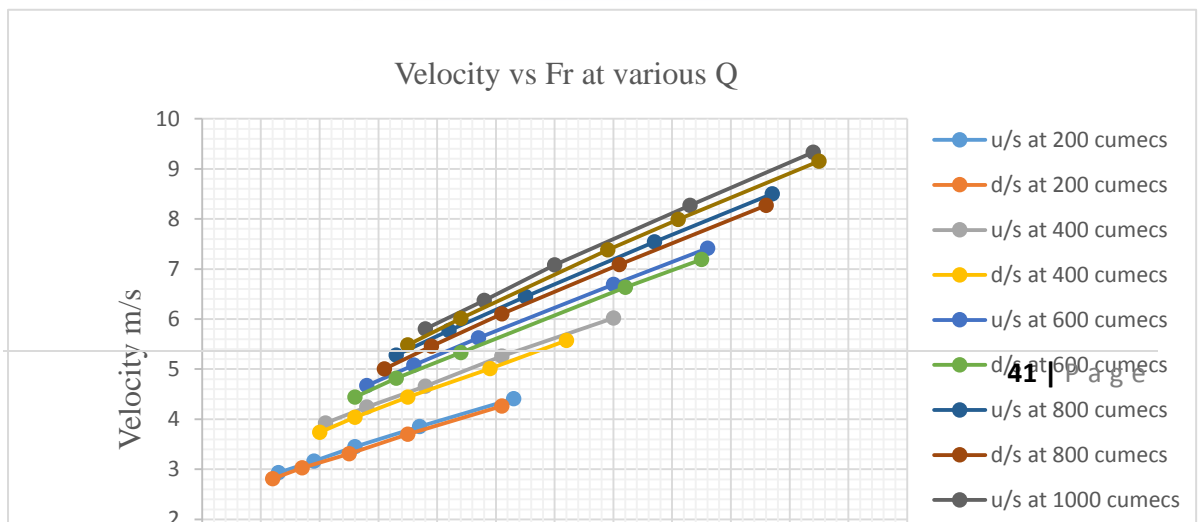


Figure 3.20: Water Surface Elevation vs Flow Area at various Q

(Velocity vs Froude no. (Fr) at various Q)



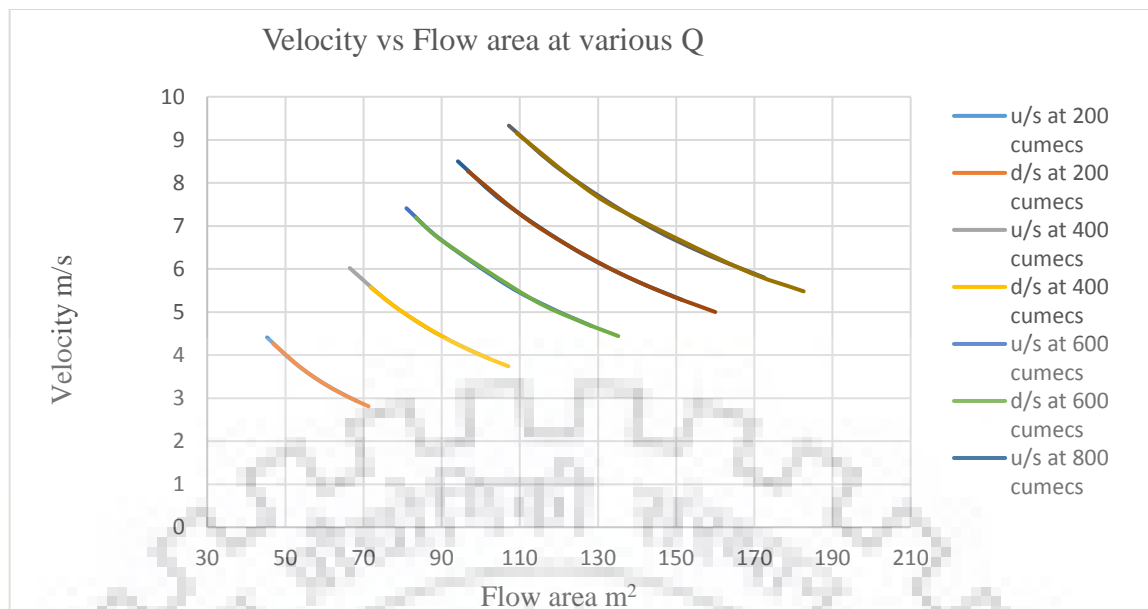


Figure 3.21: Velocity vs Froude no. (Fr) at various Q

Here, observing all the results for No Bridge Condition and for all steady flows ($Q = 200, 400, 600, 800$ and $1000 \text{ m}^3/\text{sec}$) while varying the **Manning's coefficient n**, the water surface elevation (WSE) increases as the Manning's coefficient n increases at the both upstream and downstream side of the bridge i.e. water surface elevation and Manning's coefficient are directly proportional to each other at the upstream and downstream of bridge section. Hence **Water Surface Elevation vs Manning's coefficient** curve at the upstream and downstream side run parallel with each other because there is no obstruction in the flow.

Also, when the **water surface elevation** increases, velocity decreases as the Manning's coefficient n increases at the both upstream and downstream side of the bridge i.e. water surface elevation and velocity are inversely proportional to each other as the Manning's coefficient n increases at the upstream and downstream side of the bridge section. Hence the **Water Surface Elevation vs Velocity** curve at both upstream and downstream are parallel with each other because there is no obstruction in the flow at both the sides.

Similarly, when the flow area increases, water surface elevation increases as the Manning's coefficient increases at the both upstream and downstream side of the bridge i.e. water surface elevation and flow area are directly proportional to each other as the Manning's coefficient increases at the upstream and downstream side of the bridge section. Hence **Water Surface Elevation vs Flow area** curve at the upstream and downstream site are parallel with each other.

Also, when the water surface elevation increases, Froude no. (Fr) decreases as the Manning's coefficient increases at the both upstream and downstream side of the bridge i.e. water surface elevation and Fr are inversely proportional to each other at the upstream and downstream side of the bridge section. Hence **Water Surface Elevation vs Froude no.** curve at the upstream and downstream side are parallel with each other as there is no obstruction in the flow at both the sides.

Now, when the flow area at bridge section increases, velocity decreases as the Manning's coefficient increases at the both upstream and downstream sides of the bridge i.e. velocity and flow area are inversely proportional to each other at the upstream and downstream side of the bridge section. Hence **Velocity vs Flow area** curve at the upstream and downstream side are connected with each other and seems to be a single line.

Similarly, when the velocity increases, Froude no. (Fr) also increases as the Manning's coefficient increases at the both upstream and downstream side of the bridge i.e. velocity and Fr are directly proportional to each other at the upstream and downstream side of the bridge section. And here the **Velocity vs Froude no.** curve at the upstream and downstream side are parallel with each other as there is no obstruction in the flow at both upstream and downstream sides.

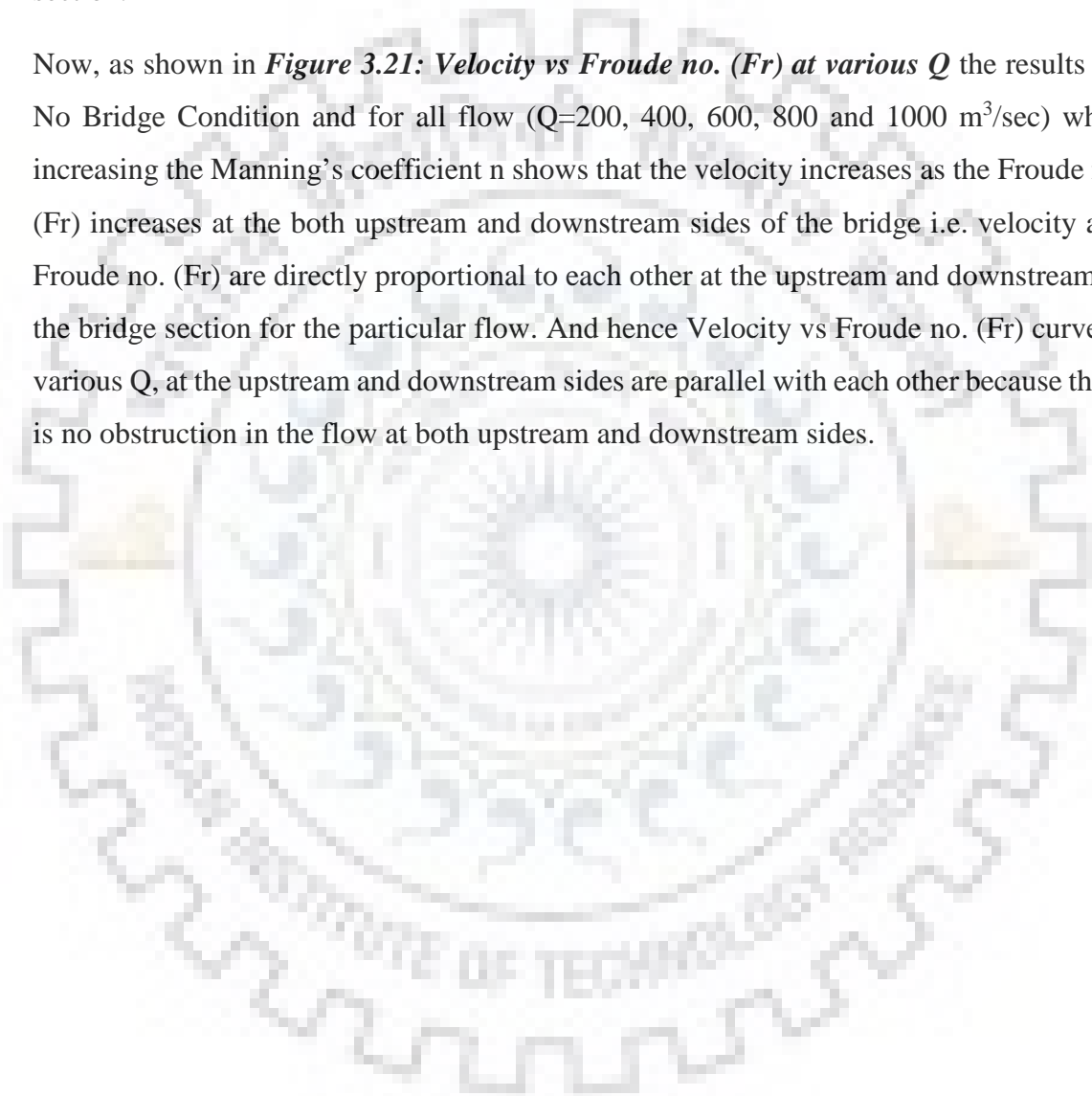
Also when the Manning's coefficient increases velocity decreases at the both upstream and downstream side of the bridge i.e. Manning's coefficient and velocity are inversely proportional to each other at both the sides of the bridge section. Hence **Velocity vs Manning's coefficient** curve at the upstream and downstream side are parallel with each other.

Now, as shown in **Figure 3.19: Water Surface Elevation vs Manning's coefficient n at various Q** , the results for No Bridge Condition and for all steady flows ($Q = 200, 400, 600, 800$ and $1000 \text{ m}^3/\text{sec}$) while varying the Manning's coefficient n shows that the water surface elevation increases as the Manning's coefficient increases at the both upstream and downstream side of the bridge i.e. water surface elevation and n are directly proportional to each other at the upstream and downstream of bridge section for the particular flow. So the **Water Surface Elevation vs Manning's coefficient** curve at various Q , at both sides of the bridge are parallel with each other.

Also, as shown in **Figure 3.20: Water Surface Elevation vs Flow Area at various Q** the results for No Bridge Condition and for all flow ($Q = 200, 400, 600, 800$ and $1000 \text{ m}^3/\text{sec}$)

while increasing the Manning's coefficient n shows that the water surface elevation increases as the flow area increases at the both upstream and downstream side of the bridge i.e. water surface elevation and flow area are directly proportional to each other at both sides of bridge section for the particular flow. Hence the **Water Surface Elevation vs Flow area** curve at various Q , at the upstream and downstream sides are overlapped on the corresponding upstream and downstream curves as the flow is unobstructed at any section.

Now, as shown in *Figure 3.21: Velocity vs Froude no. (Fr) at various Q* the results for No Bridge Condition and for all flow ($Q=200, 400, 600, 800$ and $1000 \text{ m}^3/\text{sec}$) while increasing the Manning's coefficient n shows that the velocity increases as the Froude no. (Fr) increases at the both upstream and downstream sides of the bridge i.e. velocity and Froude no. (Fr) are directly proportional to each other at the upstream and downstream of the bridge section for the particular flow. And hence Velocity vs Froude no. (Fr) curve at various Q , at the upstream and downstream sides are parallel with each other because there is no obstruction in the flow at both upstream and downstream sides.

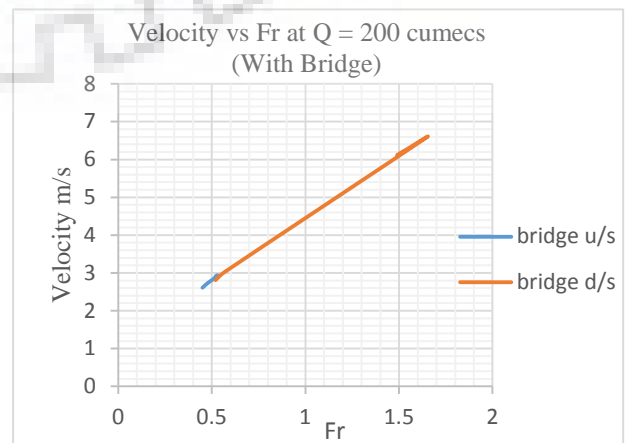
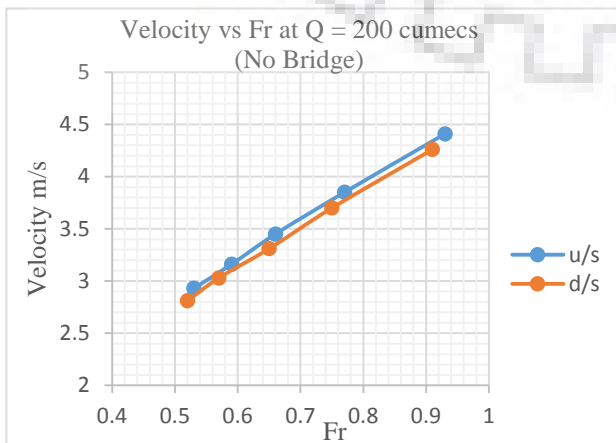
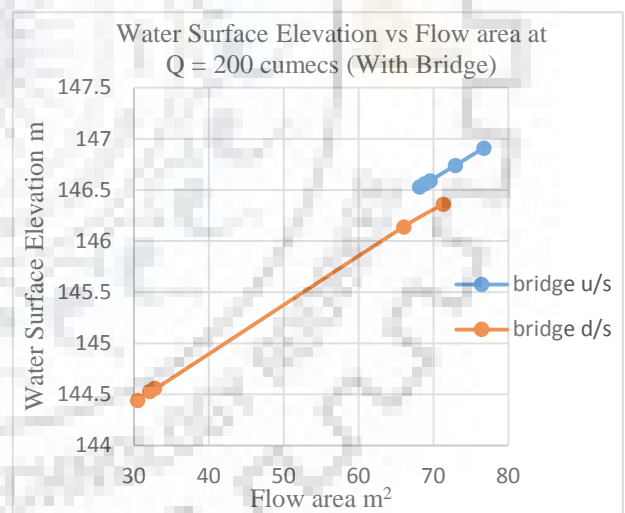
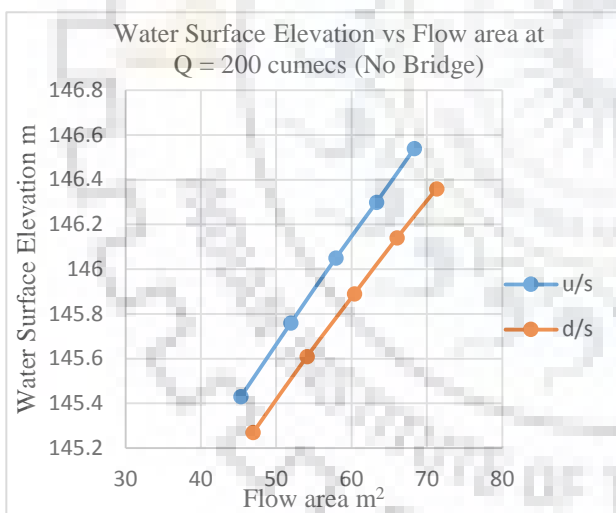
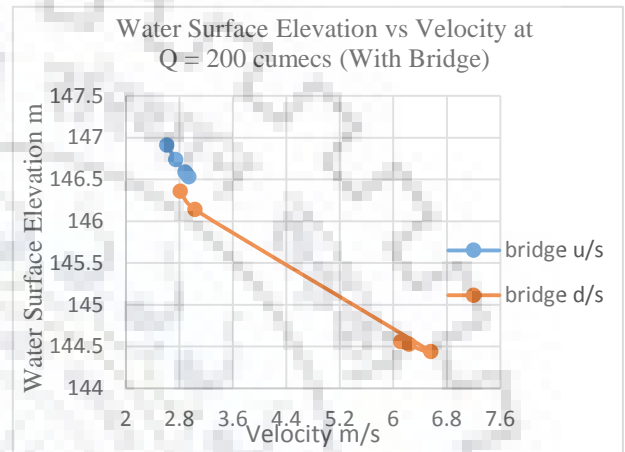
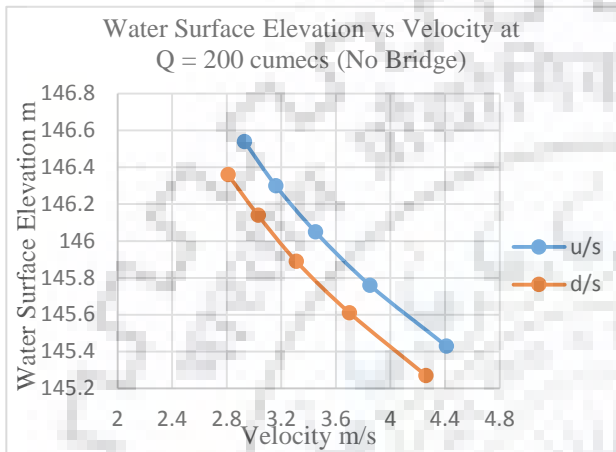
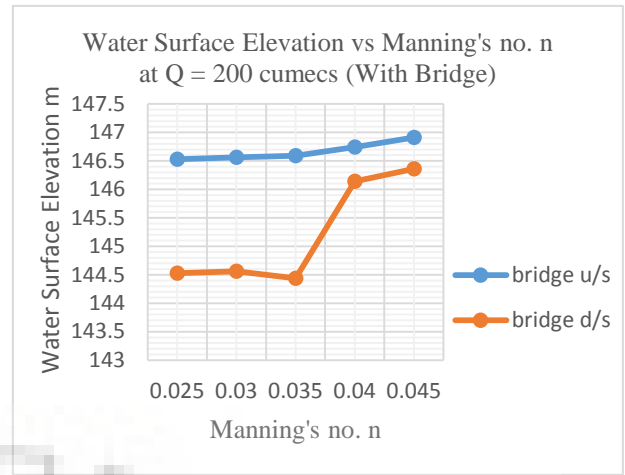
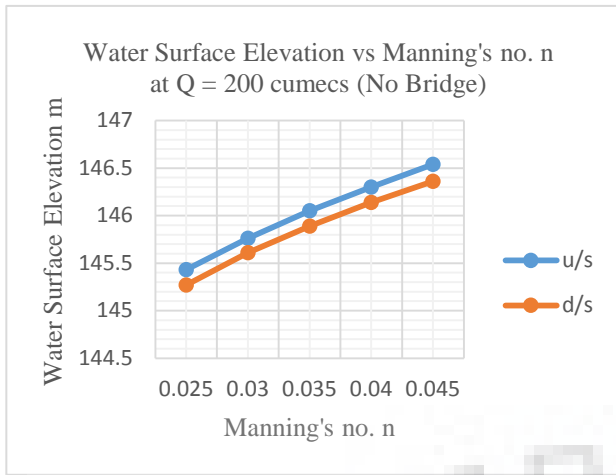


3.4.2 WITH BRIDGE AND COMPARISON WITH NO BRIDGE CONDITION

3.4.2.1 Variation of Water Surface Profiles with Manning's coefficient n ($Q = 200 \text{ m}^3/\text{s}$)

No Bridge								1 bridge 2 m pier 10 m spacing										n	Afflux m	
u/s RS 953				d/s RS 903				u/s RS 953					d/s RS 903						u/s	d/s
WSE (m)	Velocity (m/s)	Flow area m^2	Fr	WSE (m)	Velocity (m/s)	Flow area m^2	Fr	WSE (m)	CWS Elv (m)	Velocity (m/s)	Flow area m^2	Fr	WSE (m)	CWS Elv (m)	Velocity (m/s)	Flow area m^2	Fr			
145.43	4.41	45.31	0.93	145.27	4.26	46.94	0.91	146.53	145.3	2.94	68.14	0.53	144.53	145.12	6.23	32.09	1.53	0.025	1.1	-0.74
145.76	3.85	51.95	0.77	145.61	3.7	54.09	0.75	146.56	145.3	2.91	68.82	0.52	144.56	145.12	6.11	32.72	1.49	0.03	0.8	-1.05
146.05	3.45	57.91	0.66	145.89	3.31	60.37	0.65	146.59	145.3	2.88	69.56	0.52	144.44	145.12	6.56	30.49	1.64	0.035	0.54	-1.45
146.3	3.16	63.31	0.59	146.14	3.03	66.02	0.57	146.74	145.3	2.74	72.9	0.48	146.14	145.12	3.03	66.02	0.57	0.04	0.44	0.00
146.54	2.93	68.33	0.53	146.36	2.81	71.28	0.52	146.91	145.3	2.61	76.71	0.45	146.36	145.12	2.81	71.28	0.52	0.045	0.37	0.00

Table 3.7: Variation of Water Surface Profiles with Manning's coefficient n ($Q = 200 \text{ m}^3/\text{s}$)



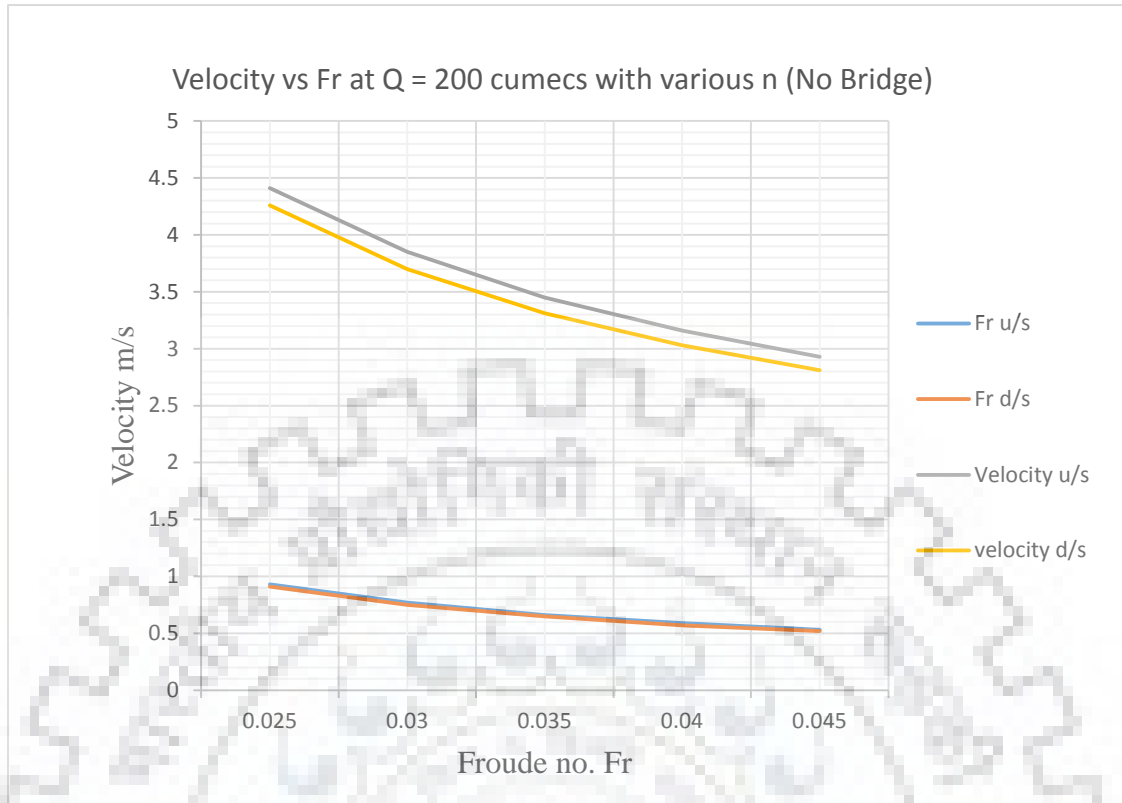


Figure 3.22: Velocity vs Fr at Q = 200 cumecs with various n (No Bridge)

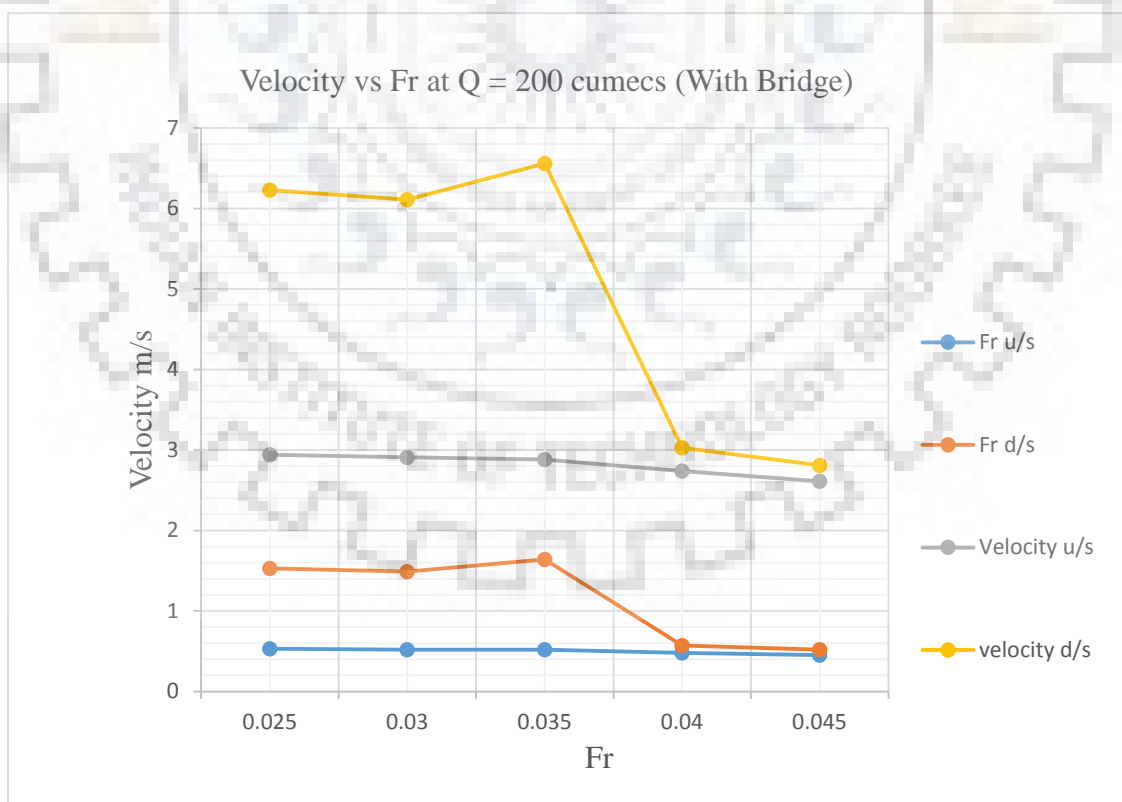
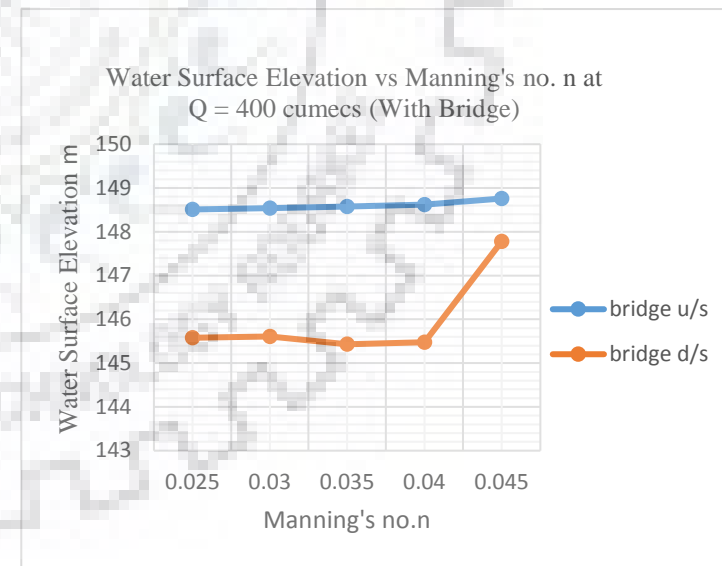
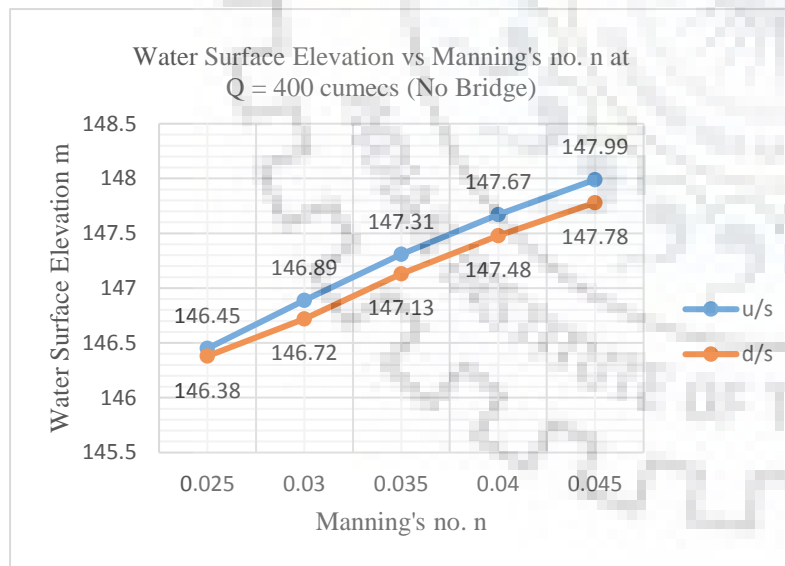


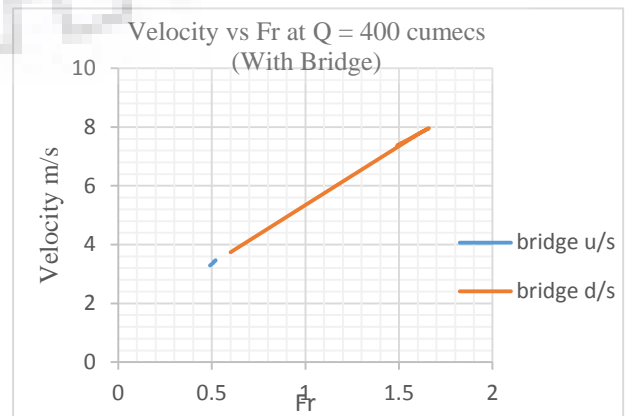
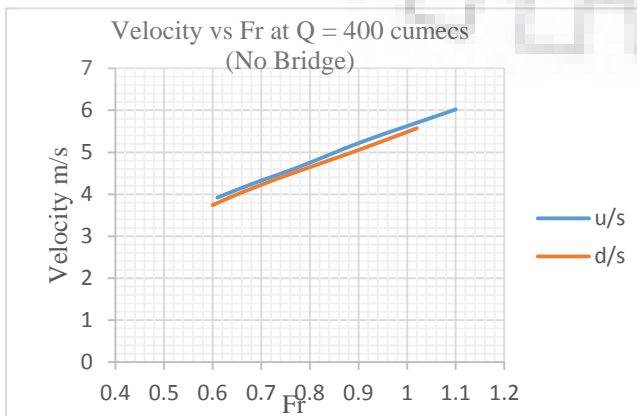
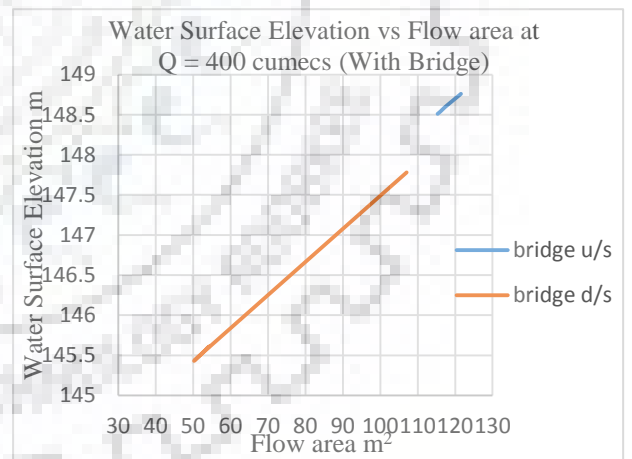
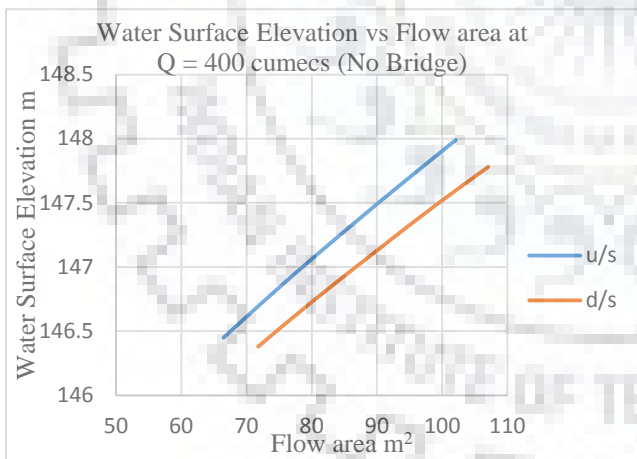
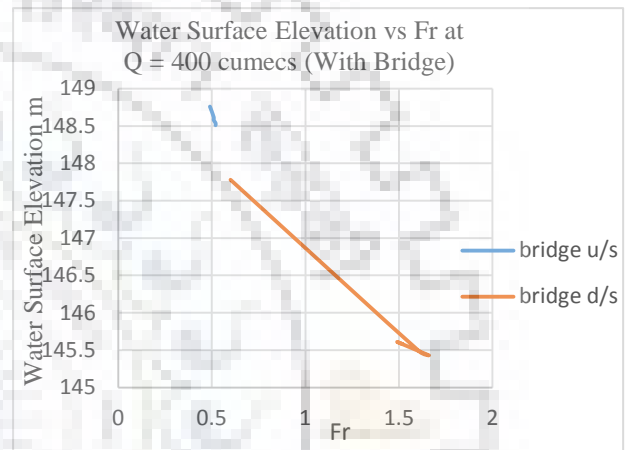
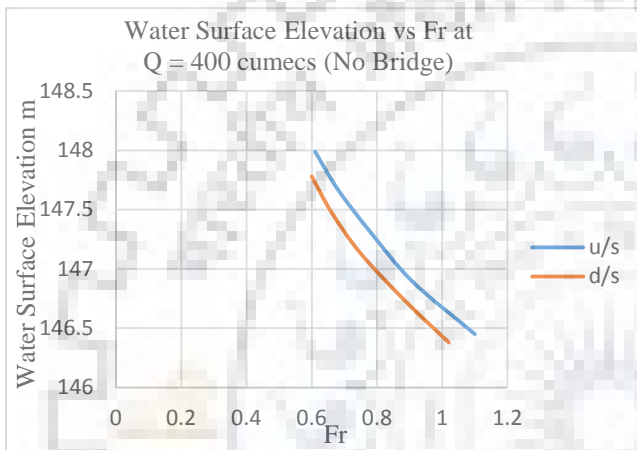
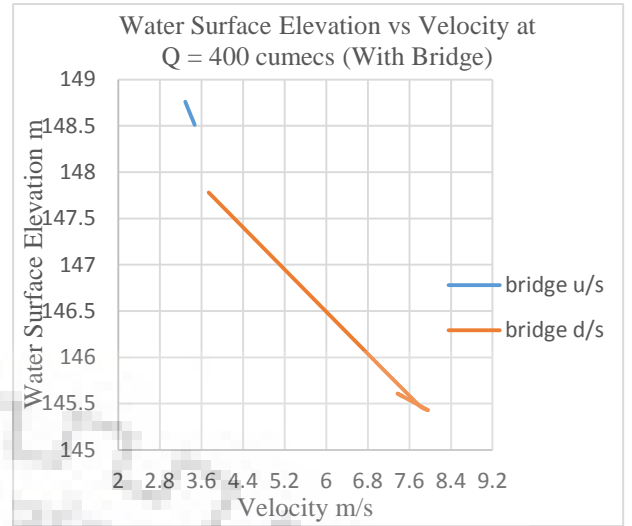
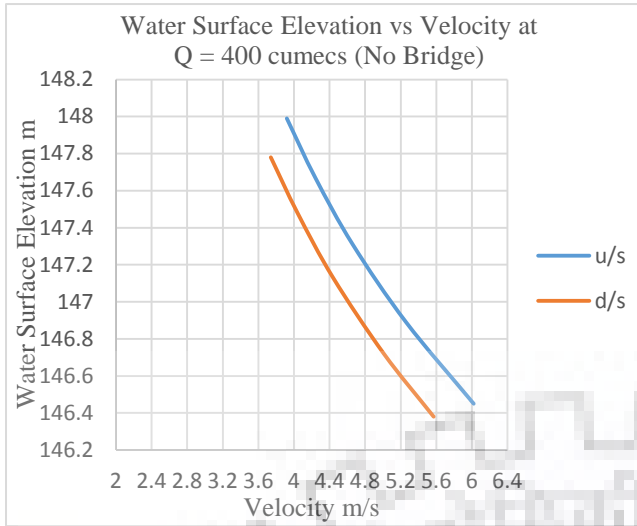
Figure 3.23: Velocity vs Fr at Q = 200 cumecs (With Bridge)

($Q = 400 \text{ m}^3/\text{s}$)

No Bridge								1 bridge 2 m pier 10 m spacing										n	Afflux m	
u/s RS 953				d/s RS 903				u/s RS 953					d/s RS 903						u/s	d/s
WSE (m)	Velocity (m/s)	Flow area m^2	Fr	WSE (m)	Velocity (m/s)	Flow area m^2	Fr	WSE (m)	CWS Elv (m)	Velocity (m/s)	Flow area m^2	Fr	WSE (m)	CWS Elv (m)	Velocity (m/s)	Flow area m^2	Fr			
146.45	6.02	66.48	1.1	146.4	5.57	71.79	1.02	148.51	146.66	3.47	115.3	0.52	145.58	146.42	7.47	53.55	1.52	0.025	2.06	-0.8
146.89	5.26	76.09	0.91	146.7	5.01	79.81	0.89	148.54	146.66	3.45	116.1	0.52	145.61	146.42	7.37	54.28	1.49	0.03	1.65	-1.11
147.31	4.66	85.74	0.78	147.1	4.44	90.02	0.75	148.58	146.66	3.42	117	0.51	145.43	146.42	7.96	50.26	1.66	0.035	1.27	-1.7
147.67	4.24	94.29	0.68	147.5	4.04	98.94	0.66	148.62	146.66	3.39	117.9	0.51	145.48	146.42	7.79	51.35	1.61	0.04	0.95	-2
147.99	3.92	102.1	0.61	147.8	3.74	107	0.6	148.76	146.66	3.29	121.6	0.49	147.78	146.42	3.74	107.04	0.6	0.045	0.77	0

Table 3.8: Variation of Water Surface Profiles with Manning's coefficient n ($Q = 400 \text{ m}^3/\text{s}$)





$$(Q = 600 \text{ m}^3/\text{s})$$

No Bridge								1 bridge 2 m pier 10 m spacing										n	Afflux m	
u/s RS 953				d/s RS 903				u/s RS 953					d/s RS 903						u/s	d/s
WSE (m)	Velocity (m/s)	Flow area m ²	Fr	WSE (m)	Velocity (m/s)	Flow area m ²	Fr	WSE (m)	CWS Elv (m)	Velocity (m/s)	Flow area m ²	Fr	WSE (m)	CWS Elv (m)	Velocity (m/s)	Flow area m ²	Fr			
147.10	7.41	80.98	1.26	146.86	7.19	83.41	1.25	150.08	147.74	3.79	158.29	0.52	146.41	147.45	8.29	72.37	1.52	0.025	2.98	-0.45
147.47	6.69	89.67	1.10	147.15	6.63	90.50	1.12	150.11	147.74	3.77	159.15	0.52	146.20	147.45	8.90	67.40	1.67	0.03	2.64	-0.95
148.18	5.62	106.80	0.87	147.99	5.33	112.54	0.84	150.15	147.74	3.75	160.14	0.51	146.25	147.45	8.73	68.74	1.62	0.035	1.97	-1.74
148.63	5.08	118.18	0.76	148.42	4.82	124.48	0.73	150.19	147.74	3.72	161.27	0.51	146.27	147.45	8.69	69.06	1.61	0.04	1.56	-2.15
149.02	4.67	128.46	0.68	148.79	4.44	135.19	0.66	150.23	147.74	3.69	162.50	0.51	148.79	147.45	4.44	135.19	0.66	0.045	1.21	0.00

Table 3.9: Variation of Water Surface Profiles with Manning's coefficient n (Q = 600 m³/s)

$$(Q = 800 \text{ m}^3/\text{s})$$

No Bridge								1 bridge 2 m pier 10 m spacing										n	Afflux m	
u/s RS 953				d/s RS 903				u/s RS 953					d/s RS 903						u/s	d/s
WSE (m)	Velocity (m/s)	Flow area m ²	Fr	WSE (m)	Velocity (m/s)	Flow area m ²	Fr	WSE (m)	CWS Elv (m)	Velocity (m/s)	Flow area m ²	Fr	WSE (m)	CWS Elv (m)	Velocity (m/s)	Flow area m ²	Fr			
147.66	8.5	94.16	1.37	147.4	8.27	96.74	1.36	151.41	148.66	4	199.8	0.52	147.1	148.34	8.96	89.3	1.52	0.025	3.75	-0.29
148.15	7.54	106	1.17	148	7.09	112.8	1.11	151.44	148.66	3.99	200.7	0.52	146.85	148.34	9.64	82.97	1.68	0.03	3.29	-1.15
148.85	6.45	124.1	0.95	148.7	6.1	131.2	0.91	151.47	148.66	3.96	201.8	0.51	146.91	148.34	9.46	84.53	1.64	0.035	2.62	-1.74
149.39	5.77	138.6	0.82	149.2	5.46	146.5	0.79	151.51	148.66	3.94	203	0.51	146.95	148.34	9.34	85.65	1.61	0.04	2.12	-2.22
149.85	5.28	151.6	0.73	149.6	5	160	0.71	151.55	148.66	3.91	204.4	0.5	146.98	148.34	9.27	86.27	1.59	0.045	1.7	-2.63

Table 3.10: Variation of Water Surface Profiles with Manning's coefficient n (Q = 800 m³/s)

(Q = 1000 m³/s)

No Bridge								1 bridge 2 m pier 10 m spacing										n	Afflux m	
u/s RS 953				d/s RS 903				u/s RS 953					d/s RS 903						u/s	d/s
WSE (m)	Velocity (m/s)	Flow area m ²	Fr	WSE (m)	Velocity (m/s)	Flow area m ²	Fr	WSE (m)	CWS Elv (m)	Velocity (m/s)	Flow area m ²	Fr	WSE (m)	CWS Elv (m)	Velocity (m/s)	Flow area m ²	Fr			
148.19	9.33	107.2	1.44	147.9	9.15	109.3	1.45	152.54	149.49	4.2	238.4	0.52	147.72	149.12	9.49	105.33	1.52	0.025	4.35	-0.15
148.73	8.27	120.9	1.23	148.4	7.99	125.1	1.21	152.57	149.49	4.18	239.4	0.52	147.75	149.12	9.41	106.26	1.51	0.03	3.84	-0.69
149.49	7.08	141.2	1	148.8	7.38	135.4	1.09	152.6	149.49	4.16	240.6	0.51	147.49	149.12	10.07	99.33	1.65	0.035	3.11	-1.31
150.04	6.37	156.9	0.88	149.8	6.01	166.4	0.84	152.64	149.49	4.13	241.9	0.51	147.84	149.12	9.2	108.66	1.46	0.04	2.6	-1.98
150.56	5.8	172.6	0.78	150.3	5.48	182.6	0.75	152.68	149.49	4.11	243.4	0.5	147.56	149.12	9.89	101.09	1.61	0.045	2.12	-2.75

Table 3.11: Variation of Water Surface Profiles with Manning's coefficient n (Q = 1000 m³/s)

Here, analyzing all the results for *Bridge Condition and at $Q = 200 \text{ m}^3/\text{sec}$* , while varying the Manning's coefficient n , the water surface elevation at the upstream side increases with smooth rate as the Manning's coefficient increases and at the downstream side between the Manning's coefficient 0.030 to 0.035 there is sudden increase in water surface elevation as the flow changes from subcritical to supercritical condition at which the Hydraulic Jump occurs.

Likewise as shown in **Table 3.7**, when there was no bridge at RS 928, the upstream side of the bridge at 50 m u/s from bridge axis (u/s RS 953) the water surface elevation was 145.43 m but after providing the bridge (1 bridge 2m pier 10 m pier spacing) the water surface elevation at the same river section (u/s RS 953) was found to be 146.53 m (i.e. afflux of 1.10 m). But at the downstream side which is 50 m d/s from the bridge axis when there was no bridge (d/s RS 903) the water surface elevation was 145.27 m but after providing the bridge (1 bridge 2m pier 10 m pier spacing) the water surface elevation at the same section of the river (d/s RS 903) it was found to be 144.53 m (i.e. decrease in water surface elevation by 0.74 m) for the same value of Manning's coefficient n . (0.025) and steady flow $200 \text{ m}^3/\text{sec}$. Also after providing the bridge the water surface elevation determined at u/s site RS 953 was 146.53 m whereas the critical water surface elevation was 145.30 m, it means that the water surface elevation observed was higher than the critical water surface elevation, which is the definition of subcritical flow at upstream side. Also at the d/s side of the bridge (d/s RS 903) the water surface elevation determined at RS 903 was 144.53 m whereas the critical water surface elevation was 145.12 m, it means that the water surface elevation observed was lower than the critical water surface elevation, which is the definition of supercritical flow at downstream side. It means that the flow changes from subcritical to the supercritical flow as a result of which the Hydraulic Jump occurs at d/s of bridge.

Similarly as shown in the same **Table 3.7**, and for Manning's coefficient n . 0.030 when there was no bridge at the upstream side of the bridge (u/s RS 953) the water surface elevation was 145.76 m but after providing the bridge (1 bridge 2m pier 10 m pier spacing) the water surface elevation at the same section of the river (u/s RS 953) was found to be 146.56 m (i.e. afflux of 0.80 m). But at the downstream side when there was no bridge (d/s RS 903) the water surface elevation was 145.61 m but after providing the bridge the water surface elevation at the same downstream side of the bridge (d/s RS 903) it was found to be 144.56 m (i.e. decrease in water surface elevation by 1.05 m) for the steady flow of 200

m^3/sec . Also after providing the bridge the water surface elevation determined at u/s side RS 953 was 146.56 m whereas the critical water surface elevation was 145.30 m, it means that the water surface elevation observed was higher than the critical water surface elevation which is the definition of subcritical flow at upstream side. Also at the d/s side of the bridge (d/s RS 903) the water surface elevation determined at RS 903 was 144.56 m whereas the critical water surface elevation was 145.12 m, it means that the water surface elevation observed was lower than the critical water surface elevation, which is the definition of supercritical flow at downstream side. It means that the flow changes from subcritical to the supercritical flow as a result of which the Hydraulic Jump occurs for the Manning's coefficient 0.030.

Hence, by observing all the Tables (*Table 3.7 to 3.11*) we found the similar trends of variation of water surface elevations with the changes in other related parameters and hence following conclusions have been made:

- ✓ As the Manning's coefficient n increases the water surface elevation increases, velocity decreases, flow area at bridge location increases, and thus Froude no. (Fr) decreases.
- ✓ But as the river cross section remaining constant for the same discharge, the flow may change from subcritical to the supercritical condition.
- ✓ Upstream flow condition is always subcritical but the downstream flow may be subcritical or supercritical depending upon the river section geometry.

3.4.2.2 Variation of Water Surface Profiles with Contraction and Expansion Reach Length

Contraction (upstream) Length 20 m

River Station	For Upstream Length = 20 m (Contraction Length = Expansion Length)																				
	Discharge	Q = 200 m ³ /s					Q = 400 m ³ /s					Q = 600 m ³ /s					Q = 800 m ³ /s				
	Min Ch El (m)	WSE (m)	CWSE (m)	Velocity (m/s)	Flow area m ²	Fr	WSE (m)	CWSE (m)	Velocity (m/s)	Flow area m ²	Fr	WSE (m)	CWSE (m)	Velocity (m/s)	Flow area m ²	Fr	WSE (m)	CWSE (m)	Velocity (m/s)	Flow area m ²	Fr
953.00*	141.93	146.51	145.30	2.95	67.82	0.53	148.50	146.66	3.48	114.97	0.52	150.07	147.74	3.80	157.89	0.52	151.40	148.66	4.01	199.33	0.52
928	Bridge																				
903.00*	141.86	144.56	145.12	6.11	32.73	1.49	145.42	146.42	7.99	50.06	1.67	146.18	147.45	8.95	67.04	1.68	146.83	148.34	9.70	82.51	1.69

Table 3.12: Variation of Water Surface Profiles with Contraction and Expansion Reach Length (for contraction length 20 m)

Contraction (upstream) Length 25 m

River Station	For Upstream Length = 25 m																				
	Discharge	Q = 200 m ³ /s					Q = 400 m ³ /s					Q = 600 m ³ /s					Q = 800 m ³ /s				
	Min Ch El (m)	WSE (m)	CWSE (m)	Velocity (m/s)	Flow area m ²	Fr	WSE (m)	CWSE (m)	Velocity (m/s)	Flow area m ²	Fr	WSE (m)	CWSE (m)	Velocity (m/s)	Flow area m ²	Fr	WSE (m)	CWSE (m)	Velocity (m/s)	Flow area m ²	Fr
953.00*	141.93	146.53	145.3	2.94	68.14	0.53	148.51	146.7	3.47	115.31	0.52	150.1	147.74	3.79	158.29	0.52	151.4	148.66	4	199.77	0.52
928	Bridge																				
903.00*	141.86	144.53	145.12	6.23	32.09	1.53	145.58	146.4	7.47	53.55	1.52	146.4	147.45	8.29	72.37	1.52	147.1	148.34	8.96	89.3	1.52

Table 3.13: Variation of Water Surface Profiles with Contraction and Expansion Reach Length (for contraction length 25 m)

Contraction (upstream) Length 30 m

River Station	For Upstream Length = 30 m																				
	Discharge	Q = 200 m ³ /s					Q = 400 m ³ /s					Q = 600 m ³ /s					Q = 800 m ³ /s				
	Min Ch El (m)	WSE (m)	CWSE (m)	Velocity (m/s)	Flow area m ²	Fr	WSE (m)	CWSE (m)	Velocity (m/s)	Flow area m ²	Fr	WSE (m)	CWSE (m)	Velocity (m/s)	Flow area m ²	Fr	WSE (m)	CWSE (m)	Velocity (m/s)	Flow area m ²	Fr
953.00*	141.93	146.54	145.3	2.92	68.45	0.53	148.53	146.7	3.46	115.67	0.52	150.1	147.74	3.78	158.68	0.52	151.4	148.66	4	200.19	0.52
928	Bridge																				
903.00*	141.86	144.5	145.12	6.36	31.47	1.57	145.55	146.4	7.57	52.86	1.55	146.4	147.45	8.38	71.56	1.54	147.1	148.34	9.04	88.45	1.54

Table 3.14: Variation of Water Surface Profiles with Contraction and Expansion Reach Length (for contraction length 30 m)

Contraction (upstream) Length 35 m

River Station	For Upstream Length = 35 m																				
	Discharge	Q = 200 m ³ /s					Q = 400 m ³ /s					Q = 600 m ³ /s					Q = 800 m ³ /s				
	Min Ch El (m)	WSE (m)	CWSE (m)	Velocity (m/s)	Flow area m ²	Fr	WSE (m)	CWSE (m)	Velocity (m/s)	Flow area m ²	Fr	WSE (m)	CWSE (m)	Velocity (m/s)	Flow area m ²	Fr	WSE (m)	CWSE (m)	Velocity (m/s)	Flow area m ²	Fr
953.00*	141.93	146.56	145.3	2.91	68.75	0.52	148.54	146.7	3.45	116.01	0.52	150.1	147.74	3.77	159.07	0.52	151.4	148.66	3.99	200.62	0.52
928	Bridge																				
903.00*	141.86	144.46	145.12	6.48	30.87	1.61	145.52	146.4	7.67	52.13	1.58	146.3	147.45	8.48	70.79	1.56	147	148.34	9.13	87.6	1.56

Table 3.15: Variation of Water Surface Profiles with Contraction and Expansion Reach Length (for contraction length 35 m)

Rearranging above data

For Q = 200 cumecs											
u/s RS 953					d/s RS 903					Contraction/ Expansion Length m	
WSE (m)	CWSE (m)	Velocity (m/s)	Flow area m ²	Fr	WSE (m)	CWSE (m)	Velocity (m/s)	Flow area m ²	Fr		
146.51	145.30	2.95	67.82	0.53	144.56	145.12	6.11	32.73	1.49	20	
146.53	145.30	2.94	68.14	0.53	144.53	145.12	6.23	32.09	1.53	25	
146.54	145.30	2.92	68.45	0.53	144.50	145.12	6.36	31.47	1.57	30	
146.56	145.30	2.91	68.75	0.52	144.46	145.12	6.48	30.87	1.61	35	

Table 3.16: Rearranging data for various Contraction Lengths (Q = 200 cumecs)

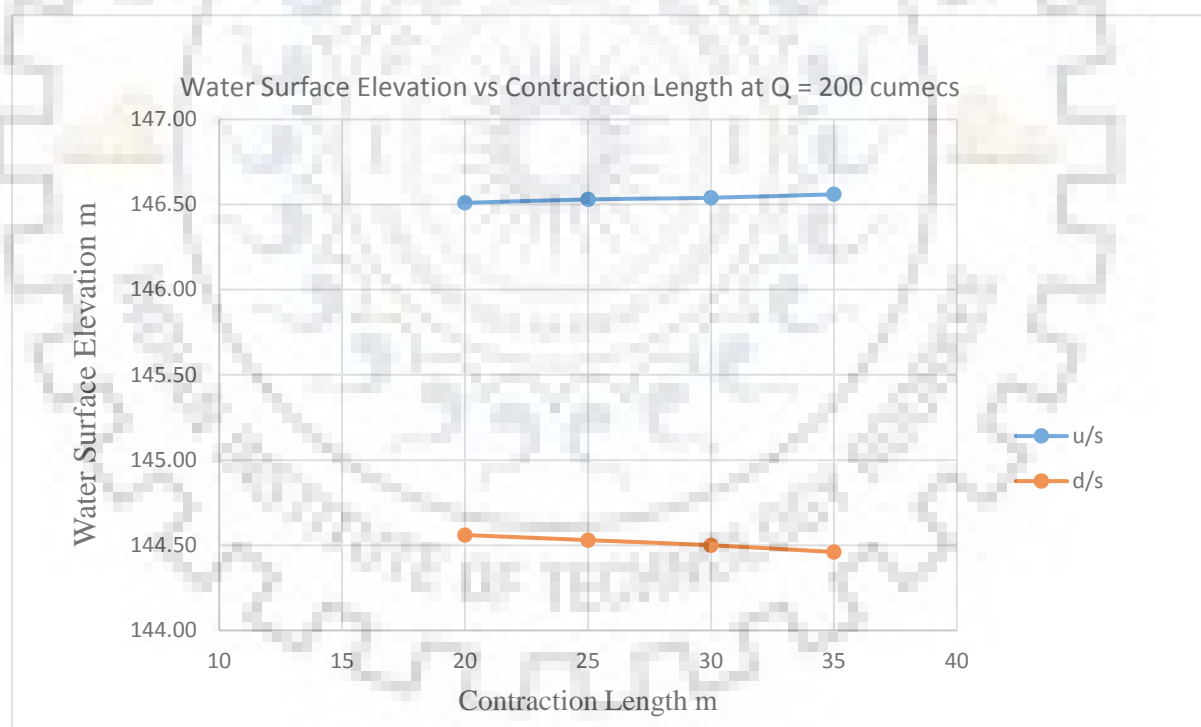


Figure 3.24: Water Surface Elevation vs Contraction Length at Q = 200 cumecs

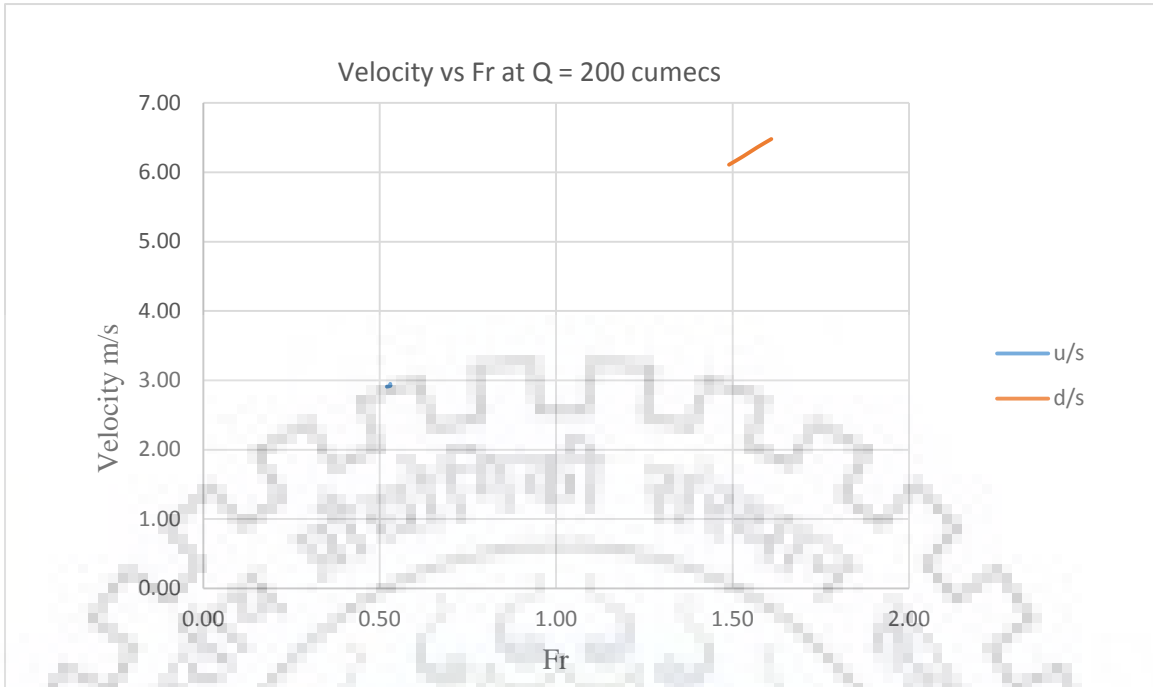


Figure 3.25: Velocity vs Fr

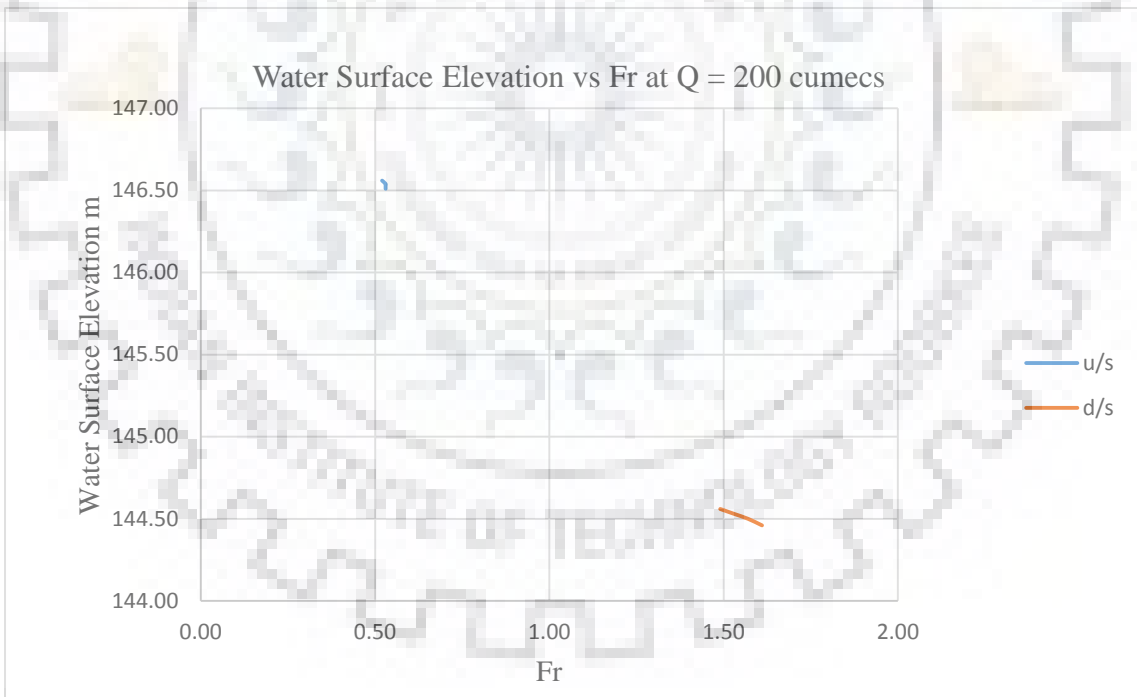


Figure 3.26: Water Surface Elevation vs Fr

For Q = 400 cumecs											
u/s RS 953					d/s RS 903					Contraction/ Expansion Length m	
WSE (m)	CWS E(m)	Velocity (m/s)	Flow area m ²	Fr	WSE (m)	CWSE (m)	Velocity (m/s)	Flow area m ²	Fr		
148.50	146.66	3.48	114.97	0.52	145.42	146.42	7.99	50.06	1.67	20	
148.51	146.66	3.47	115.3	0.52	145.58	146.42	7.47	53.55	1.52	25	
148.53	146.66	3.46	115.7	0.52	145.55	146.42	7.57	52.86	1.55	30	
148.54	146.66	3.45	116	0.52	145.52	146.42	7.67	52.13	1.58	35	

Table 3. 17: Rearranging data for various Contraction Lengths (Q = 200 cumecs)

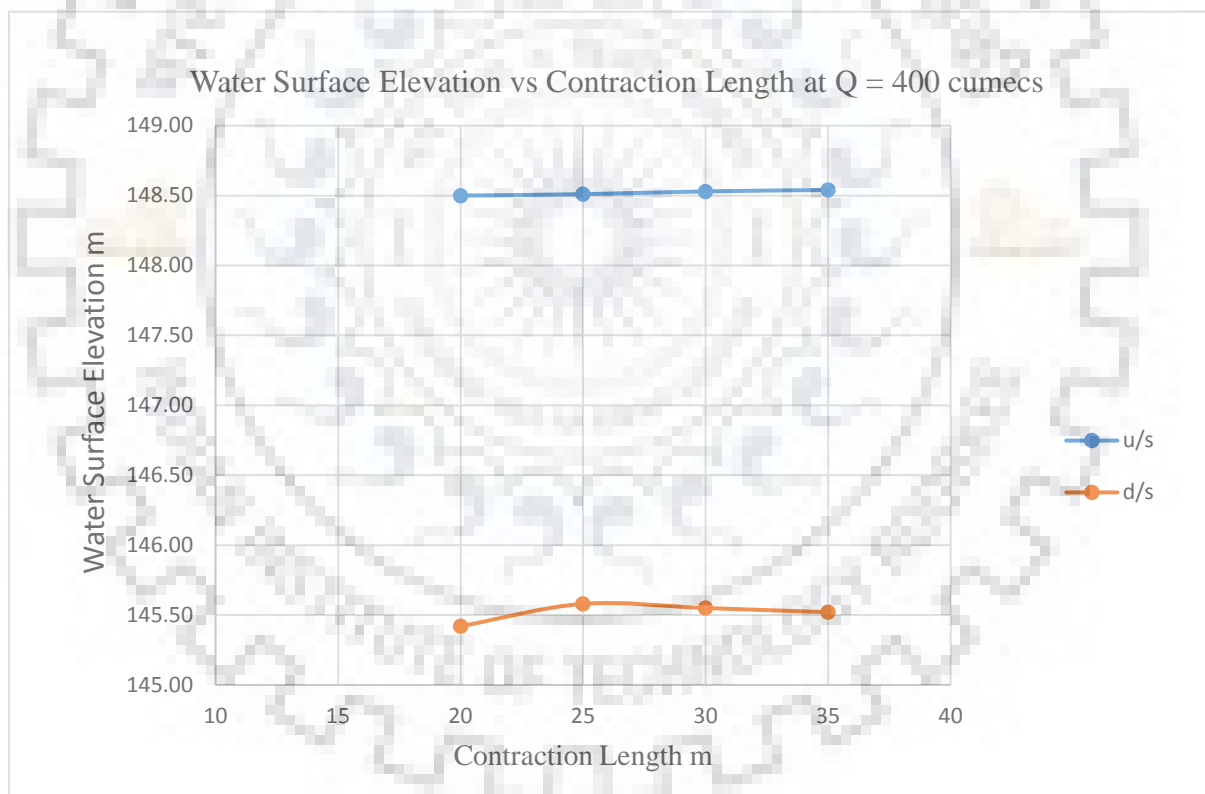


Figure 3.27: Water Surface Elevation vs Contraction Length at Q = 400 cumecs

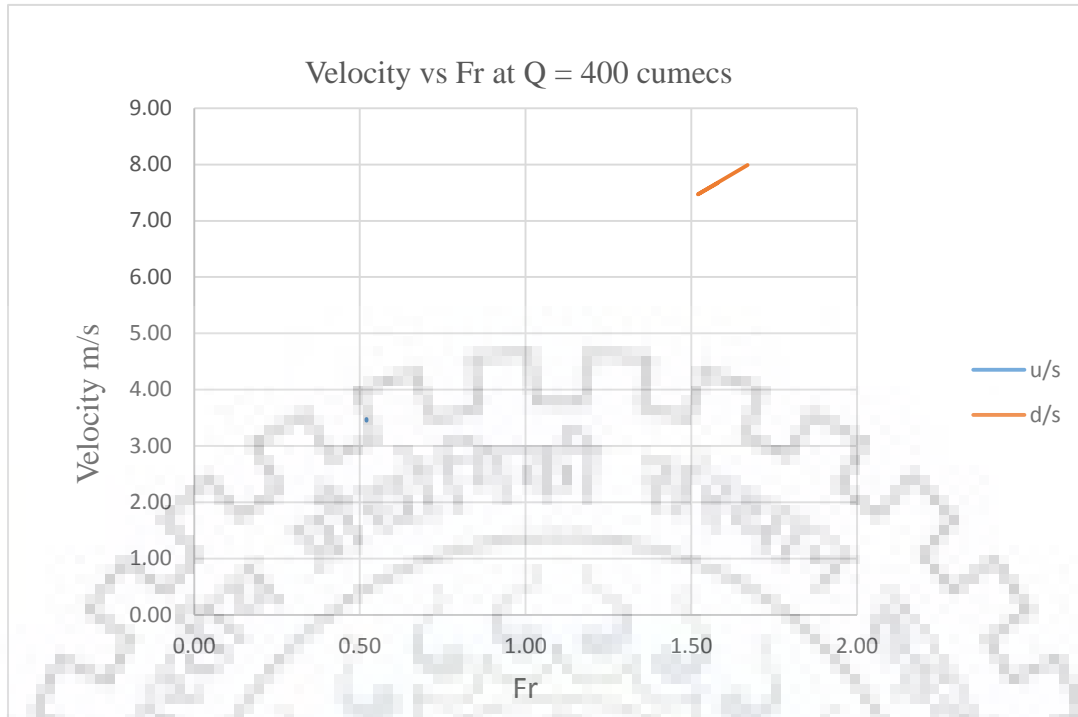


Figure 3.28: Velocity vs Fr

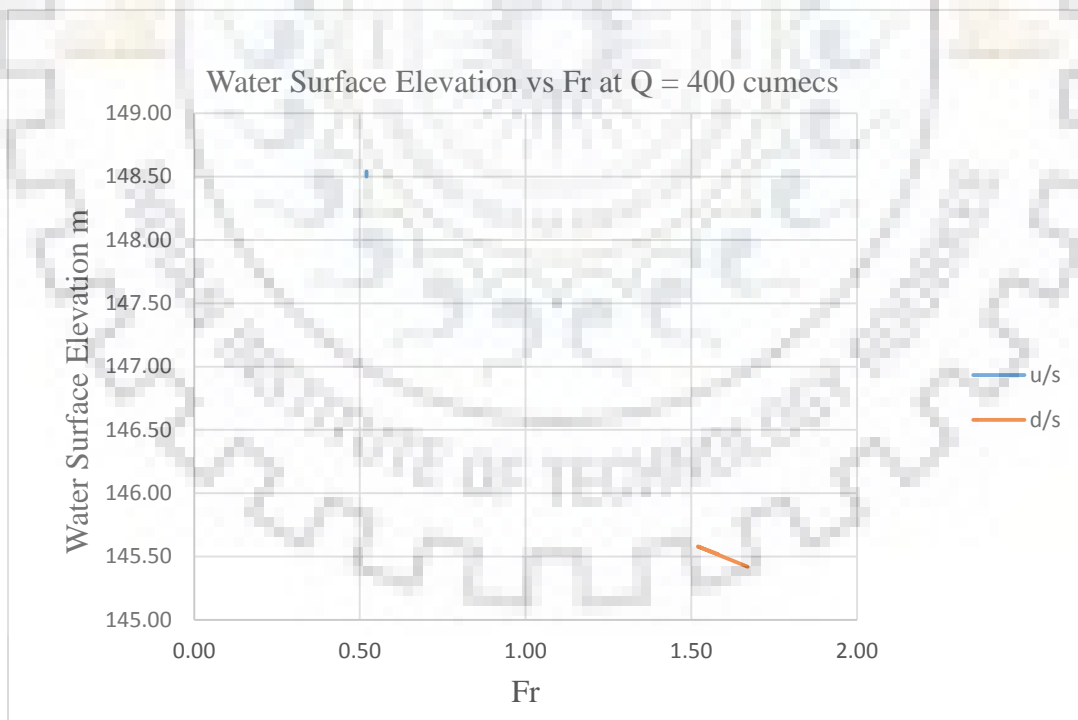


Figure 3.29: Water Surface Elevation vs Fr

For Q = 600 cumecs											
u/s RS 953					d/s RS 903					Contraction/ Expansion Length m	
WSE (m)	CWSE (m)	Velocity (m/s)	Flow area m ²	Fr	WSE (m)	CWSE (m)	Velocity (m/s)	Flow area m ²	Fr		
150.07	147.74	3.80	157.89	0.52	146.18	147.45	8.95	67.04	1.68	20	
150.08	147.74	3.79	158.3	0.52	146.4	147.45	8.29	72.37	1.52	25	
150.1	147.74	3.78	158.7	0.52	146.4	147.45	8.38	71.56	1.54	30	
150.11	147.74	3.77	159.1	0.52	146.3	147.45	8.48	70.79	1.56	35	

Table 3.18: Rearranging data for various Contraction Lengths (Q = 600 cumecs)

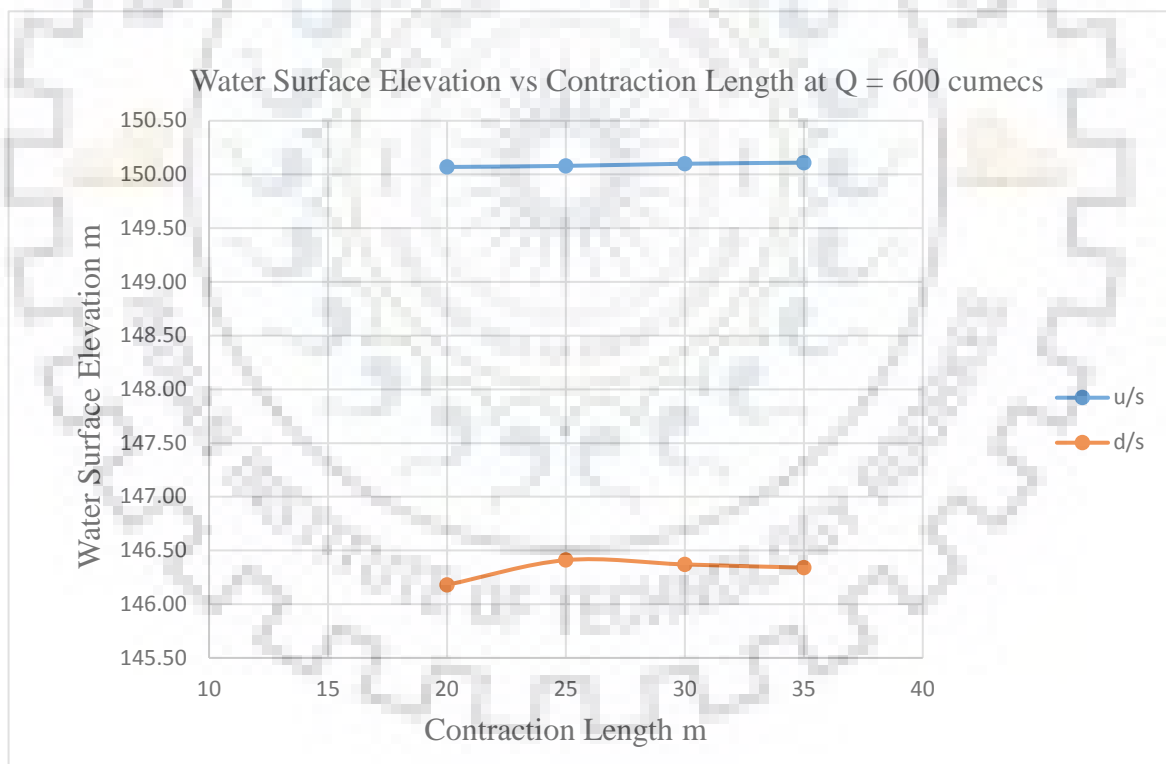


Figure 3.30: Water Surface Elevation vs Contraction Length at Q = 600 cumecs

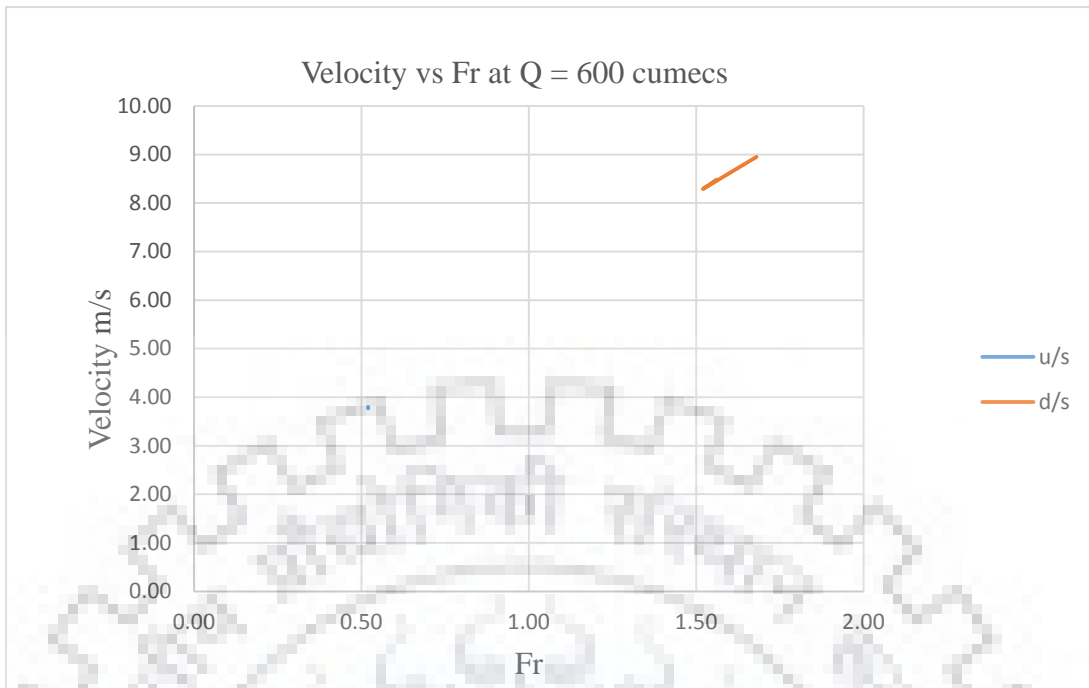


Figure 3.31: Velocity vs Fr

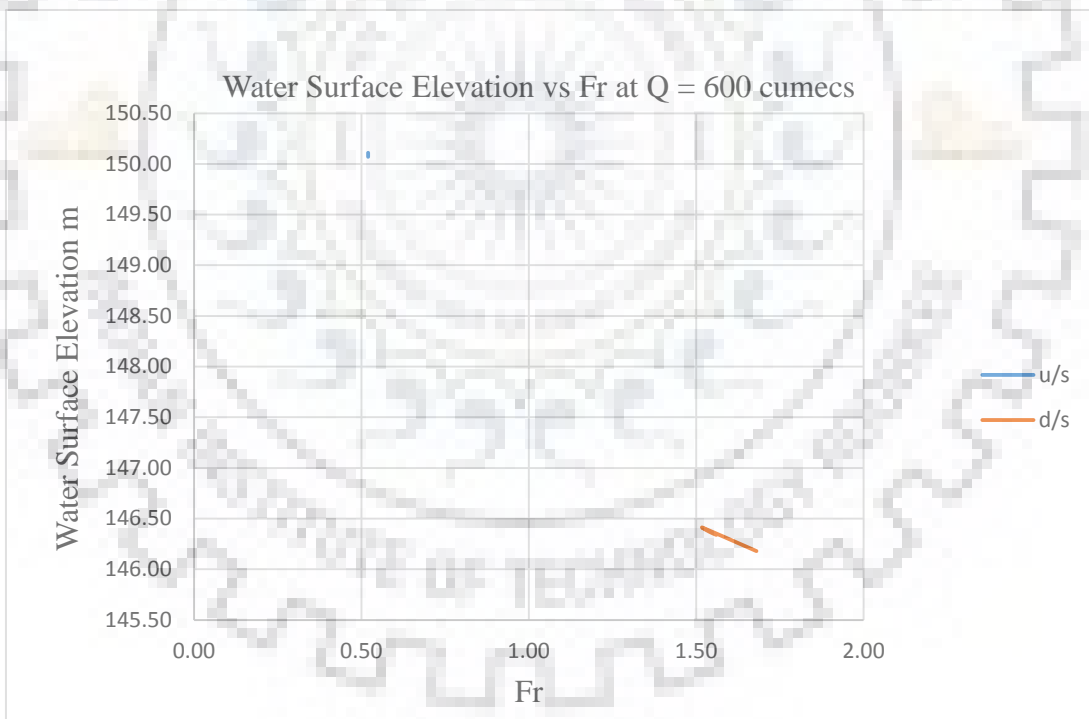


Figure 3.32: Water Surface Elevation vs Fr

For Q = 800 cumecs											
u/s RS 953					d/s RS 903					Contraction/ Expansion Length m	
WSE (m)	CWSE (m)	Velocity (m/s)	Flow area m ²	Fr	WSE (m)	CWSE (m)	Velocity (m/s)	Flow area m ²	Fr		
151.40	148.66	4.01	199.33	0.52	146.83	148.34	9.70	82.51	1.69	20	
151.4	148.66	4	199.77	0.52	147.1	148.34	8.96	89.3	1.52	25	
151.4	148.66	4	200.19	0.52	147.1	148.34	9.04	88.45	1.54	30	
151.4	148.66	3.99	200.62	0.52	147	148.34	9.13	87.6	1.56	35	

Table 3.19: Rearranging data for various Contraction Lengths (Q = 800 cumecs)

For Q = 1000 cumecs											
u/s RS 953					d/s RS 903					Contraction/ Expansion Length m	
WSE (m)	CWSE (m)	Velocity (m/s)	Flow area m ²	Fr	WSE (m)	CWSE (m)	Velocity (m/s)	Flow area m ²	Fr		
152.53	149.49	4.20	237.90	0.52	147.41	149.12	10.28	97.32	1.69	20	
152.5	149.49	4.2	238.37	0.52	147.7	149.12	9.49	105.33	1.52	25	
152.6	149.49	4.19	238.83	0.52	147.7	149.12	9.58	104.43	1.54	30	
152.6	149.49	4.18	239.31	0.52	147.7	149.12	9.66	103.51	1.56	35	

Table 3.20: Rearranging data for various Contraction Lengths (Q = 1000 cumecs)

Now, for the analysis of results for variation of Water Surface Profiles with Contraction and Expansion reach length, we take the contraction and expansion length equal to each other. i.e. 20.0, 25.0, 30.0 and 35.0 m towards upstream and downstream from the Bridge axis (at RS 928 m).

From **Table 3.16**, for steady flow $200 \text{ m}^3/\text{sec}$ and Manning's coefficient 0.025, the water surface elevation for contraction length 20.0 m (at upstream) RS 948 is 146.51 m whereas at d/s RS 908 it is found to be 144.56 m. The flow area at u/s side of bridge is 67.82 m^2 but it is only 32.73 m^2 at d/s side. Velocity at u/s side is 2.95 m/sec but at d/s side it is 6.11 m/sec which is very high as compared with velocity at u/s side. Obviously the Froude no. (Fr) also changes with the variation in all above parameters. Also at u/s side the critical water surface elevation is 145.30 m which is lower than the observed water surface elevation of 146.51 m at u/s side, it means the flow at u/s side is subcritical flow. But at the d/s side (RS 908) for expansion length 20.0 m, the water surface elevation observed is 144.56 m but the critical water surface elevation is 145.12 m. Here the critical water surface elevation is higher than the observed water surface elevation so the flow at d/s side is said to be in supercritical flow.

Similarly, from the same **Table 3.16**, the water surface elevation for contraction length 25.0 m at upstream RS 953 is 146.53 m whereas at d/s RS 903 it is found to be 144.53 m. The flow area at u/s side of bridge is 68.14 m^2 but it is only 32.09 m^2 at d/s side. Velocity at u/s side is 2.94 m/sec but at d/s side it is 6.23 m/sec which is very high as compared with velocity at u/s side. Obviously the Froude no. (Fr) also changes with the variation in all above parameters. Also at u/s side the critical water surface elevation is 145.30 m which is lower than the observed water surface elevation of 146.53 m at u/s side, it means the flow at u/s side is subcritical flow. But at the d/s side (RS 903) for expansion length 25.0 m, the water surface elevation observed is 144.53 m but the critical water surface elevation is 145.12 m. Here the critical water surface elevation is higher than the observed water surface elevation so the flow at d/s side is said to be in supercritical flow.

Observing all the results for contraction/expansion reach lengths, when the contraction/expansion reach lengths increases the water surface elevation at u/s side increases but decreases at d/s side. Similarly velocity at u/s side goes on decreasing but increasing at d/s side, flow area at u/s side increasing but decreasing at d/s side as a result

of which the Froude no. (Fr) at u/s side is almost constant but at d/s side it is continuously increasing as the contraction/expansion reach lengths increasing.

After analyzing all the above tables (*Table 3.12 to 3.20*) we have the following results/conclusions.

- ✓ When the contraction/expansion reach lengths increases for the particular steady flow, the water surface elevation at u/s side increases, velocity decreases, flow area decreases and thus the Fr remains constant. But at the d/s side water surface elevation initially increases or decreases depending on the river section geometry as a result of which the velocity, flow area and the Fr fluctuates accordingly.
- ✓ Flow changes from subcritical to supercritical depending on the river section geometry and flow condition.



3.4.2.3 Variation of Water Surface Profiles with Pier Size (2.0, 2.5, 3.0 m)

For 2.0 m pier size and $n = 0.025$, different pier spacing ($Q = 200 \text{ m}^3/\text{s}$)

Contraction or expansion length = 25.0 m

u/s RS 953					d/s RS 903					pier spacing m
WSE (m)	CWS (m)	Velocity (m/s)	Flow area m^2	Fr	WSE (m)	CWSE (m)	Velocity (m/s)	Flow area m^2	Fr	
146.53	145.3	2.94	68.14	0.53	144.53	145.12	6.23	32.09	1.53	10.00
146.52	145.3	2.95	67.9	0.53	144.49	145.12	6.37	31.4	1.57	15.00
146.4	145.3	3.06	65.26	0.56	144.57	145.12	6.1	32.81	1.48	20.00

Table 3.21: Variation of Water Surface Profiles with Pier Size (2 m pier size)

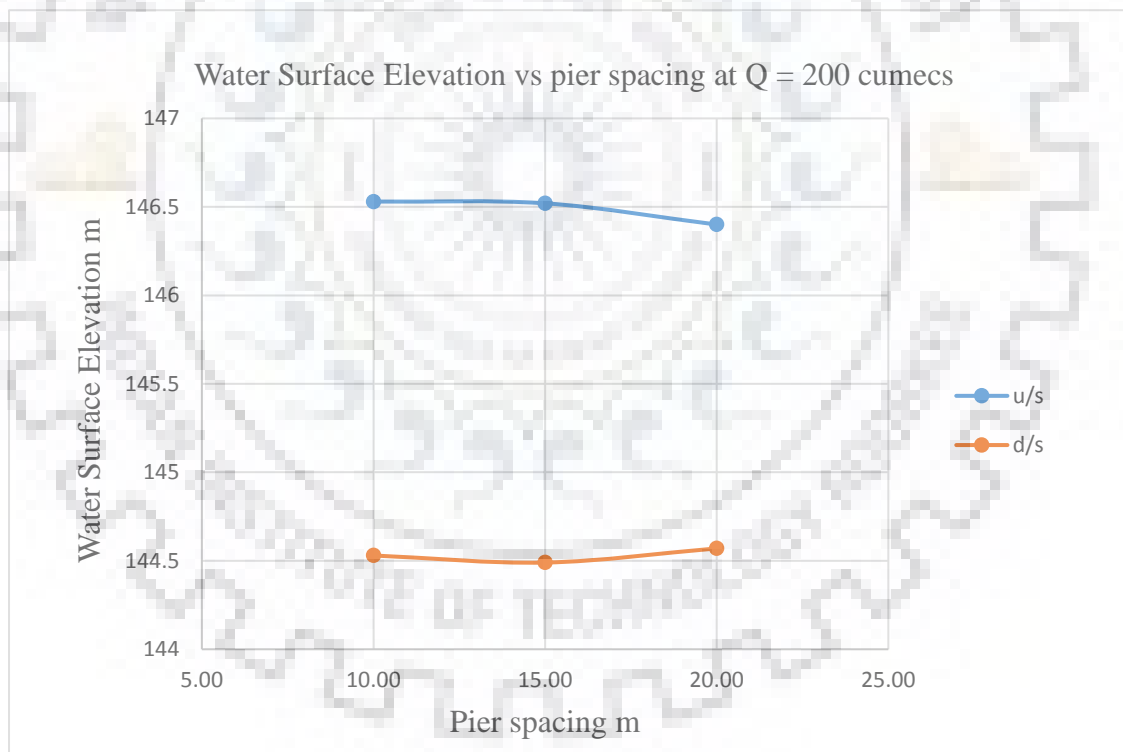


Figure 3.33: Water Surface Elevation vs pier spacing at $Q = 200$ cumecs

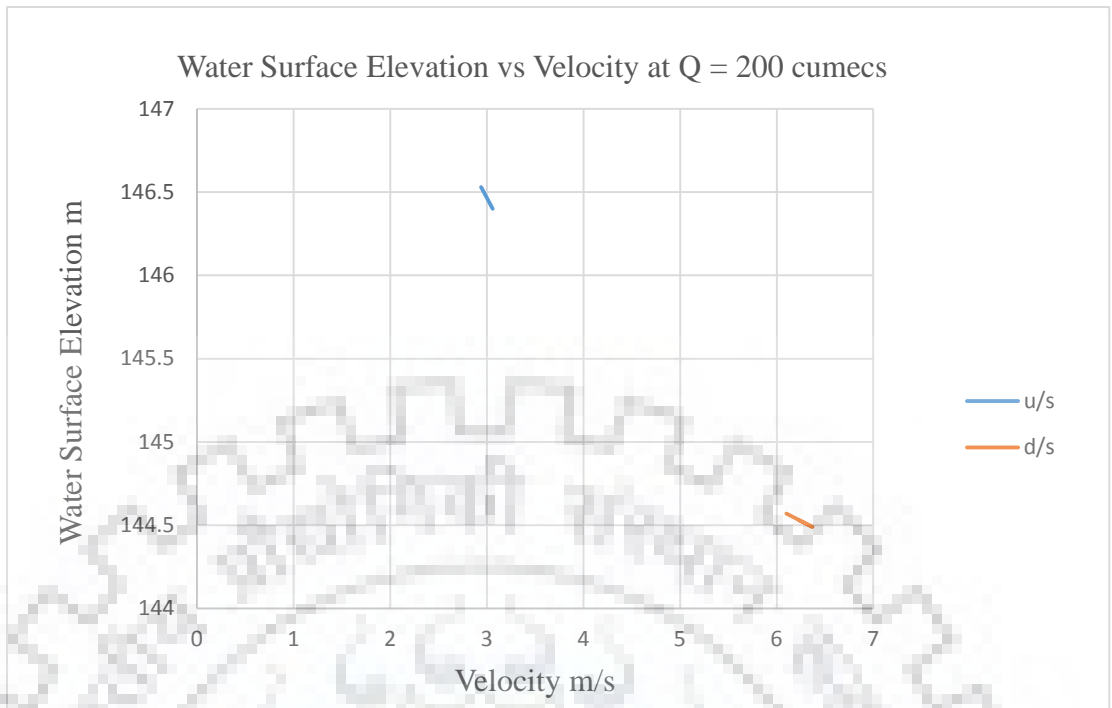


Figure 3.34: Water Surface Elevation vs Velocity

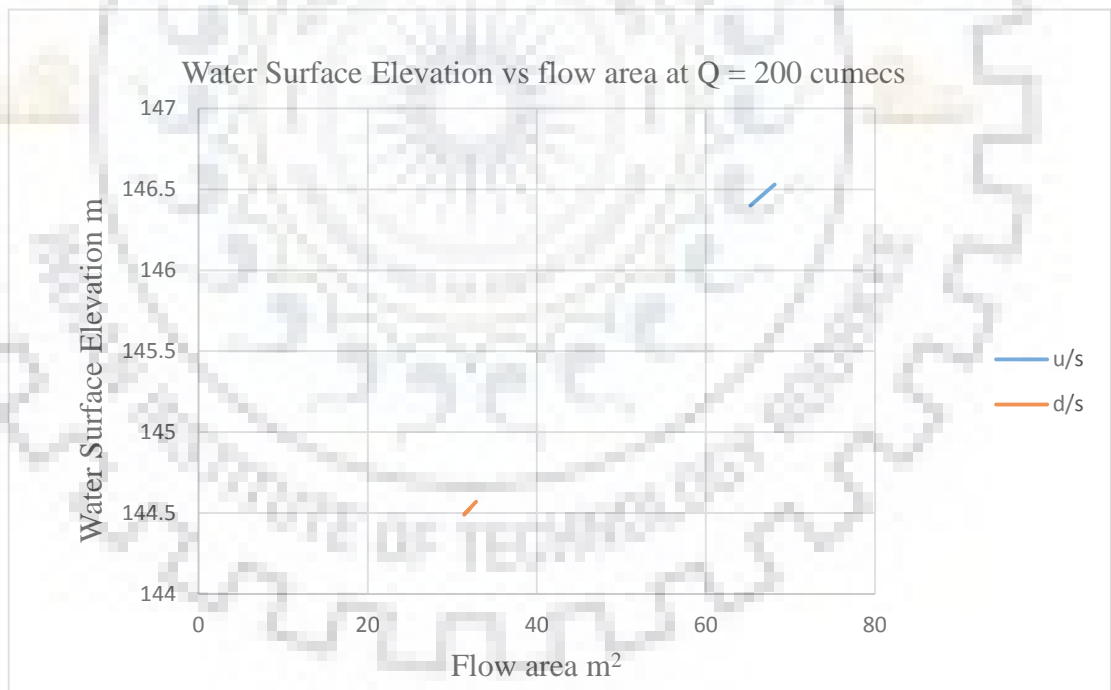


Figure 3.35: Water Surface Elevation vs flow area

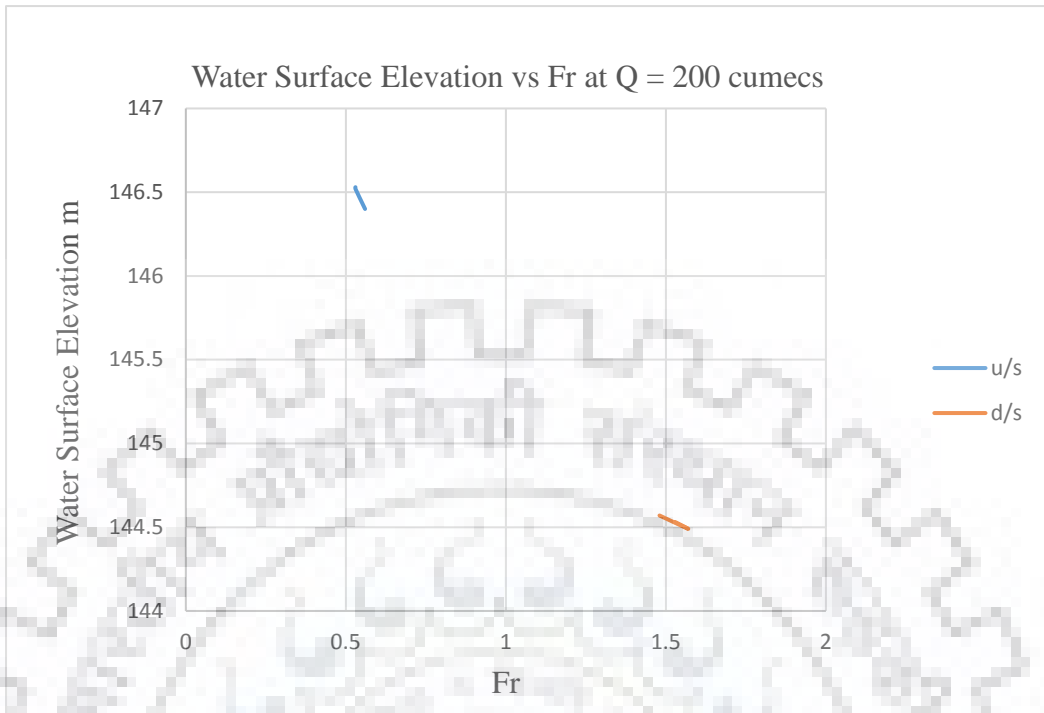


Figure 3.36: Water Surface Elevation vs Fr

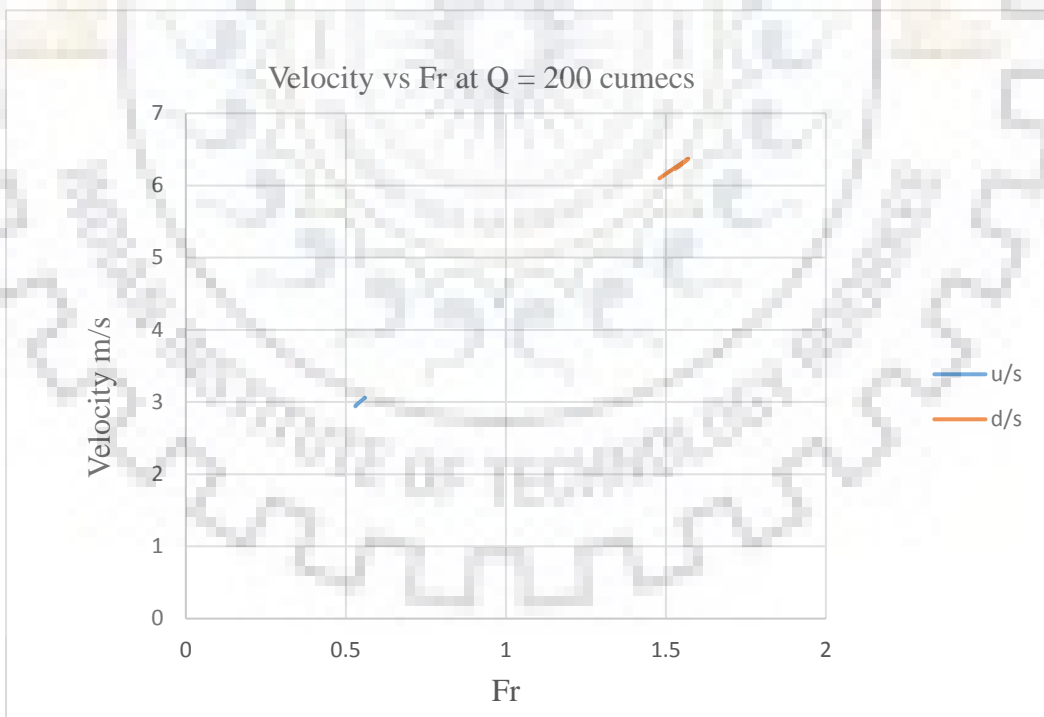


Figure 3.37: Velocity vs Fr

For 2.5 m pier size and $n = 0.025$, different pier spacing and $Q = 200 \text{ m}^3/\text{s}$

u/s RS 953					d/s RS 903					pier spacing m
WSE (m)	CWSE (m)	Velocity (m/s)	Flow area m^2	Fr	WSE (m)	CWSE (m)	Velocity (m/s)	Flow area m^2	Fr	
146.68	145.3	2.8	71.38	0.5	144.44	145.12	6.57	30.46	1.64	10.00
146.66	145.3	2.82	71.04	0.5	144.54	145.12	6.19	32.29	1.51	15.00
146.51	145.3	2.95	67.76	0.53	144.49	145.12	6.39	31.28	1.58	20.00

Table 3.22: Variation of Water Surface Profiles with Pier Size (2.5 m pier size)

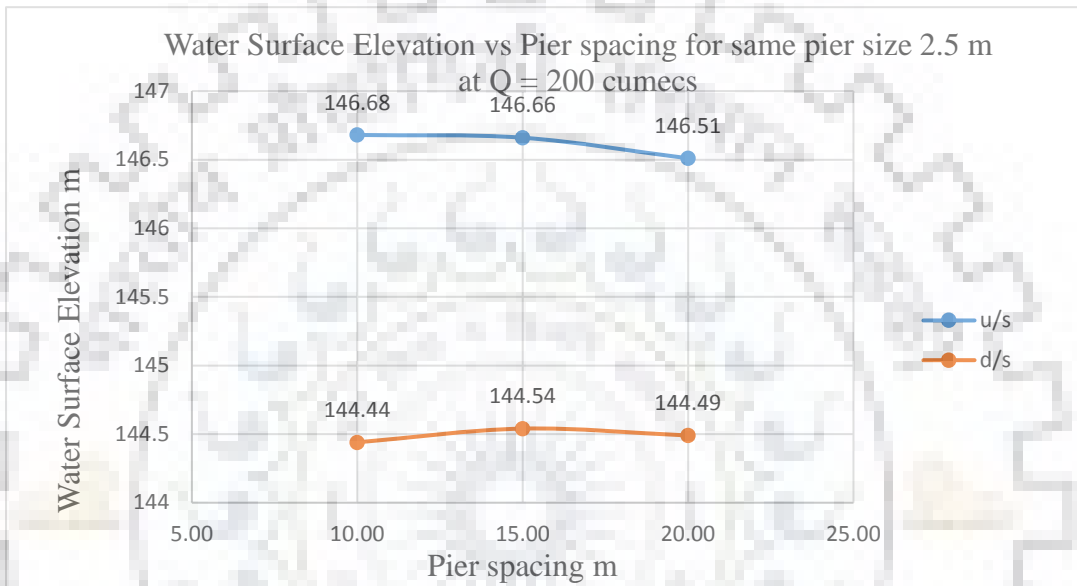


Figure 3.38: Water Surface Elevation vs Pier spacing for same pier size 2.5 m at $Q = 200$ cumecs

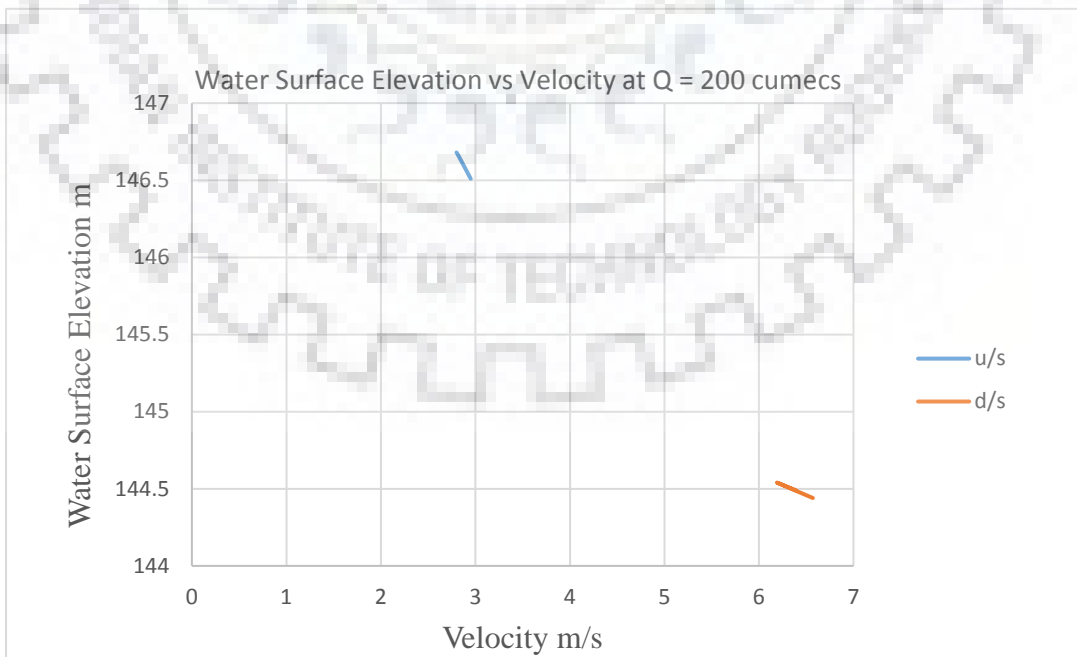


Figure 3.39: Water Surface Elevation vs Velocity

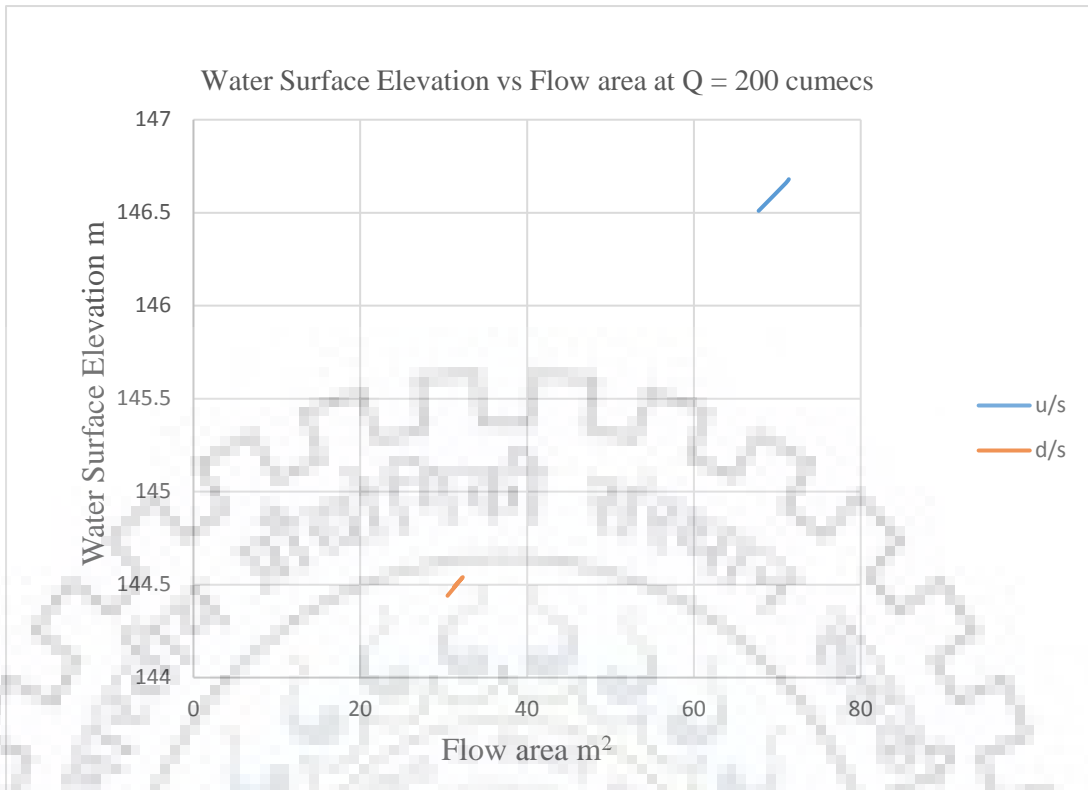


Figure 3.40: Water Surface Elevation vs Flow area

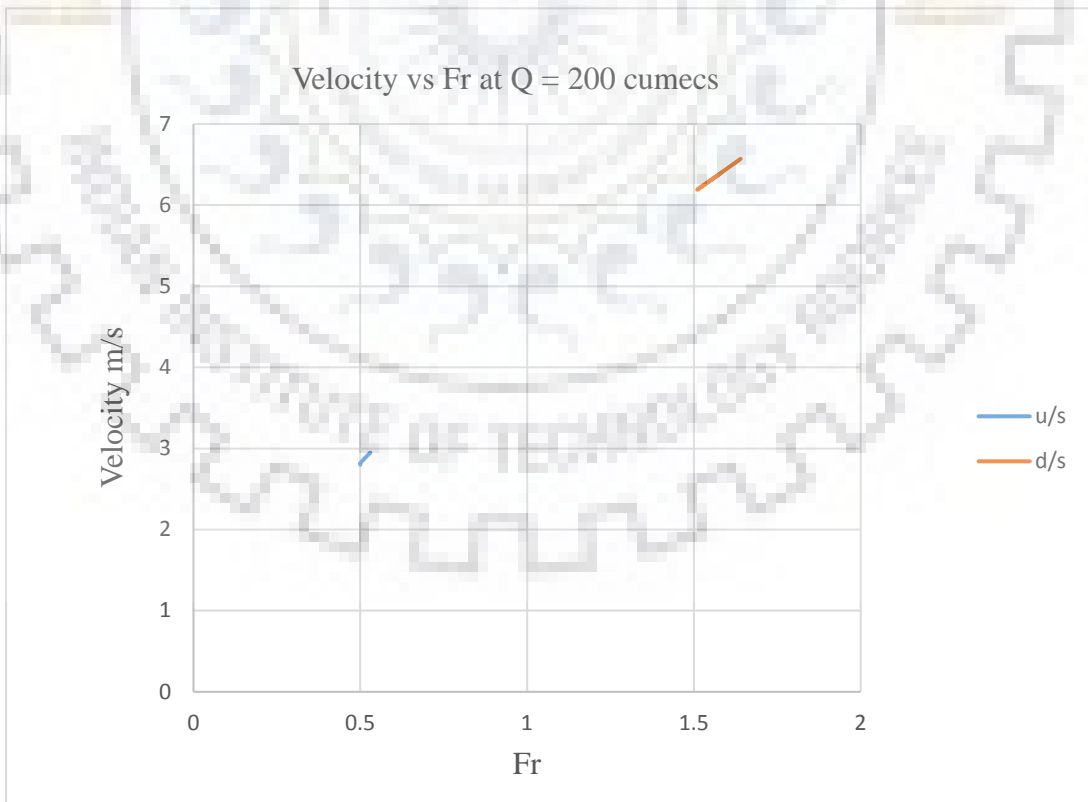


Figure 3.41: Velocity vs Fr

For 3.0 m pier size and $n = 0.025$, different pier spacing and $Q = 200 \text{ m}^3/\text{s}$

u/s RS 953					d/s RS 903					pier spacing m
WSE (m)	CWSE (m)	Velocity (m/s)	Flow area m^2	Fr	WSE (m)	CWSE (m)	Velocity (m/s)	Flow area m^2	Fr	
146.83	145.3	2.68	74.72	0.47	144.36	145.12	6.89	29.03	1.75	10.00
146.8	145.3	2.7	74.11	0.47	144.47	145.12	6.45	31	1.6	15.00
146.62	145.3	2.85	70.15	0.51	144.55	145.12	6.14	32.55	1.5	20.00

Table 3.23: Variation of Water Surface Profiles with Pier Size (3 m pier size)

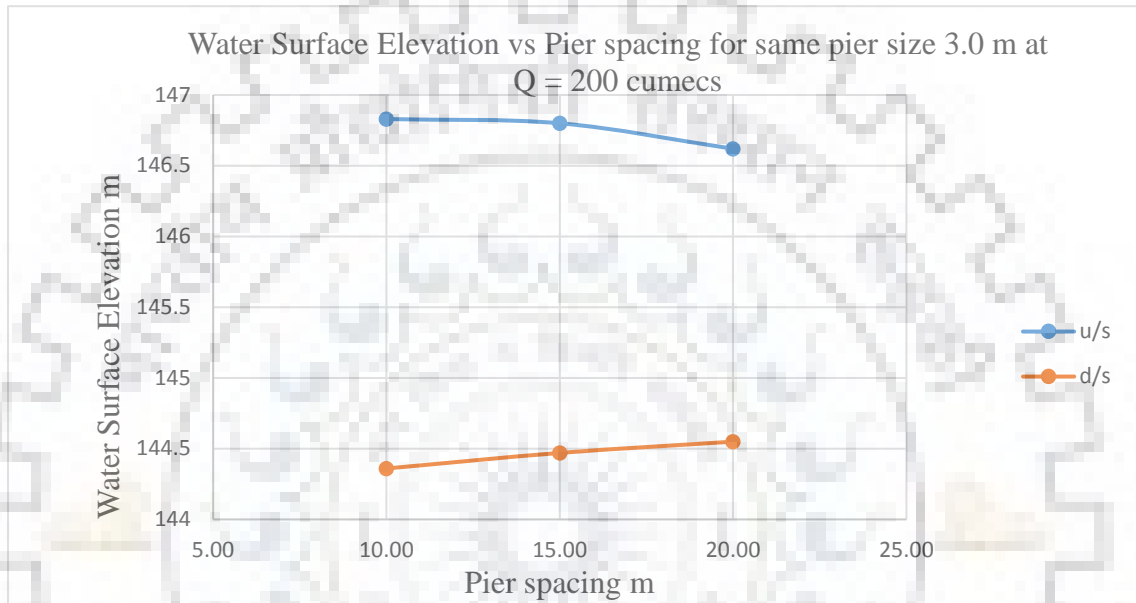


Figure 3.42: Water Surface Elevation vs Pier spacing for same pier size 3.0 m at $Q = 200$ cumecs

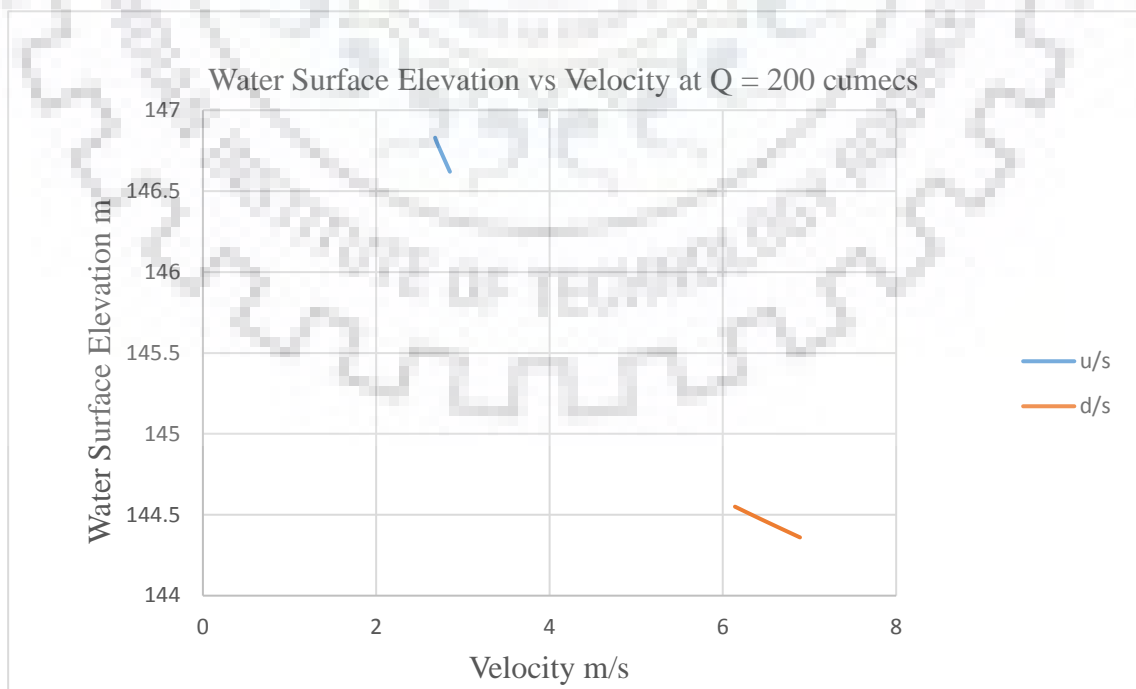


Figure 3.43: Water Surface Elevation vs Velocity

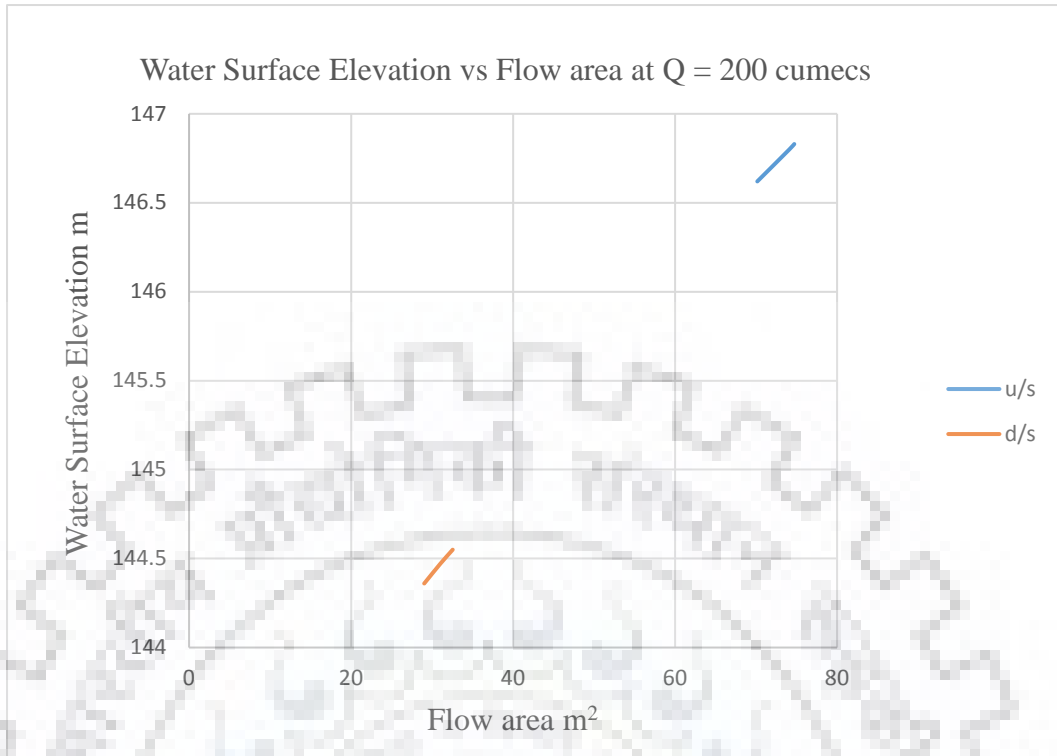


Figure 3.44: Water Surface Elevation vs Flow area at $Q = 200$ cumecs

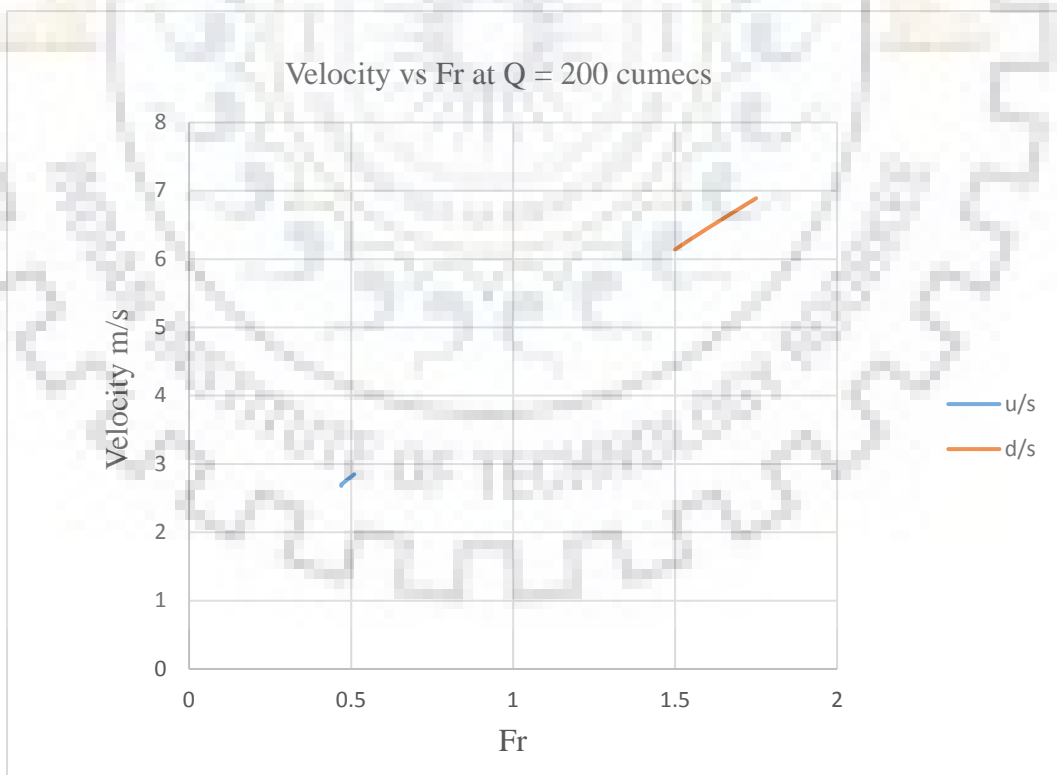


Figure 3.45: Velocity vs Fr

Now, for the analysis of variation of Water Surface Profiles with Pier Size, we take 2.0, 2.5 and 3.0 m pier size for different pier spacing and steady flow 200 m³/s.

Now, observing the results in **Table 3.21**, for 2.0 m pier size, when pier spacing is 10.0 m the WSE at u/s side (RS 953) is 146.53 m with CWSE 145.30 m. The velocity is 2.94 m/sec, flow area is 68.14 m² and Fr 0.53. But at d/s side (RS 903) the WSE is 144.53 m with CWSE 145.12 m and flow area of 32.09 m² with high velocity 6.23 m/sec and Fr 1.53. Also for the same pier size of 2.0 m but pier spacing 15.0 m the WSE at u/s side (RS 953) is 146.52 m with CWSE 145.30 m. The velocity is 2.95 m/sec, flow area is 67.90 m² and Fr 0.53. But at d/s side (RS 903) the WSE is 144.49 m with CWSE 145.12 m and flow area of 31.40 m² with high velocity 6.37 m/sec and Fr 1.57. And for pier spacing 20.0 m the WSE at u/s side (RS 953) is 146.40 m with CWSE 145.30 m. The velocity is 3.06 m/sec, flow area is 65.26 m² and Fr 0.56. But at d/s side (RS 903) the WSE is 144.57 m with CWSE 145.12 m and flow area of 32.81 m² with a high velocity 6.10 m/sec and Fr 1.48.

Similarly, for 2.5 m pier size, when pier spacing is 10.0 m the WSE at u/s side (RS 953) is 146.68 m with CWSE 145.30 m. The velocity is 2.80 m/sec, flow area is 71.38 m² and Fr 0.50. But at d/s side (RS 903) the WSE is 144.44 m with CWSE 145.12 m and flow area of 30.46 m² with a very high velocity 6.57 m/sec and Fr 1.64. Also for the same pier size of 2.5 m but pier spacing 15.0 m the WSE at u/s side (RS 953) is 146.66 m with CWSE 145.30 m. The velocity is 2.82 m/sec, flow area is 71.04 m² and Fr 0.50. But at d/s side (RS 903) the WSE is 144.54 m with CWSE 145.12 m and flow area of 32.29 m² with velocity 6.19 m/sec and Fr 1.51. And for pier spacing 20.0 m the WSE at u/s side (RS 953) is 146.51 m with CWSE 145.30 m. The velocity is 2.95 m/sec, flow area is 67.76 m² and Fr 0.53. But at d/s side (RS 903) the WSE is 144.49 m with CWSE 145.12 m and flow area of 31.28 m² with a velocity 6.39 m/sec and Fr 1.58.

And, for 3.0 m pier size, when pier spacing is 10.0 m the WSE at u/s side (RS 953) is 146.83 m with CWSE 145.30 m. The velocity is 2.68 m/sec, flow area is 74.72 m² and Fr 0.47. But at d/s side (RS 903) the WSE is 144.36 m with CWSE 145.12 m and flow area of 29.03 m² with a very high velocity 6.89 m/sec and Fr 1.75. Also for the same pier size of 3.0 m but pier spacing 15.0 m the WSE at u/s side (RS 953) is 146.80 m with CWSE 145.30 m. The velocity is 2.70 m/sec, flow area is 74.11 m² and Fr 0.47. But at d/s side (RS 903) the WSE is 144.47 m with CWSE 145.12 m and flow area of 31.00 m² with

velocity 6.45 m/sec and Fr 1.60. And for pier spacing 20.0 m the WSE at u/s side (RS 953) is 146.62 m with CWSE 145.30 m. The velocity is 2.85 m/sec, flow area is 70.15 m² and Fr 0.51. But at d/s side (RS 903) the WSE is 144.55 m with CWSE 145.12 m and flow area of 32.55 m² with a velocity 6.14 m/sec and Fr 1.50.

Comparing all the results above (as shown in **Table 3.21 to 3.23**) we can conclude the following:

- with different pier spacing of 10.0, 15.0 and 20.0 m and for different pier size (2.0, 2.5 and 3.0 m), when the pier spacing increases for a *particular pier size (say 2.0 m)*, u/s WSE decreases, velocity increases, flow area decreases and Fr also increases. But at the d/s side when pier spacing increases WSE may increase or decrease as a result of which velocity, flow area and Fr may also increase or decrease accordingly which is mainly due to the flow regime and river section geometry.
- The flow at u/s side is always at subcritical flow but may change to supercritical flow at d/s side of bridge.

3.4.2.4 Variation of Water Surface Profiles with Pier Spacing (10.0, 15.0 and 20.0 m)

For 10.0 m pier spacing and $n = 0.025$, $Q = 200 \text{ m}^3/\text{s}$

u/s RS 953					d/s RS 903					pier size m
WSE (m)	CWSE (m)	Velocity (m/s)	Flow area m^2	Fr	WSE (m)	CWSE (m)	Velocity (m/s)	Flow area m^2	Fr	
146.53	145.3	2.94	68.14	0.53	144.53	145.12	6.23	32.09	1.53	2.00
146.68	145.3	2.8	71.38	0.5	144.44	145.12	6.57	30.46	1.64	2.50
146.83	145.3	2.68	74.72	0.47	144.36	145.12	6.89	29.03	1.75	3.00

Table 3.24: Variation of Water Surface Profiles with Pier Spacing (10 m pier spacing)

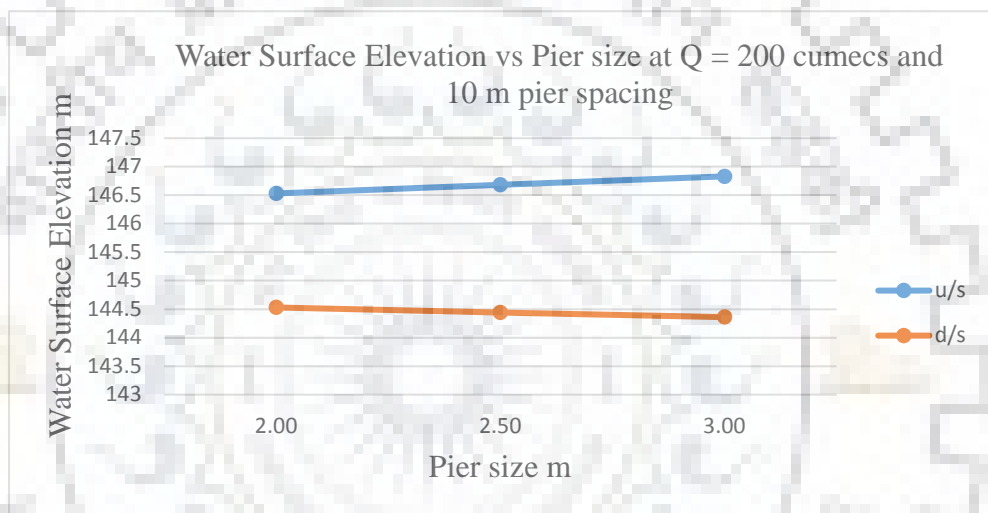


Figure 3.46: Water Surface Elevation vs Pier size at $Q = 200$ cumecs and 10 m pier spacing

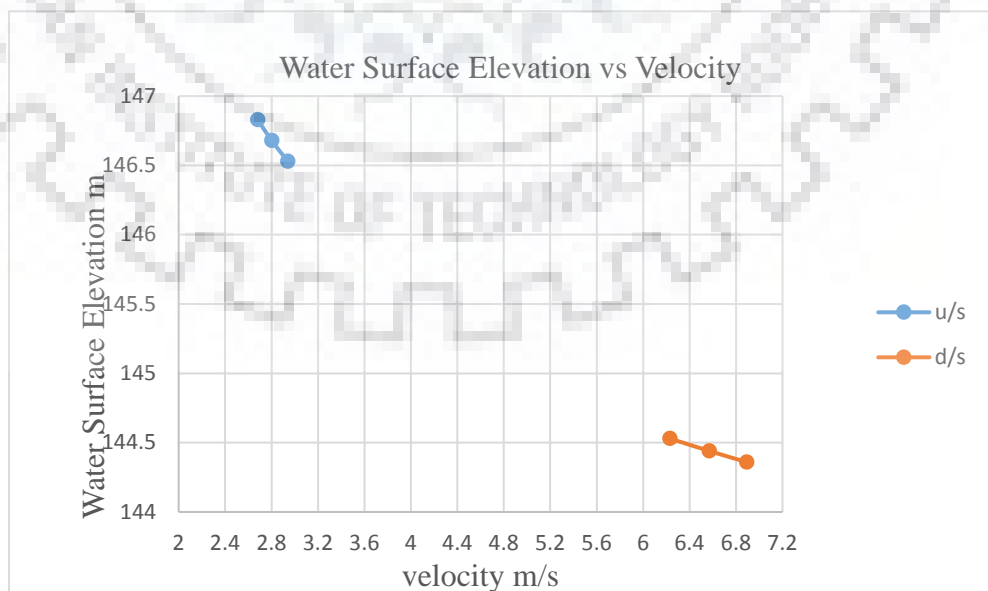


Figure 3.47: Water Surface Elevation vs Velocity

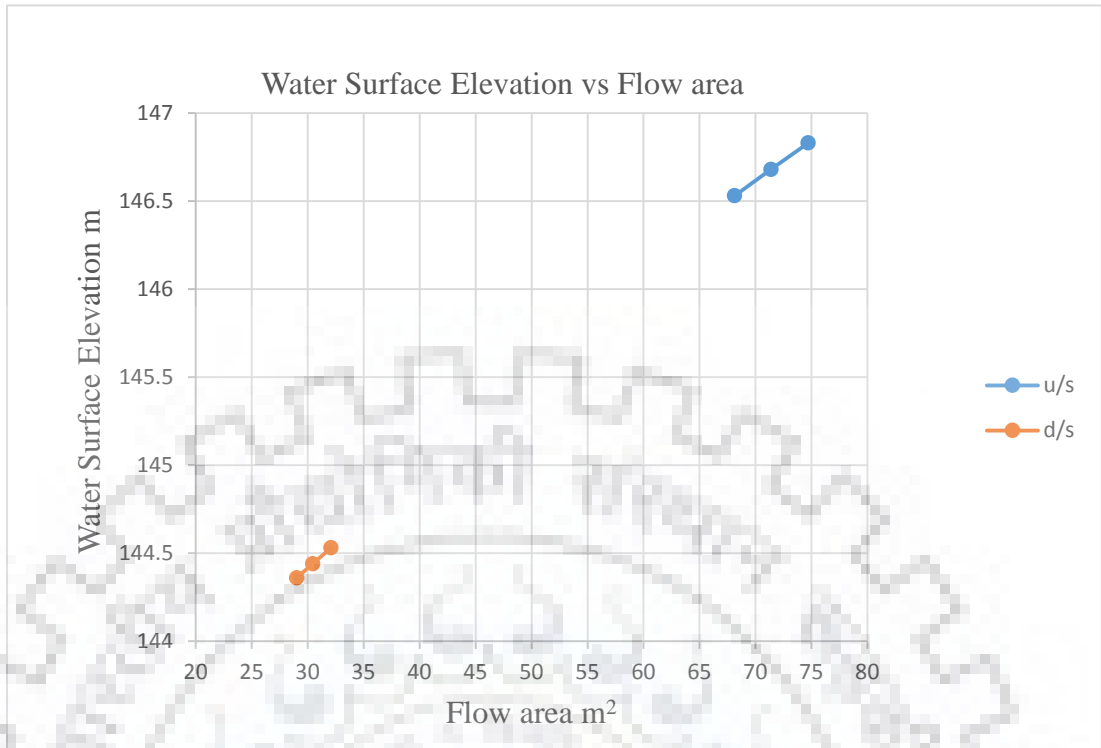


Figure 3.48: Water Surface Elevation vs Flow area

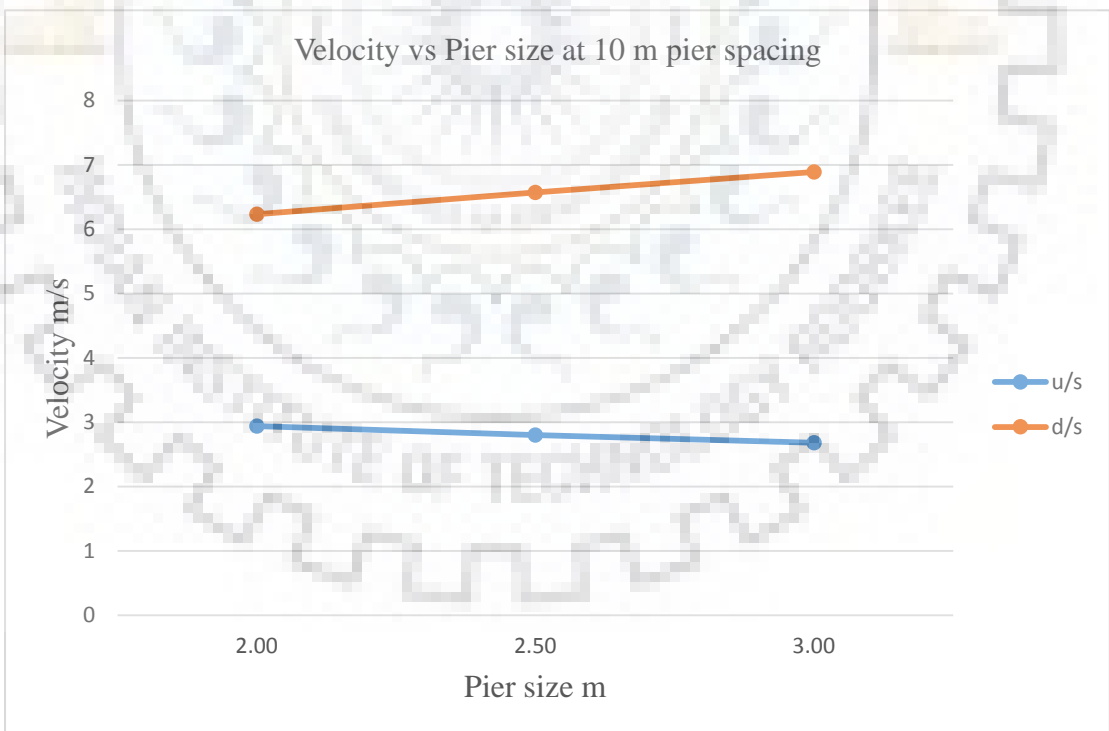


Figure 3.49: Velocity vs Pier size

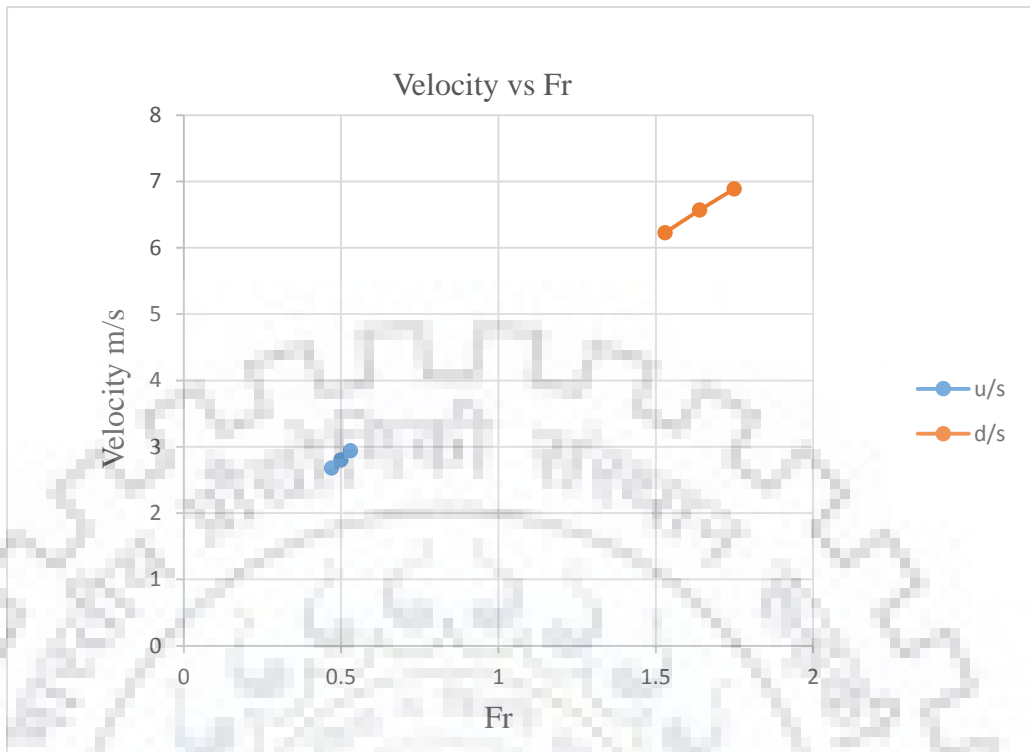


Figure 3.50: Velocity vs Fr

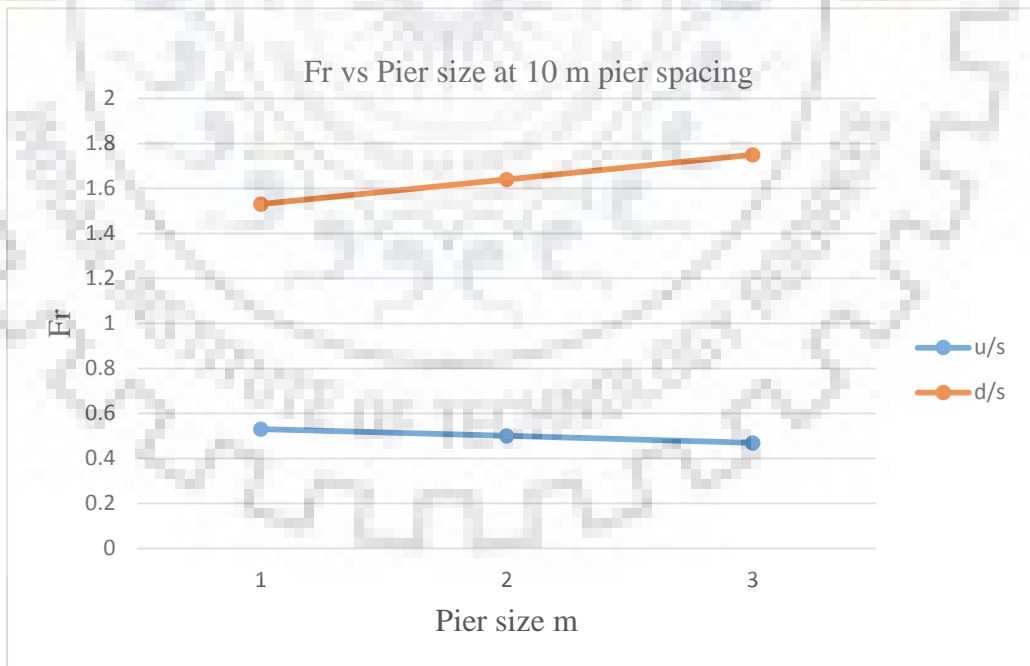


Figure 3.51: Fr vs Pier size

15.0 m pier spacing and $n = 0.025$, $Q = 200 \text{ m}^3/\text{s}$

u/s RS 953					d/s RS 903					Pier size m
WSE (m)	CWSE (m)	Velocity (m/s)	Flow area m^2	Fr	WSE (m)	CWSE (m)	Velocity (m/s)	Flow area m^2	Fr	
146.52	145.3	2.95	67.9	0.53	144.49	145.12	6.37	31.4	1.57	2.00
146.66	145.3	2.82	71.04	0.5	144.54	145.12	6.19	32.29	1.51	2.50
146.8	145.3	2.7	74.11	0.47	144.47	145.12	6.45	31	1.6	3.00

Table 3.25: Variation of Water Surface Profiles with Pier Spacing (15 m pier spacing)

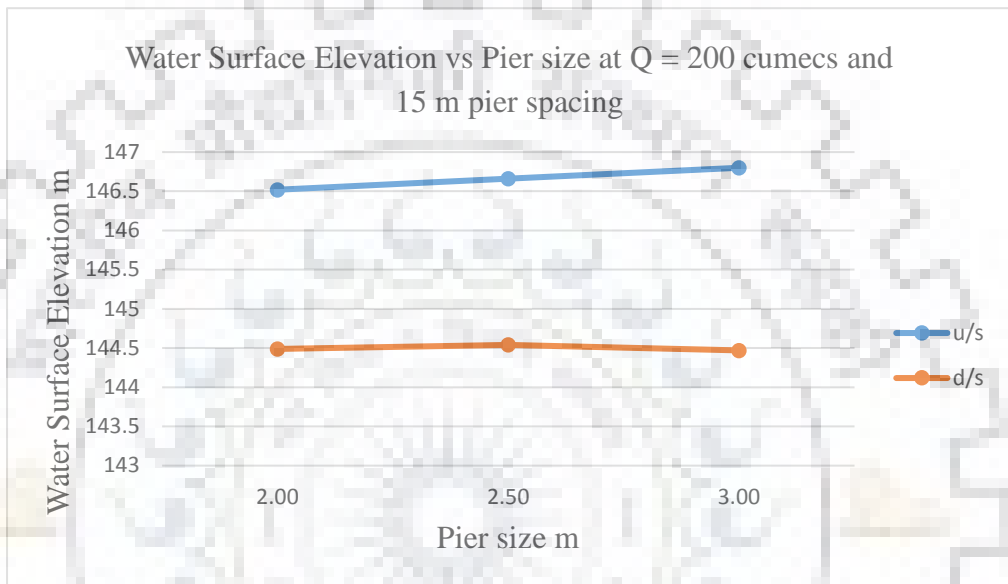


Figure 3.52: Water Surface Elevation vs Pier size at $Q = 200$ cumecs and 15 m pier spacing

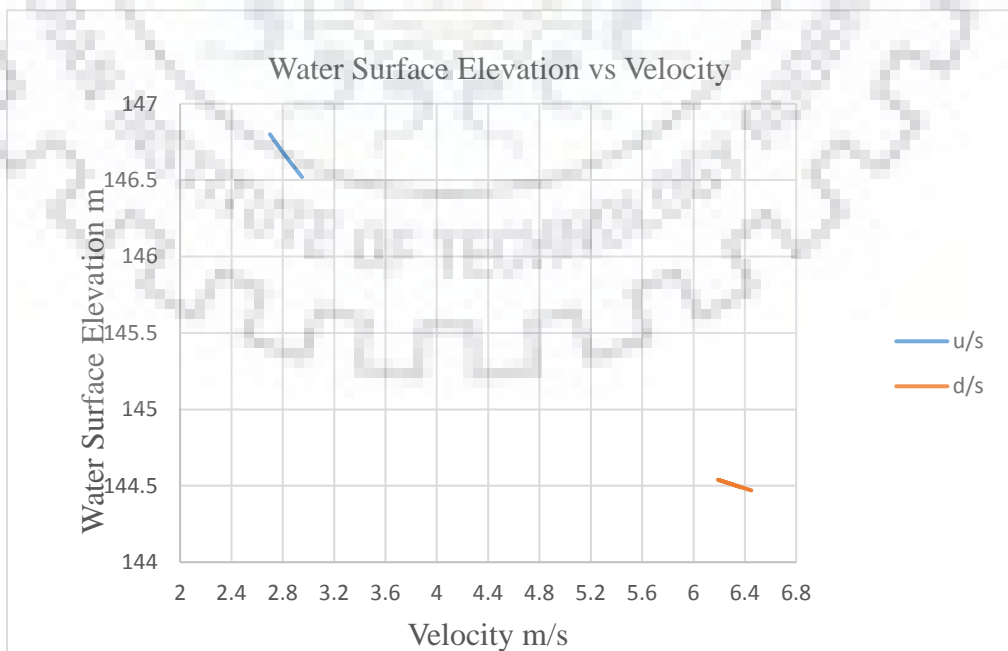


Figure 3.53: Water Surface Elevation vs Velocity

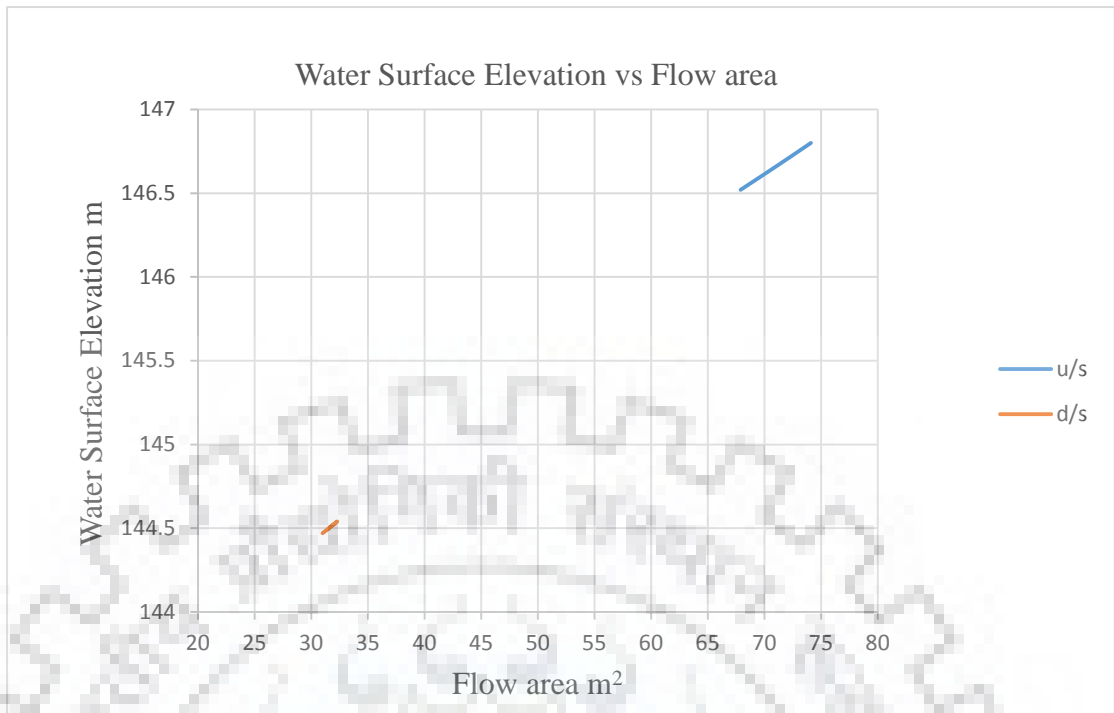


Figure 3.54: Water Surface Elevation vs Flow area

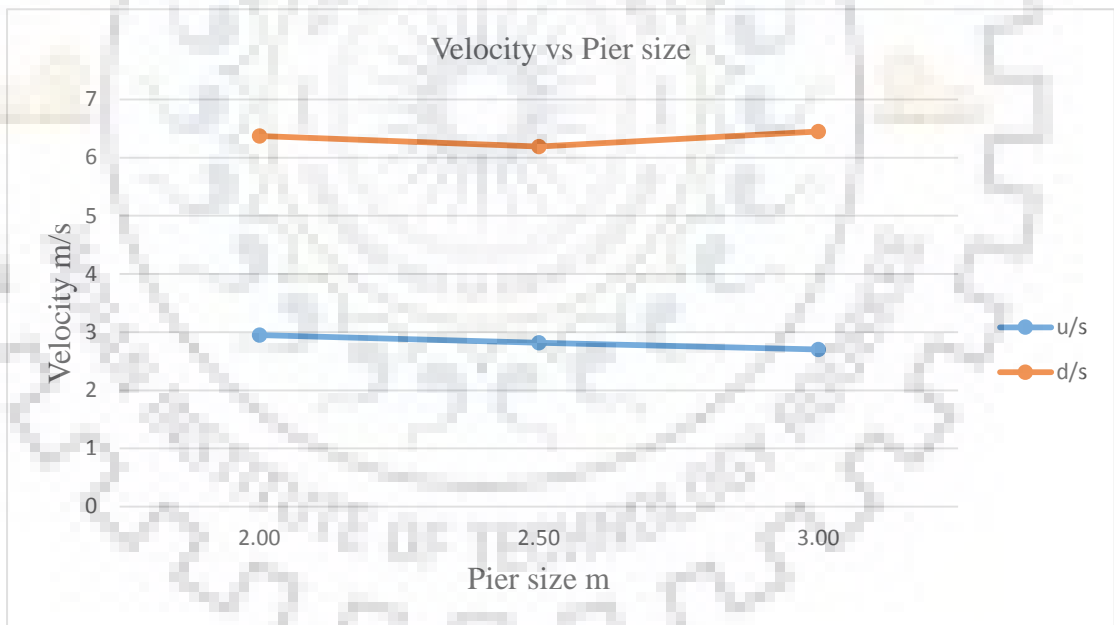


Figure 3.55: Velocity vs Pier size

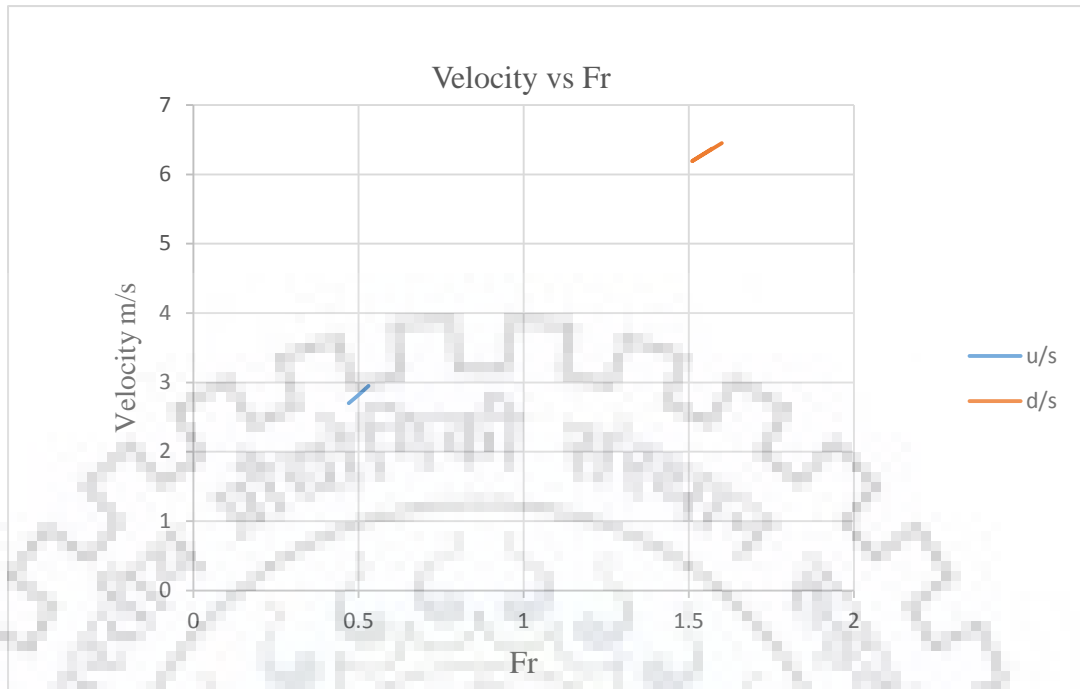


Figure 3.56: Velocity vs Fr

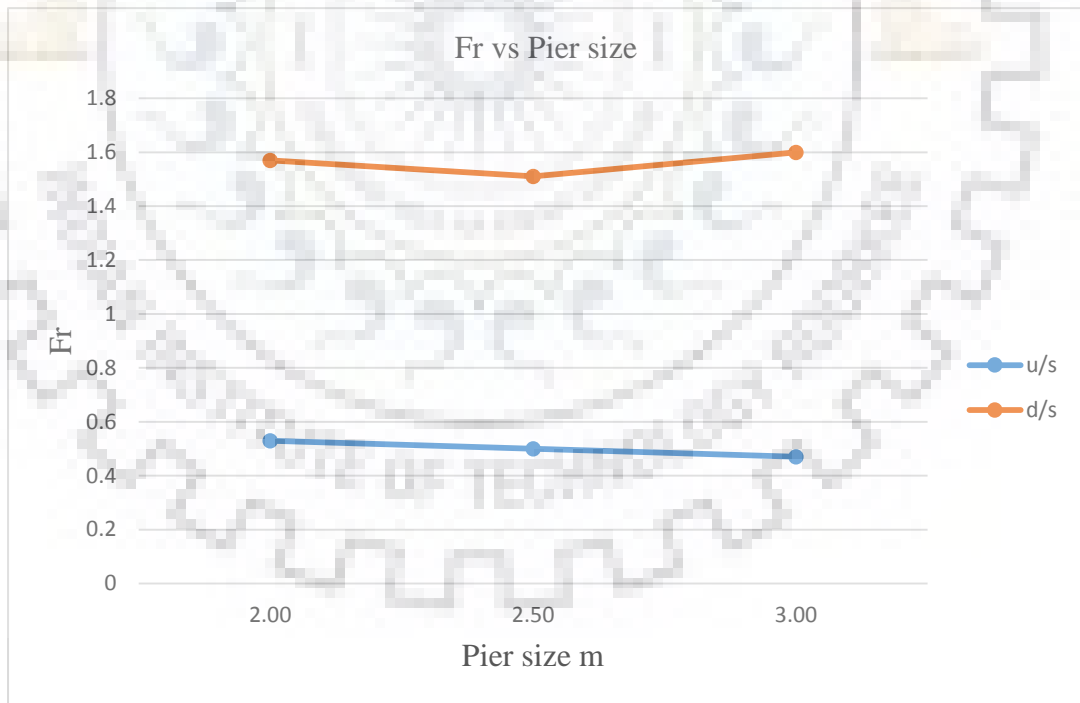


Figure 3.57: Fr vs Pier size

For 20.0 m pier spacing and $n = 0.025$, $Q = 200 \text{ m}^3/\text{s}$

u/s RS 953					d/s RS 903					pier size m
WSE (m)	CWSE (m)	Velocity (m/s)	Flow area m^2	Fr	WSE (m)	CWSE (m)	Velocity (m/s)	Flow area m^2	Fr	
146.4	145.3	3.06	65.26	0.56	144.57	145.12	6.1	32.81	1.48	2.00
146.51	145.3	2.95	67.76	0.53	144.49	145.12	6.39	31.28	1.58	2.50
146.62	145.3	2.85	70.15	0.51	144.55	145.12	6.14	32.55	1.5	3.00

Table 3.26: Variation of Water Surface Profiles with Pier Spacing (20 m pier spacing)

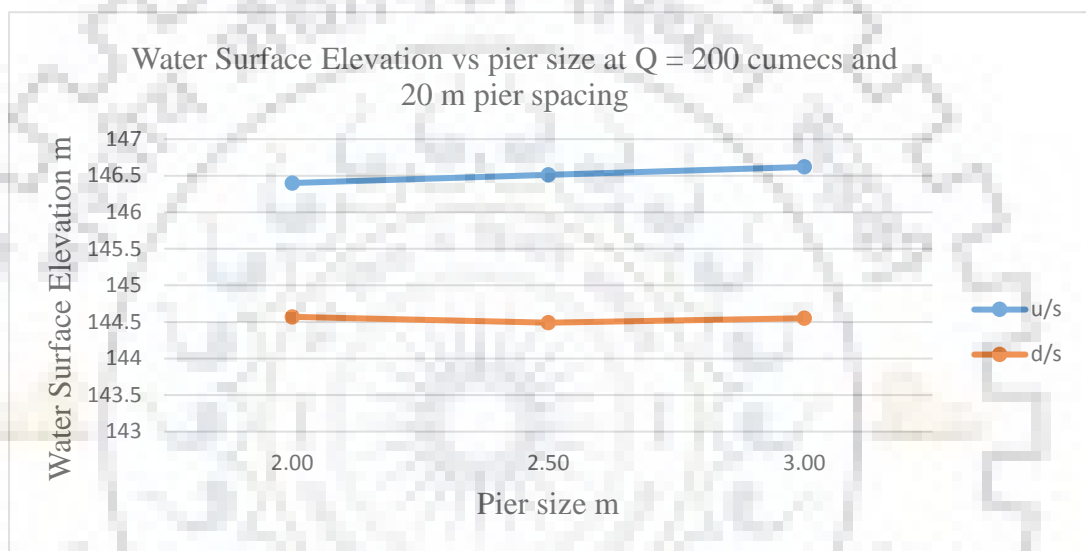


Figure 3.58: Water Surface Elevation vs pier size at $Q = 200$ cumecs and 20 m pier spacing

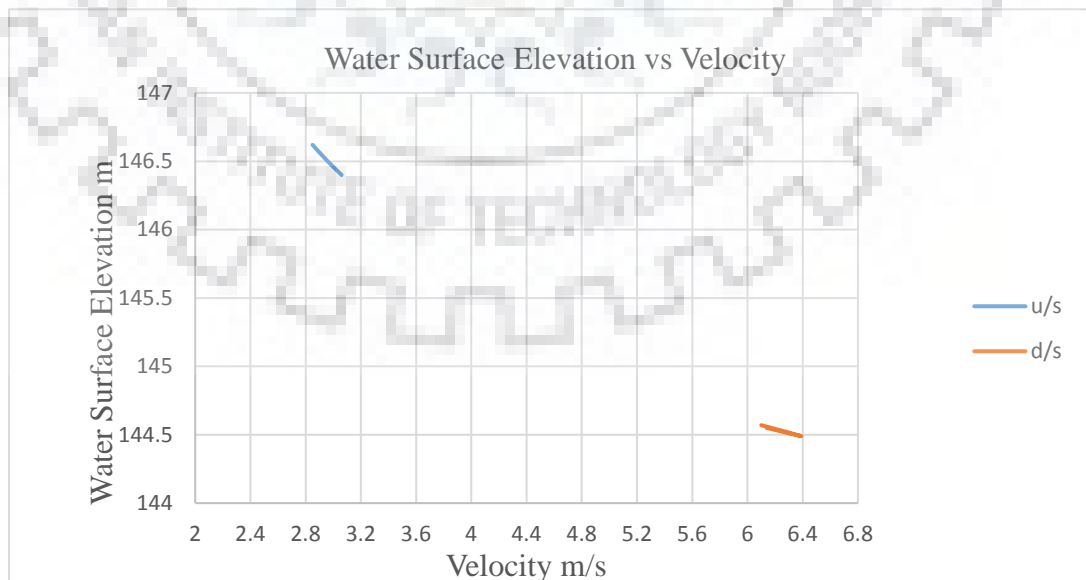


Figure 3.59: Water Surface Elevation vs Velocity

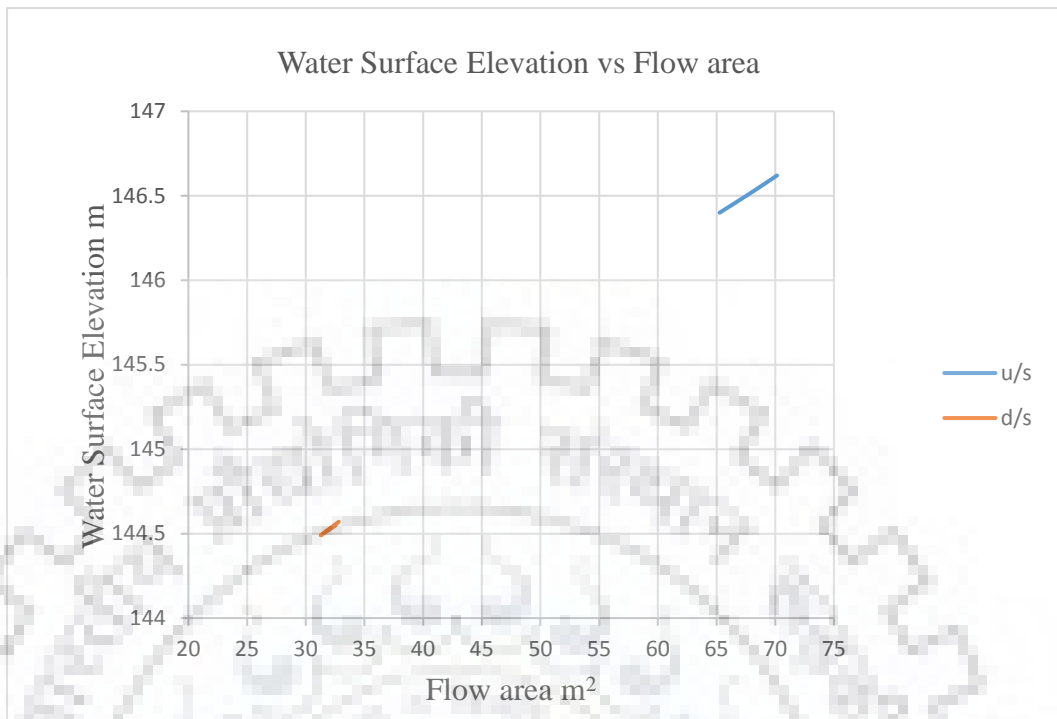


Figure 3.60: Water Surface Elevation vs Flow area

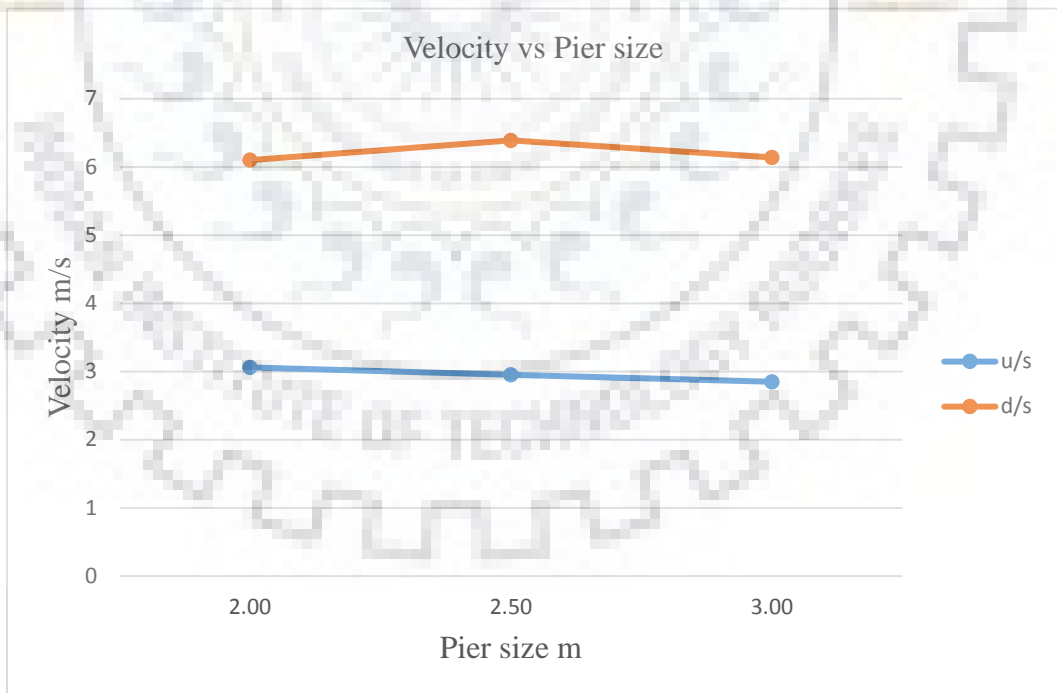


Figure 3.61: Velocity vs Pier size

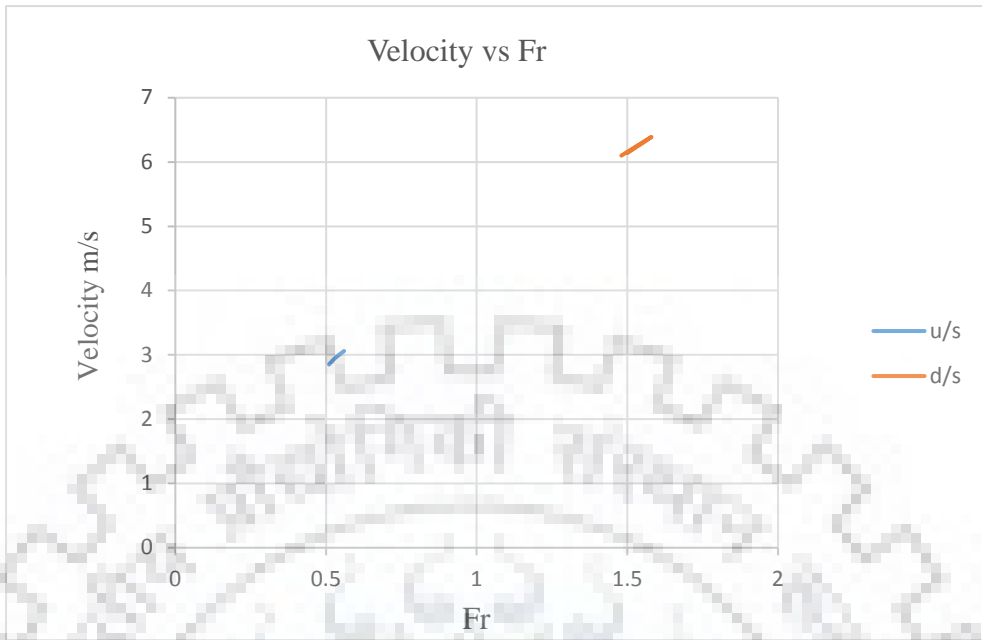


Figure 3.62: Velocity vs Fr

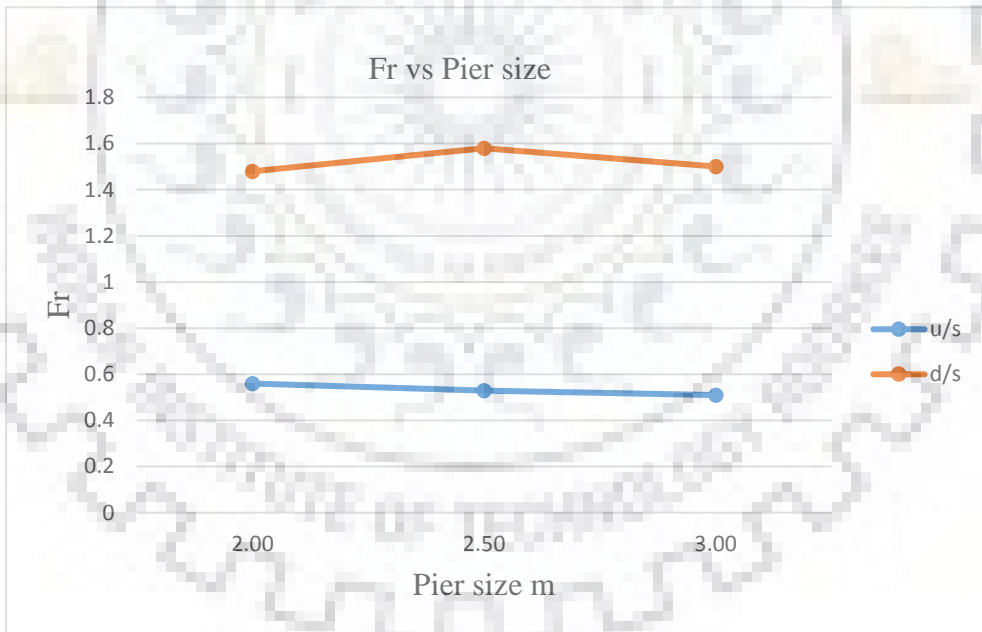


Figure 3.63: Fr vs Pier size

Here, for the analysis of variation of WSE with Pier Spacing, we take 10.0, 15.0 and 20.0 m pier spacing for different pier size (2.0, 2.5 and 3.0 m) and steady flow 200 m³/s.

Now observing the results in **Table 3.24**, for 10.0 m pier spacing, when pier size is 2.0 the WSE at u/s side (RS 953) is 146.53 m with CWSE 145.30 m. The velocity is 2.94 m/sec, flow area is 68.14 m² and Fr 0.53. But at d/s side (RS 903) the WSE is 144.53 m with CWSE 145.12 m and flow area of 32.09 m² with a velocity 6.23 m/sec and Fr 1.53. And for same pier spacing and 2.5 m pier size, the WSE at u/s side (RS 953) is 146.68 m with CWSE 145.30 m. The velocity is 2.80 m/sec, flow area is 71.38 m² and Fr 0.50. But at d/s side (RS 903) the WSE is 144.44 with CWSE 145.12 m and flow area of 30.46 m² with high velocity 6.57 m/sec and Fr 1.64. And for 3.0 m pier size, the WSE at u/s side (RS 953) is 146.83 m with CWSE 145.30 m. The velocity is 2.68 m/sec, flow area is 74.72 m² and Fr 0.47. But at d/s side (RS 903) the WSE is 144.36 with CWSE 145.12 m and flow area of 29.03 m² with high velocity 6.89 m/sec and Fr 1.75.

Again, as shown in **Table 3.25**, for 15.0 m pier spacing and 2.0 m pier size the WSE at u/s side (RS 953) is 146.52 m with CWSE 145.30 m. The velocity is 2.95 m/sec, flow area is 67.90 m² and Fr 0.53. But at d/s side (RS 903) the WSE is 144.49 m with CWSE 145.12 m and flow area of 31.40 m² with a velocity 6.37 m/sec and Fr 1.57. And for same pier spacing and 2.5 m pier size, the WSE at u/s side (RS 953) is 146.66 m with CWSE 145.30 m. The velocity is 2.82 m/sec, flow area is 71.04 m² and Fr 0.50. But at d/s side (RS 903) the WSE is 144.54 m with CWSE 145.12 m and flow area of 32.29 m² with a velocity 6.19 m/sec and Fr 1.51. And for 3.0 m pier size, the WSE at u/s side (RS 953) is 146.80 m with CWSE 145.30 m. The velocity is 2.70 m/sec, flow area is 74.11 m² and Fr 0.47. But at d/s side (RS 903) the WSE is 144.47 with CWSE 145.12 m and flow area of 31.00 m² with high velocity 6.45 m/sec and Fr 1.60.

Now again, as shown in **Table 3.26**, for 20.0 m pier spacing and 2.0 m pier size the WSE at u/s side (RS 953) is 146.40 m with CWSE 145.30 m. The velocity is 3.06 m/sec, flow area is 65.26 m² and Fr 0.56. But at d/s side (RS 903) the WSE is 144.57 m with CWSE 145.12 m and flow area of 32.81 m² with a velocity 6.10 m/sec and Fr 1.48. And for same pier spacing and 2.5 m pier size, the WSE at u/s side (RS 953) is 146.51 m with CWSE 145.30 m. The velocity is 2.95 m/sec, flow area is 67.76 m² and Fr 0.53. But at d/s side (RS 903) the WSE is 144.49 m with CWSE 145.12 m and flow area of 31.28 m² with a velocity 6.39 m/sec and Fr 1.58. And for 3.0 m pier size, the WSE at u/s side (RS 953) is

146.62 m with CWSE 145.30 m. The velocity is 2.85 m/sec, flow area is 70.15 m² and Fr 0.51. But at d/s side (RS 903) the WSE is 144.55 with CWSE 145.12 m and flow area of 32.55 m² with a velocity 6.14 m/sec and Fr 1.50

After analyzing the above results, we can conclude the following:

- For the constant pier spacing with different pier size, when the pier size increases u/s WSE increases, velocity decreases, flow area increases and Fr decreases. But at the d/s side when pier size increases WSE decreases velocity increases, flow area decreases and Fr also increases which is mainly due to the flow regime and river section geometry.
- The flow at u/s side is always at subcritical flow but it may change to supercritical flow at d/s side of bridge.



3.4.2.5 Variation of Water Surface Profiles with Pier Shape (Drag Coefficient Cd) *(Momentum Method)*

Effect of Cd for various Pier Shape (2m pier size and 10 m spacing)

u/s RS 953					d/s RS 903					Cd for various pier shape	Cd Description
WSE (m)	CWSE (m)	Velocity (m/s)	Flow area m ²	Fr	WSE (m)	CWSE (m)	Velocity (m/s)	Flow area m ²	Fr		
146.38	145.3	3.08	64.93	0.57	144.53	145.12	6.23	32.09	1.53	0.60	Elliptical piers with 2:1 length to width
146.42	145.3	3.04	65.89	0.55	144.53	145.12	6.23	32.09	1.53	1.00	Triangular nose with 30 degree angle
146.45	145.3	3.01	66.37	0.55	144.53	145.12	6.23	32.09	1.53	1.20	Circular pier
146.46	145.3	3	66.66	0.55	144.53	145.12	6.23	32.09	1.53	1.33	Elongated piers with semi-circular ends
146.47	145.3	2.99	66.8	0.54	144.53	145.12	6.23	32.09	1.53	1.39	Triangular nose with 60 degree angle
146.53	145.3	2.94	68.14	0.53	144.53	145.12	6.23	32.09	1.53	2.00	Square nose piers

Table 3.27: Variation of Water Surface Profiles with Pier Shape Cd

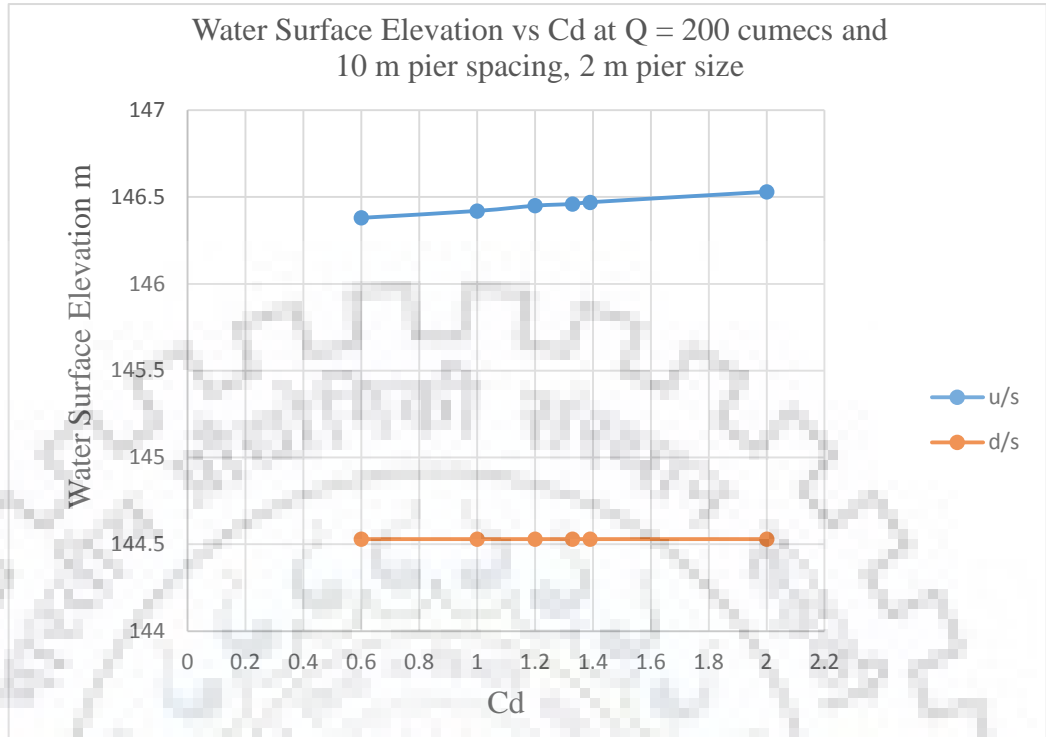


Figure 3.64: Water Surface Elevation vs Cd at Q = 200 cumecs and 10 m pier spacing, 2 m pier size

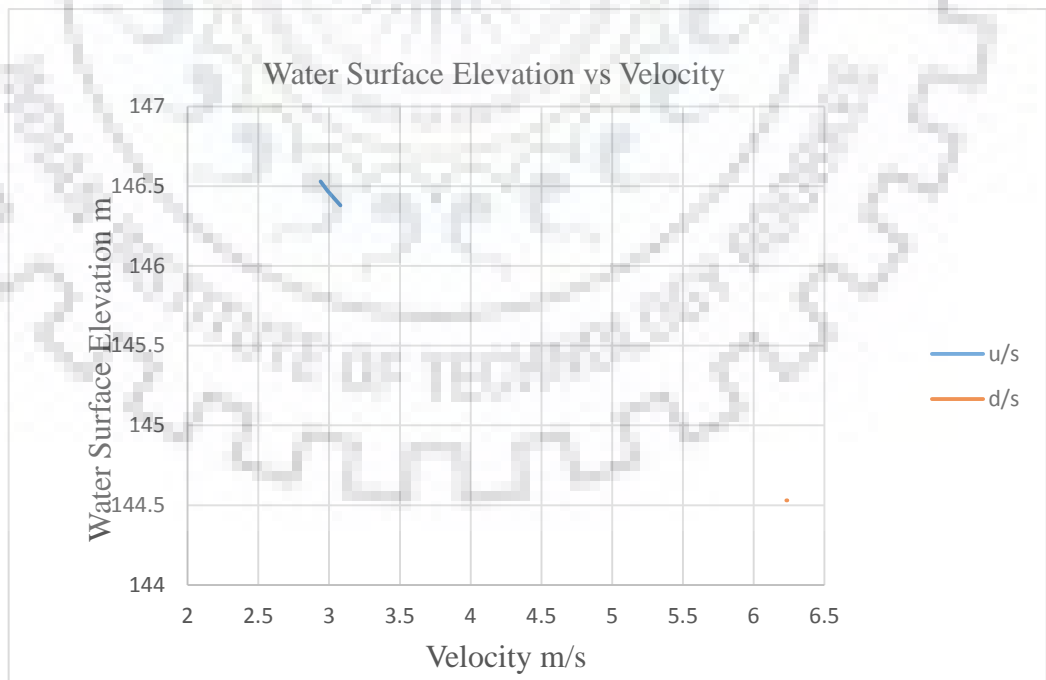


Figure 3.65: Water Surface Elevation vs Velocity

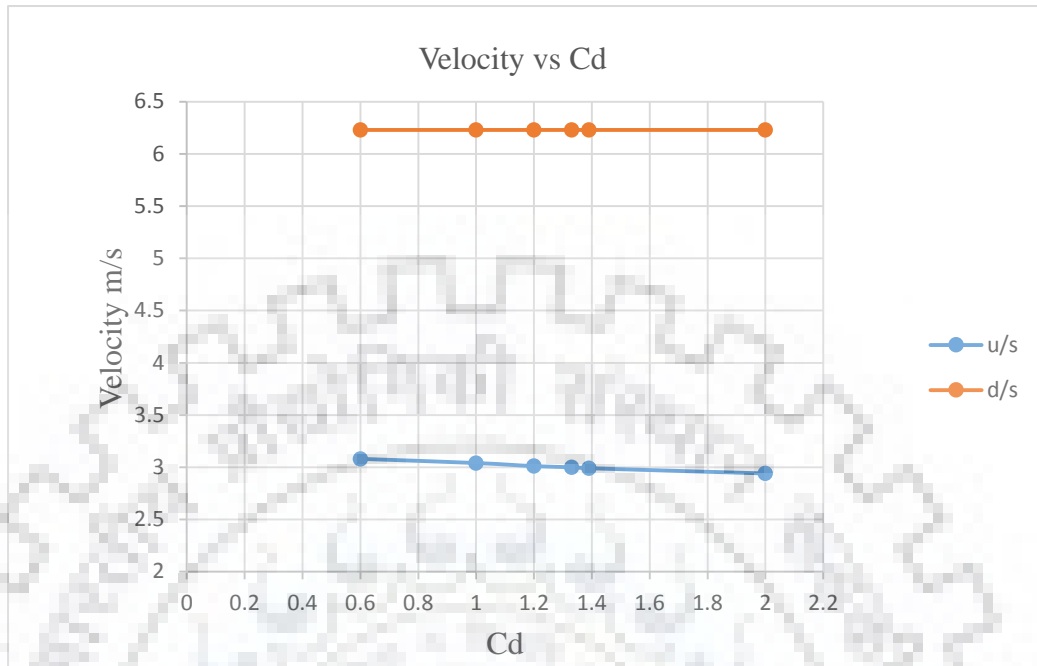


Figure 3.66: Velocity vs Cd

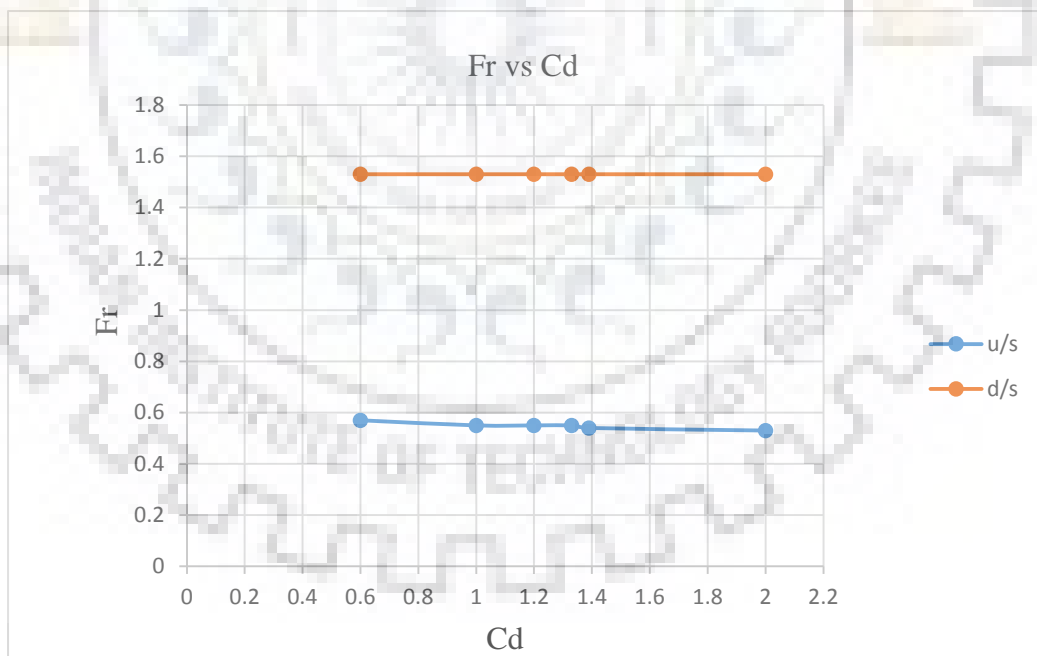


Figure 3.67: Fr vs Cd

Now, analyzing the variation of WSE with Pier Shape (Drag Coefficient C_d) in Momentum Method, we take the different values of C_d for different pier shapes. The values of C_d are taken from 0.60 to 2.0 and steady flow $200 \text{ m}^3/\text{s}$.

As shown in **Table 3.27**, for $C_d = 0.60$ (Elliptical piers with 2:1 length to width) the WSE at u/s RS 953 is 146.38 m with CWSE 145.30 m. The velocity is 3.08 m/sec, flow area is 64.93 m^2 and Fr 0.57. But at d/s RS 903 the water surface elevation is 144.53 with CWSE 145.12 m and flow area of 32.09 m^2 with high velocity 6.23 m/sec and Fr 1.53.

Also, for $C_d = 1.0$ (Triangular nose with 30 degree angle) the WSE at u/s RS 953 is 146.42 m with CWSE 145.30 m. The velocity is 3.04 m/sec, flow area is 65.89 m^2 and Fr 0.55. But at d/s RS 903 the WSE, CWSE, flow area, velocity and Fr remains same as in the case of $C_d = 0.60$.

Similarly, for $C_d = 1.2$ (Circular shape pier) the WSE at u/s (RS 953) is 146.45 m with CWSE 145.30 m. The velocity is 3.01 m/sec, flow area is 66.37 m^2 and Fr 0.55. But at d/s RS 903 the WSE, CWSE, flow area, velocity and Fr remains unchanged as in the previous case.

Again, for $C_d = 1.33$ (Elongated piers with semi-circular ends) the WSE at u/s (RS 953) is 146.46 m with CWSE 145.30 m. The velocity is 3.0 m/sec, flow area is 66.66 m^2 and Fr 0.55. But at d/s RS 903 the WSE, CWSE, flow area, velocity and Fr remains unchanged as in the previous case.

Now, for $C_d = 1.39$ (Triangular nose with 60 degree angle) the WSE at u/s (RS 953) is 146.47 m with CWSE 145.30 m. The velocity is 2.99 m/sec, flow area is 66.80 m^2 and Fr 0.54. But at d/s RS 903 the WSE, CWSE, flow area, velocity and Fr remains unchanged as in the previous case.

Now, for $C_d = 2.0$ (Square nose piers) the WSE at u/s (RS 953) is 146.53 m with CWSE 145.30 m. The velocity is 2.94 m/sec, flow area is 68.14 m^2 and Fr 0.53. But at d/s RS 903 the WSE, CWSE, flow area, velocity and Fr remains unchanged as in the previous case.

Hence, analyzing the results with different values of C_d for different pier shapes (0.60 to 2.0) when the pier shape coefficient C_d increases u/s WSE increases, velocity decreases, flow area increases and Fr decreases. But at the d/s side for all values of C_d , WSE, velocity, flow area and Fr all remain constant at d/s side as the effect of C_d is of local nature and does not extent over a large area downstream but the small change in C_d caused the

changes in all the parameters like water surface elevation, velocity, flow area and Fr at upstream side of bridge.

Hence, we can conclude that:

- ✓ The upstream WSE for square nose pier is found to be maximum among all above shape piers. The increasing order of water surface elevation at u/s side of bridge due to various shape of piers are summarized below.

Cd for various pier shape	Cd Description	Remarks
0.60	Elliptical piers with 2:1 length to width	
1.00	Triangular nose with 30 degree angle	
1.20	Circular pier	
1.33	Elongated piers with semi-circular ends	
1.39	Triangular nose with 60 degree angle	
2.00	Square nose piers	

3.4.2.6 Variation of Water Surface Profiles with Pier Shape (Yarnell Coefficient k)

u/s RS 953					d/s RS 903					k for various pier shape	Cd Description
WSE (m)	CWSE (m)	Velocity (m/s)	Flow area m ²	Fr	WSE (m)	CWSE (m)	Velocity (m/s)	Flow area m ²	Fr		
146.53	145.3	2.94	68.14	0.53	144.53	145.12	6.23	32.09	1.53	0.9	Semi-circular nose and tail
146.53	145.3	2.94	68.14	0.53	144.53	145.12	6.23	32.09	1.53	1.05	90 degree triangular nose and tail
146.53	145.3	2.94	68.14	0.53	144.53	145.12	6.23	32.09	1.53	1.25	Square nose and tail

Table 3.28: Variation of Water Surface Profiles with Pier Shape k

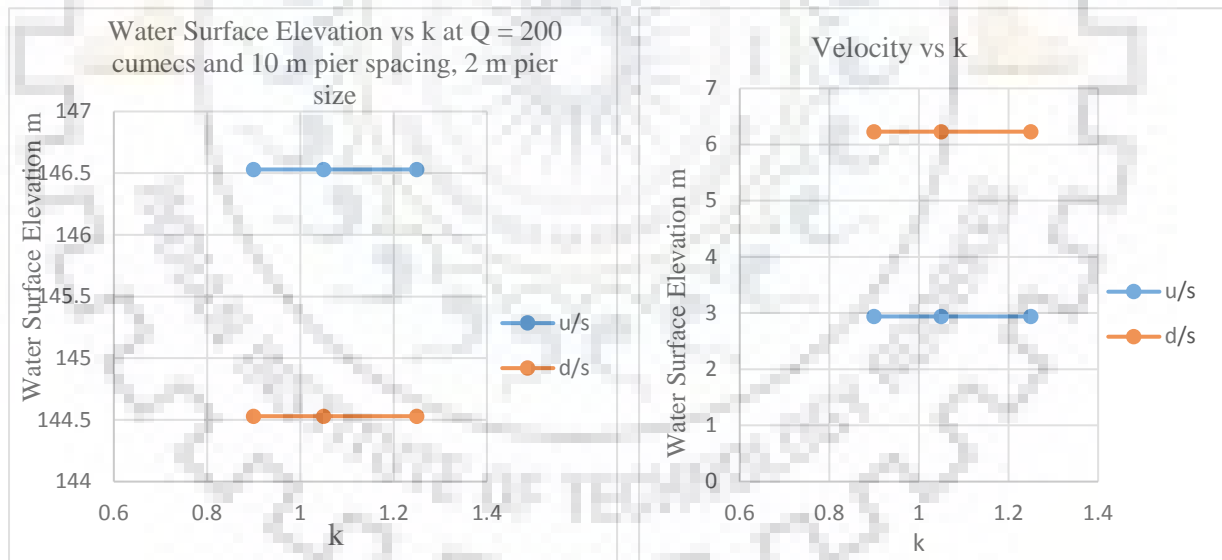


Figure 3.68: (a) Water Surface Elevation vs k at Q = 200 cumecs and 10 m pier spacing, 2 m pier size (b) Velocity vs k

Here, observing the results in **Table 3.28** for variation of WSE with Pier Shape (Yarnell Coefficient k), $k = 0.90$ (Semi-circular nose and tail) the WSE at u/s side (RS 953) is 146.53 m with CWSE 145.30 m. The velocity is 2.94 m/sec, flow area is 68.14 m² and Fr 0.53. But at d/s side (RS 903) the WSE is 144.53 with CWSE 145.12 m and flow area of 32.09 m² with a high velocity 6.23 m/sec and Fr 1.53.

Hence, analyzing the results with different values of k for different pier shapes (0.90 to 1.25), for all values of k there is no effect on WSE, velocity, flow area and Fr at u/s and d/s side of bridge section. So we can say that the Yarnell's Momentum method has no effect on WSE determination.



3.4.3 VARIATION OF WATER SURFACE PROFILES WITH AND WITHOUT BRIDGES IN SERIES (5 nos.)

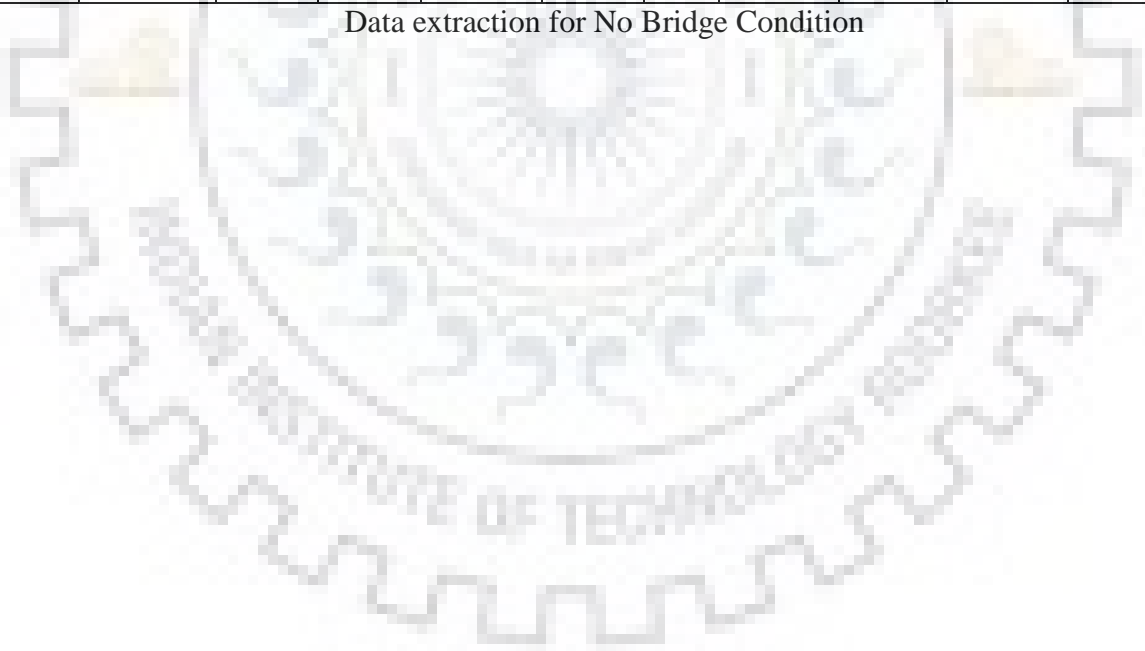
3.4.3.1 Data extraction for No Bridge Condition

River Station	n = 0.025															
	Discharge	200 m ³ /s					400 m ³ /s					600 m ³ /s				
	Min Ch El (m)	WSE (m)	CWSE (m)	Velocity (m/s)	Flow area m ²	Fr	WSE (m)	CWSE (m)	Velocity (m/s)	Flow area m ²	Fr	WSE (m)	CWSE (m)	Velocity (m/s)	Flow area m ²	Fr
8471.18*	159.11	163.07		0.94	212.69	0.18	164.58		1.17	341.85	0.2	165.68		1.34	448.5	0.2
8425.73*	159.04	163.05		1.03	194.13	0.2	164.56		1.28	312.86	0.21	165.65		1.46	411.39	0.22
6953.00*	154.56	156.93	156.9	3.71	53.86	0.98	157.66	157.79	4.86	82.34	1.09	158.26	158.51	5.57	107.69	1.14
6903.00*	154.4	156.72	156.66	3.59	55.65	0.95	157.8	157.53	3.99	100.3	0.85	158.77	158.23	4.08	147.03	0.78
5430.78*	151.28	155.71		2.12	94.3	0.44	156.9		2.75	145.69	0.49	157.77		3.23	185.94	0.52
5375.22*	151.23	155.64		2.18	91.93	0.46	156.84		2.77	144.2	0.5	157.72		3.22	186.51	0.53
3953.00*	148.52	152.18		3.35	59.67	0.74	153.29		4.24	94.42	0.81	154.15		4.8	124.95	0.84
3903.00*	148.44	152.07		3.28	61.02	0.73	153.19		4.12	97.06	0.79	154.06		4.64	129.37	0.81
2453.00*	144.91	149.03		2.04	98.14	0.4	150.91		2.27	175.97	0.37	152.55		2.37	253.19	0.34
2403.00*	144.81	148.98		2.12	94.54	0.42	150.86		2.35	170.11	0.38	152.51		2.44	245.43	0.35
953.00*	141.93	145.43	145.3	4.41	45.31	0.93	146.45	146.66	6.02	66.48	1.1	147.1	147.74	7.41	80.98	1.26
903.00*	141.86	145.27	145.12	4.26	46.94	0.91	146.38	146.42	5.57	71.79	1.02	146.86	147.45	7.19	83.41	1.25

Table 3.29: Data extraction for No Bridge Condition

River Station	n = 0.025										
	Discharge	800 m ³ /s					1000 m ³ /s				
	Min Ch El (m)	WSE (m)	CWSE (m)	Velocity (m/s)	Flow area m ²	Fr	WSE (m)	CWSE (m)	Velocity (m/s)	Flow area m ²	Fr
8471.18*	159.11	166.57		1.48	540.68	0.21	167.34		1.6	623.71	0.21
8425.73*	159.04	166.54		1.61	496.39	0.23	167.3		1.75	572.6	0.23
6953.00*	154.56	159.62	159.14	4.57	174.9	0.82	160.44	159.67	4.5	222.17	0.75
6903.00*	154.4	159.66		4.07	196.34	0.71	160.48		4.06	246.17	0.65
5430.78*	151.28	158.55		3.58	223.47	0.54	159.27		3.85	259.45	0.55
5375.22*	151.23	158.51		3.53	226.32	0.54	159.23		3.78	264.72	0.55
3953.00*	148.52	155.03		4.99	160.29	0.82	155.96		4.96	201.44	0.76
3903.00*	148.44	154.97		4.78	167.25	0.79	155.93		4.73	211.51	0.72
2453.00*	144.91	154		2.43	328.61	0.32	155.31		2.48	403.11	0.31
2403.00*	144.81	153.96		2.51	319.03	0.33	155.27		2.55	391.66	0.32
953.00*	141.93	147.66	148.66	8.5	94.16	1.37	148.19	149.49	9.33	107.2	1.44
903.00*	141.86	147.39	148.34	8.27	96.74	1.36	147.87	149.12	9.15	109.26	1.45

Data extraction for No Bridge Condition



3.4.3.2 Data extraction for Five Bridges in Series

River Station	n = 0.025															
	Discharge	200 m ³ /s					400 m ³ /s					600 m ³ /s				
	Min Ch El (m)	WSE (m)	CWSE (m)	Velocity (m/s)	Flow area (m ²)	Fr	WSE (m)	CWSE (m)	Velocity (m/s)	Flow area (m ²)	Fr	WSE (m)	CWSE (m)	Velocity (m/s)	Flow area (m ²)	Fr
8471.18*	159.11	163.07		0.94	212.69	0.18	164.58		1.17	341.85	0.2	165.68		1.34	448.5	0.2
8425.73*	159.04	163.05		1.03	194.13	0.2	164.56		1.28	312.86	0.21	165.65		1.46	411.39	0.22
6953.00*	154.56	157.83	156.9	2.24	89.15	0.49	159.11	157.78	2.71	147.63	0.51	160.08	158.51	2.99	200.96	0.51
6928	Bridge															
6903.00*	154.4	156.2	156.66	5.39	37.08	1.64	156.99	157.53	6.05	66.14	1.49	157.54	158.23	6.74	88.96	1.49
5430.78*	151.28	155.89	154.55	1.96	101.88	0.4	157.3	155.48	2.44	163.66	0.41	158.39	156.23	2.79	215.32	0.42
5428	Bridge															
5375.22*	151.23	155.64		2.17	91.99	0.46	156.85		2.77	144.66	0.5	157.76		3.18	188.42	0.52
3953.00*	148.52	152.87	151.72	2.49	80.43	0.5	154.42	152.86	2.95	135.53	0.51	155.61	153.72	3.23	185.92	0.51
3928	Bridge															
3903.00*	148.44	151.11	151.59	5.63	35.54	1.48	152	152.7	6.77	59.06	1.51	152.68	153.55	7.51	79.87	1.53
2453.00*	144.91	149.17	147.69	1.94	103.12	0.38	151.09	148.66	2.17	183.98	0.34	152.74	149.42	2.28	262.67	0.32
2428	Bridge															
2403.00*	144.81	148.99		2.11	94.85	0.42	150.88		2.34	170.89	0.38	152.53		2.44	246.31	0.34
953.00*	141.93	146.53	145.3	2.93	68.15	0.53	148.51	146.66	3.47	115.31	0.52	150.08	147.74	3.79	158.28	0.52
928	Bridge															
903.00*	141.86	144.53	145.12	6.23	32.09	1.53	145.58	146.42	7.47	53.54	1.52	146.41	147.45	8.29	72.37	1.52

Table 3.30: Data extraction for Bridges in Series (Five Bridges in Series)

River Station	n = 0.025										
	Discharge	800 m ³ /s					1000 m ³ /s				
	Min Ch El (m)	WSE (m)	CWSE (m)	Velocity (m/s)	Flow area m ²	Fr	WSE (m)	CWSE (m)	Velocity (m/s)	Flow area m ²	Fr
8471.18*	159.11	166.57		1.48	540.68	0.21	167.34		1.6	623.71	0.21
8425.73*	159.04	166.54		1.61	496.39	0.23	167.3		1.75	572.6	0.23
6953.00*	154.56	160.9	159.14	3.2	249.84	0.51	161.81	159.7	3.24	308.56	0.48
6928	Bridge										
6903.00*	154.4	160.1		3.59	222.72	0.6	161.01		3.57	279.89	0.55
5430.78*	151.28	159.34	156.84	3.04	263.01	0.43	160.19	157.4	3.25	308.11	0.43
5428	Bridge										
5375.22*	151.23	158.58		3.47	230.4	0.53	159.34		3.69	270.86	0.53
3953.00*	148.52	156.58	154.45	3.47	230.82	0.5	157.4	155.1	3.68	271.49	0.51
3928	Bridge										
3903.00*	148.44	153.27	154.26	8.02	99.75	1.53	153.77	154.9	8.45	118.34	1.52
2453.00*	144.91	154.19	150.07	2.36	338.56	0.3	155.48	150.7	2.42	413.41	0.3
2428	Bridge										
2403.00*	144.81	153.97		2.5	319.51	0.33	155.26		2.56	391.14	0.32
953.00*	141.93	151.41	148.66	4.01	199.75	0.52	152.54	149.5	4.19	238.45	0.52
928	Bridge										
903.00*	141.86	147.1	148.34	8.96	89.3	1.52	147.72	149.1	9.49	105.34	1.52

Data extraction for Bridges in Series (Five Bridges in Series)

3.4.3.2 Comparison of Water Surface Elevations with and without Bridges

No Bridge Condition						With 5 Bridges in Series					Afflux at various Q (n = 0.025)					Remarks
Discharges (Q) m ³ /s	200	400	600	800	1000	200	400	600	800	1000	200	400	600	800	1000	
RS	WSE (m)					WSE (m)					Afflux (m)					
8471.18*	163.07	164.58	165.68	166.57	167.34	163.07	164.58	165.68	166.57	167.34	0.00	0.00	0.00	0.00	0.00	
8425.73*	163.05	164.56	165.65	166.54	167.30	163.05	164.56	165.65	166.54	167.30	0.00	0.00	0.00	0.00	0.00	
6953.00*	156.93	157.66	158.26	159.62	160.44	157.83	159.11	160.08	160.90	161.81	0.90	1.45	1.82	1.28	1.37	u/s of Bridge at RS 6928
6903.00*	156.72	157.80	158.77	159.66	160.48	156.20	156.99	157.54	160.10	161.01	-0.52	-0.81	-1.23	0.44	0.53	d/s of Bridge at RS 6928
5430.78*	155.71	156.90	157.77	158.55	159.27	155.89	157.30	158.39	159.34	160.19	0.18	0.40	0.62	0.79	0.92	u/s of Bridge at RS 5428
5375.22*	155.64	156.84	157.72	158.51	159.23	155.64	156.85	157.76	158.58	159.34	0.00	0.01	0.04	0.07	0.11	d/s of Bridge at RS 5428
3953.00*	152.18	153.29	154.15	155.03	155.96	152.87	154.42	155.61	156.58	157.40	0.69	1.13	1.46	1.55	1.44	u/s of Bridge at RS 3928
3903.00*	152.07	153.19	154.06	154.97	155.93	151.11	152.00	152.68	153.27	153.77	-0.96	-1.19	-1.38	-1.70	-2.16	d/s of Bridge at RS 3928
2453.00*	149.03	150.91	152.55	154.00	155.31	149.17	151.09	152.74	154.19	155.48	0.14	0.18	0.19	0.19	0.17	u/s of Bridge at RS 2428
2403.00*	148.98	150.86	152.51	153.96	155.27	148.99	150.88	152.53	153.97	155.26	0.01	0.02	0.02	0.01	-0.01	d/s of Bridge at RS 2428
953.00*	145.43	146.45	147.10	147.66	148.19	146.53	148.51	150.08	151.41	152.54	1.10	2.06	2.98	3.75	4.35	u/s of Bridge at RS 928
903.00*	145.27	146.38	146.86	147.39	147.87	144.53	145.58	146.41	147.10	147.72	-0.74	-0.80	-0.45	-0.29	-0.15	d/s of Bridge at RS 928

Table 3.31: Comparison of Water Surface Elevations with and without Bridges

Here, comparing the results between *Bridge Condition and Without Bridge Condition* for the multiple bridges in series in the same river reach at the upstream and downstream side of the bridges.

The modelling is done for *five bridges* which are located at RS 928, 2428, 3928, 5428 and 6928 m and are at equal distance (1500 m) apart from each other in the same river reach. The flow simulation is done for the five nos. of steady flow (200, 400, 600, 800 and 1000 cumecs) and the results for the Water Surface Elevations obtained are expressed in the tabular form as shown above tables. (Tables 3.28 to 3.30).

From the results as shown in Tables above, at the u/s side of Bridge at RS 6928 i.e. at ch. 6953.00* the WSE for steady flow at 200 cumecs when there was no bridge is 156.93 m, but after placing the bridge at RS 6928 it was found to be 157.83 m (i.e. afflux 0.90 m at u/s). Also at the d/s side of bridge at RS 6928 i.e. at ch. 6903.00* the WSE for steady flow at 200 cumecs when there was no bridge is 156.72 m, but after but after placing the bridges at RS 6928 it was found to be 156.20 m (i.e. decrease in water surface elevation by 0.52 m).

Similarly, from the results as shown in Tables above, at the u/s side of Bridge at RS 5428 i.e. at ch. 5430.78* the WSE when there was no bridge is 155.71 m, but after placing the bridge at RS 5428 it was found to be 155.89 m (i.e. afflux 0.18 m at us). Also at the d/s side of bridge at RS 5428 i.e. at ch. 5375.22* the water surface elevation for steady flow at 200 cumecs when there was no bridge is 155.64 m, but after but after placing the bridge at RS 5428 it was found to be 155.64 m (i.e. there is no change in water surface elevation at d/s side).

All the flows and their corresponding WSE and afflux values are shown in above Table. Hence, we can say that there is a similar trends of changing water surface elevation and other parameters and there is always some rise in backwater (afflux) at the upstream side of bridge for any steady flow. But the condition may always not be true at the downstream side of bridge. At the d/s side, the water surface elevation may rise or fall as compared with the u/s WSE depending upon the width of channel, river geometry and river section at the site of consideration. Hence the effect of backwater vicinity at the bridge location due to bridge parameters is of localized nature and cannot be extent up to a large area of upstream and downstream of bridge.

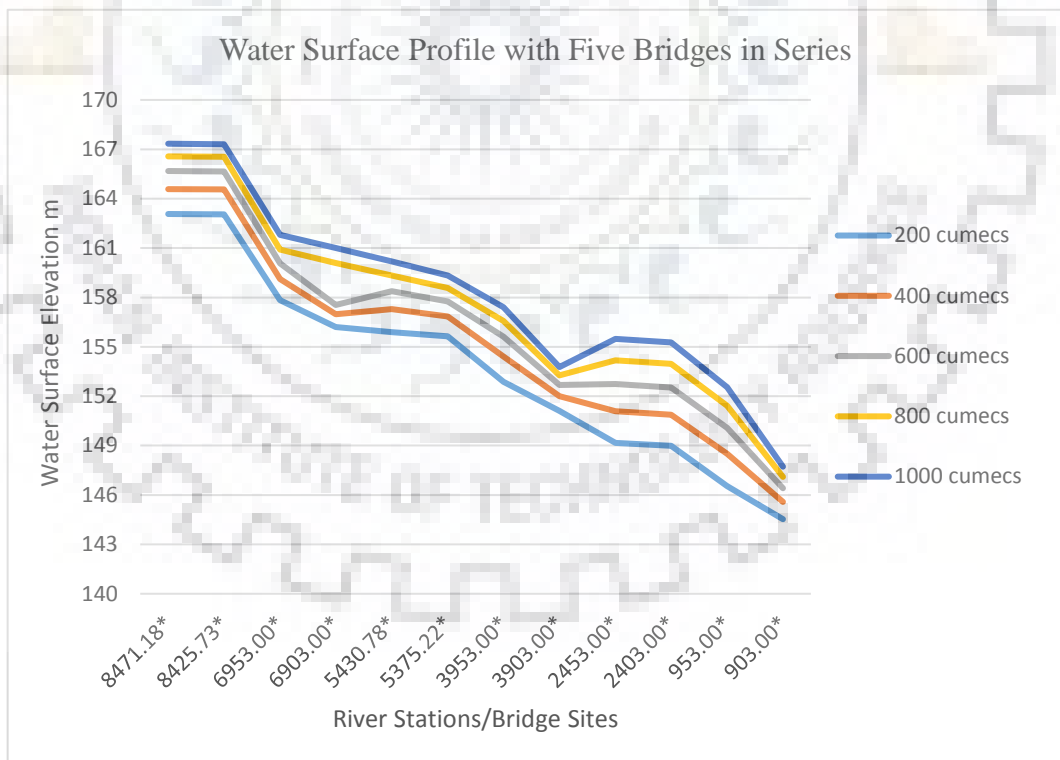
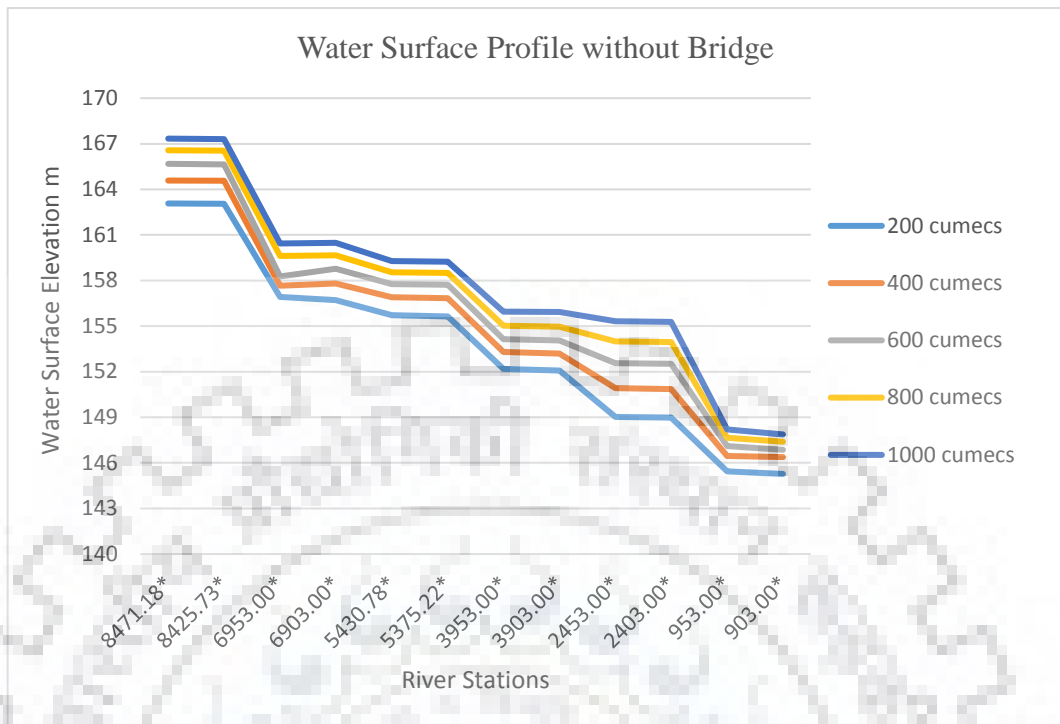


Table 3.32: Water Surface Elevations with and without Bridges (Drawn in Excel)

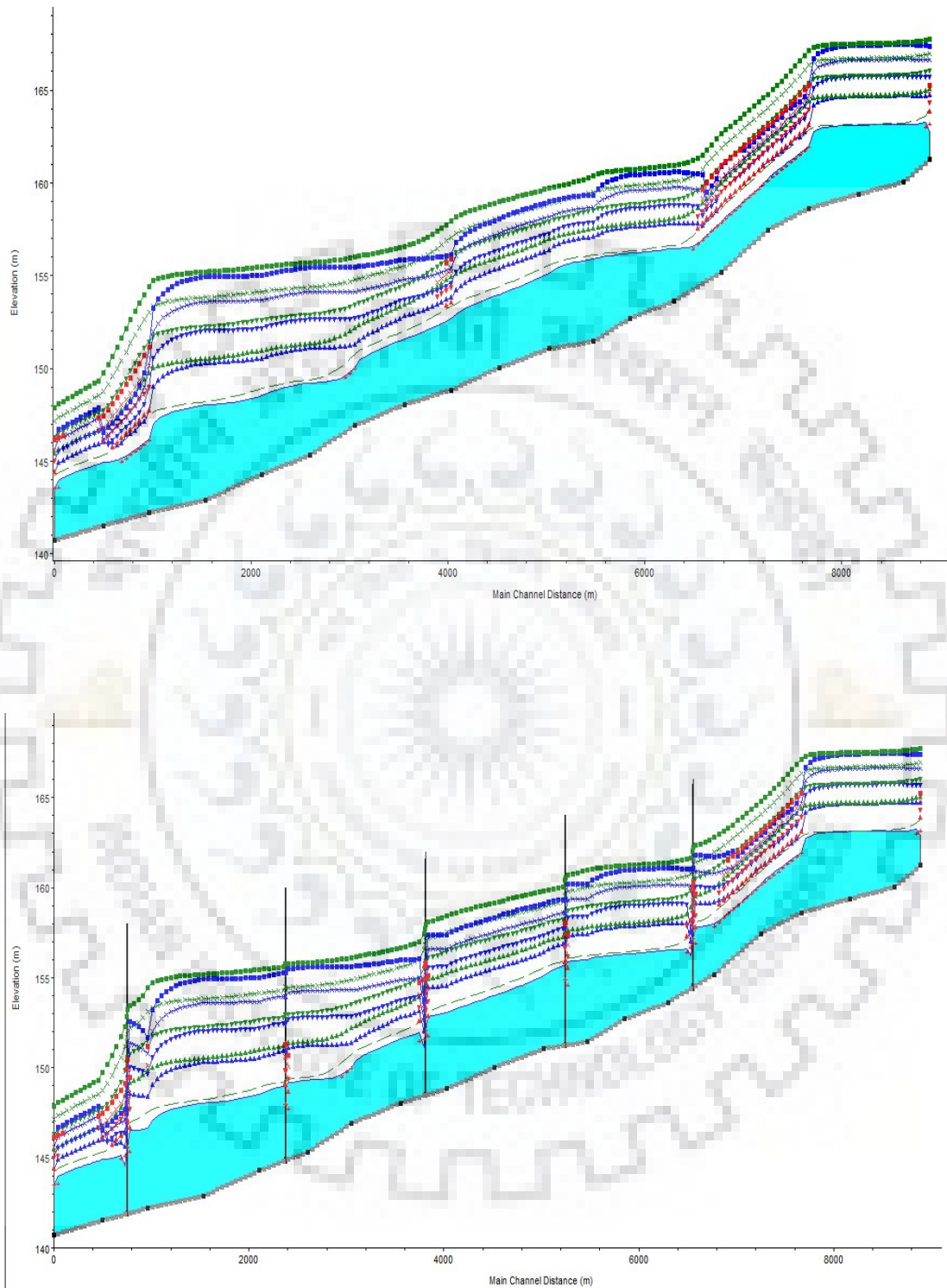


Table 3.33: Water Surface Profiles with and without Bridges (Obtained from HEC -RAS)

SUMMARY AND DISCUSSION OF RESULTS

4.1 SUMMARY AND CONCLUSION

After analysis of the all the parameters related to cause the change in water surface elevation in the one dimension steady flow with bridge and without bridge condition, following results and conclusions are obtained. The summary of all results can be expressed in the Tabular form as shown below:

Parameters	Effect	WSE	Velocity	Flow Area at bridge site	Froude no. (Fr)
Manning's coefficient n	Increases	Increases	Decreases	Increases	Decreases
Pier Spacing	Increases	Decreases	Increases	Decreases	Increases
Different pier size at equal spacing (2.0, 2.5, 3 m piers @ 10 m spacing)	Increases	Increases	Decreases	Increases	Decreases
Same pier size at different spacing (2.0 m pier @ 10, 15, 20 m spacing)	Increases	Decreases	Increases	Decreases	Increases
Shape of piers					
Cd (Momentum Method)	Increases	u/s increases/ d/s constant	u/s decreases/d/s constant	u/s increases/d/s constant	u/s decreases/d/s constant
k (Yarnell's Method)	No effect				
For the constant k					
Discharge Q	Increases	Increases	Increases	Increases	Constant
For the constant n					
Discharge Q	Increases	Increases	Increases	Increases	u/s decreases/d/s increases
Spacing of piers	Increases	Decreases	u/s increases/d/s decreases	u/s decreases/d/s increases	Increases

Table 3.34: Summary Table of Results

For no bridge condition and steady flow

For the Constant Steady Flow, when Manning's no. n increases Water Surface Elevation increases, Velocity decreases, Flow area at Bridge site increases, and thus Froude no. (Fr) decreases.

For bridge condition and steady flow

But after placing the bridge at the same location, the bridge piers obstruct the flow at upstream and downstream side of the bridge and hence there is significant changes in the water surface elevations at both sides of the bridge.

On the basis of variation of the different bridge parameters, the water surface elevations also varies accordingly.

For the same Discharge, when the bridge pier spacing increases, Water Surface Elevation decreases, Velocity increases, Flow area at Bridge site decreases, and thus Froude no. (Fr) increases.

Also for different pier size at equal spacing i.e. 2.0, 2.5, 3.0 m piers @ 10 m spacing and for the same Q , when the bridge pier size increases, Water Surface Elevation increases, Velocity decreases, Flow area at Bridge site increases, and thus Froude no. (Fr) decreases.

Also for Same pier size at different spacing i.e. 2 m pier @ 10, 15, 20 m spacing and for the same Q , when the bridge pier spacing increases, Water Surface Elevation decreases, Velocity increases, Flow area at Bridge site decreases, and thus Froude no. (Fr) increases.

Now, according to the shape of piers or as per pier geometry, when the coefficient of discharge C_d increases, Water Surface Elevation at u/s side of bridge increases whereas it is constant at d/s side, Velocity at u/s side decreases and no change at d/s side, similarly Flow area at u/s Bridge side increases but no change at d/s side, and thus Froude no. (Fr) at u/s side decreases and is constant at d/s side.

Now as per the effect of Yarnell coefficient k , for the steady flow Q , it has no effect on any of the above parameters.

For constant k

Now as per the effect of Yarnell coefficient k , for the same k , when the Discharge Q increases, there is no change in Water Surface Elevation, Velocity and Flow area at Bridge site, and thus no change in Froude no. (Fr).

For constant C_d and n together

Now for the same C_d and n at the same time, when the Discharge Q increases, Water Surface Elevation increases, Velocity also increases, Flow area at Bridge site increases, and thus Froude no. (Fr) at u/s side decreases while it decreased at d/s side of bridge.

Now for the same n , when the Discharge Q increases, Water Surface Elevation increases, Velocity also increases, Flow area at Bridge site increases, and thus Froude no. (Fr) at u/s side decreases while it decreased at d/s side of bridge.

For same n and same pier size, if Spacing of piers increases, Water Surface Elevation decreases, Velocity at u/s side increases and d/s side decreases, Flow area at Bridge u/s side decreases and d/s side increases and thus Froude no. (Fr) at u/s side increases while it decreased at d/s side of bridge.

The results and conclusions are of much more important because the variation of water surface elevation and corresponding water surface profiles due to bridge are not only related to bridge hydraulics but are caused due to the river section geometry and bridge modelling method. The results are very useful for finding stagnation zones of bridge site and are also the measure of finding the afflux and backwater effect to the vicinity of the bridge site.

4.2 FUTURE SCOPE OF WORKS

The stability of bridge is very important aspect as it is used for transportation purpose because without stable bridge structure in the roads there is no possibility of communication between the two places. The well-functioning of bridge can be assured only by the effective hydraulic and geometric design of bridges. So in the designing stage, maximum backwater (afflux), effective area, stagnation zones, contraction and expansion lengths of river reach and effects of piers (size, shape, spacing, numbers etc.) can be well designed and their effects should also be considered very efficiently. The simulation of steady flow in HEC-RAS gives the effects of such bridge parameters on the water surface profiles.

1. Therefore, it is advisable to use the HEC-RAS programming for the fast, efficient and reliable results for the determination of backwater effects due to road bridge in any natural channel (like river). The afflux or backwater analysis can be used for the bridge designing and modelling and also for the design of river training structures around the bridge.
2. The modelling in the river reach can be used widely in the determination of effects of contraction and expansion lengths. The modelling greatly affects the upstream and downstream reach as the flow can be changed from one regime to the another at the same river section after providing the bridges.
3. The effect of single bridge at the particular river station and its vicinity can be measured. Also the effect of multiple bridges in series at the particular spacing upstream and downstream of the river cross section can be determined with the HEC-RAS programming which can be very beneficial in the analysis of flood and stagnation zones due to those bridges.
4. For bridges over major rivers the guide bunds and other protection measures should be designed at least for floods and soil erosion controlling purposes. The effective zones can safely be handled with the help of HEC-RAS.
5. Since the area near bridge site is of high concern, the hydraulics related to bridge and river should be treated as major importance for the stability and smooth functioning of bridge.

REFERENCES:

1. Biswas S. K. (2010), Effect of bridge pier on waterways constriction: a case study using 2-D mathematical modeling.
2. Brandimarte L. (2012), Uncertainty in the estimation of backwater effects at bridge crossings.
3. Chaochao Q., Yamada T. (2013), A Study on Water Surface Profiles of Rivers with Constriction.
4. Department of Primary Industries and Regional Development, Government of Western Australia. <https://www.agric.wa.gov.au/>
5. Hydraulic Reference Manual (2016), US Army Corps of Engineer, Hydrologic Engineering Center.
6. J. Allen & K.J. Enever (2012), Water surface profiles in gradually varied open-channel flow.
7. J. Randall, Charbeneau, Holley R.E. (2001), Backwater Effects of Bridges Piers in Subcritical Flow.
8. Johnson K.G., Quinones F., Gonzalez R. (1987), Hydraulics Analysis of Water Surface Profiles in the Vicinity of the Coamo Dam.
9. Kidson R.L. (2006), Hydraulic model calibration for extreme floods in bedrock-confined channels: case study from northern Thailand.
10. Kocaman S. (2014), Prediction of Backwater Profiles due to Bridges in a Compound Channel Using CFD.
11. Liu Y., Pender G. (2015), A flood inundation modelling using v-support vector machine regression model, Engineering Applications of Artificial Intelligence.
12. Loughborough University Leicestershire, UK <https://dspace.lboro.ac.uk/dspace-jspui/>
13. Merkel W. H., Donald E.W. (1992), SCS Water Surface Profile Model - WSP2.
14. National University of Ireland, Galway <http://www.nuigalway.ie/>
15. National University of Singapore <https://scholarbank.nus.edu.sg/>
16. NIH Roorkee (1999), Computation of Water Surface Profile by using HEC River Analysis System.
17. Norwegian University of Science and Technology, Norway : <https://www.ntnu.edu/>

18. Peck W.W. (2001), Evaluation of Alternatives for Hydraulic Design of Bridges with HEC-RAS.
19. Pilotti M. (2012), Environmental Hydraulics Using HEC-RAS for computing water surface profiles.
20. Salah El, Kassem A. (2009), Backwater Rise due to Flow Constriction by Bridge Piers.
21. Schwab G., Fangmeier D., Elliot W. & Frevert R. (1992), Soil and water conservation engineering, 4th edn, John Wiley and Sons Inc., Toronto, Canada.
22. Subedi A.S., Sharma S., Islam A. and Lamichhane N. (2019), Quantification of the Effect of Bridge Pier Encasement on Headwater Elevation Using HEC-RAS, Civil and Environmental Engineering, Youngstown State University, USA.
23. Torlapati J. (2017), Open Channel Flow – Worksheet-3 Water Surface Profiles.
24. U.S. Bureau of Land Management Papers (1992), Steady and Unsteady Flow Profiles in Reclamation.
25. Universiti Teknologi MARA (UiTM) Malaysia : <https://uitm.edu.my/index.php/en/>
26. University of Melbourne, Australia : <https://www.unimelb.edu.au/>
27. University of Sheffield Western Sheffield UK : <https://www.sheffield.ac.uk/>
28. Wang H. (2016), Backwater effect of multiple bridges along Huaihe River, China.
29. Woltemade J.C. (1997), Water Level Management Opportunities for Ecological Benefit, Pool 5 Mississippi River, Journal of the American Water Resources Association
30. Xinbao Y., Tao J., and Xiong B.Y. (2011), Comparison Study on Computer Simulations for Bridge Scour Estimation.